SEASONALITY AND ENVIRONMENTAL HETEROGENEITY DURING A LATE CARBONIFEROUS HIGHSTAND: BRACHIOPOD SHELL GEOCHEMICAL RECORDS FROM THE PANGEAN TROPICS

A Thesis

by

ANDREW PEARSON ROARK

Submitted to the Office of Graduate and Professional Studies of
Texas A&M University
in partial fulfillment of the requirements for the degree of

MASTER OF SCIENCE

Chair of Committee,	Ethan L. Grossman
Committee Members,	Debbie J. Thomas
	Thomas D. Olszewski
Head of Department,	John R. Giardino

December 2014

Major Subject: Geology

Copyright 2014 Andrew Pearson Roark

ABSTRACT

The relationship between Permo-Carboniferous glacial cycles and low-latitude climate remains a subject of vigorous debate. This study investigated seasonality and regional environmental variability in a portion of central equatorial Pangea during a late Pennsylvanian highstand using stable isotope and trace element analyses of brachiopod shells from the Virgilian Ames Member of the Conemaugh Group in the Appalachian Basin, U.S.A. Well-preserved, thick-shelled *Neospirifer dunbari* specimens were serially sampled across growth bands to elucidate a record of seasonal variability during the life of the organisms. Because *Neospirifer* only colonized this marginal basin during near-maximum highstands when stable marine salinities were established, these data are a direct proxy for intra-annual climate fluctuations during interglacial times. Additionally, well-preserved specimens of the thinner-shelled brachiopod *Crurithyris planoconvexa*, which has a wider spatial and stratigraphic distribution within the basin, were analyzed individually.

Neospirifer specimens show remarkably little internal chemical variability, with $\delta^{18}O$ generally fluctuating by 0.4‰ or less and $\delta^{13}C$ by less than 1.5‰ within a single specimen. Moreover, total variability between all specimens is only ~1.5‰. This lack of variation reflects a homogenous, nonseasonal to weakly seasonal climate during the Ames highstand. Both $\delta^{18}O$ and $\delta^{13}C$ are ~1.5 lower than those of other Virgilian specimens from regions with a more proximal connection to the open ocean, suggesting relatively high freshwater influence in the Appalachian Basin during this time, although salinities remained close to marine levels. Thus, brachiopod seasonal records indicate

normal moist tropical conditions during this penultimate Carboniferous interglacial, with no evidence for strong monsoonal variations in temperature or rainfall. *Crurithyris* specimens show similarly homogenous isotopic values that are slightly depleted relative to more nearly marine specimens. There is a weak gradient towards increasing $\delta^{18}O$ and $\delta^{13}C$ in *Crurithyris* specimens to the west, consistent with decreasing influence of Appalachian runoff waters in that direction. *Crurithyris* from two sites show anomalously enriched isotopic values, potentially indicating rare, sporadic periods of net evaporation. However, because of *Crurithyris*' wider temporal distribution, these events may not have occurred during the highstand.

DEDICATION

SDG

A generation goes and a generation comes, but the earth remains forever
Ecclesiastes 1:4

ACKNOWLEDGEMENTS

To kick off a long list of acknowledgements, I would like to thank my advisor, Ethan Grossman, for his excellent help and guidance throughout this project. Ethan's commitment to personally mentoring me throughout my time at A&M has meant more than he could know. He successfully applied for a Chevron Fellowship from the Berg-Hughes center on my behalf, which provided two years of financial support during my time here, and has generously paid for research expenses out of his Michel T. Halbouty endowed chair in geology. I would also like to thank my other committee member, Tom Olszewski and Debbie Thomas. National Science Foundation Grant EAR-0643309, for which Debbie was the PI, provided one semester of support for me in the form of a research assistantship and paid additional research expenditures. Debbie provided an essential oceanographic perspective to this effort, in addition to insightful manuscript reviews. Tom provided priceless feedback and engaging discussions on climatic-eustatic-stratigraphic teleconnections.

On the technical side, Chris Maupin, Brendan Roark, and the Stable Isotope Geoscience Facility staff kept the mass spectrometer and peripheral equipment running smoothly. Ray Guillemette skillfully operated the microprobe; his insight in interpreting mineralogy and trace element data will be greatly missed following his retirement this year. Blake Herber, our undergraduate lab assistant, significantly shortened my days (and nights) at the thin section polishing wheel.

My family and friends have been a haven of support throughout my years in school; I can't wait to celebrate reaching this milestone with them.

TABLE OF CONTENTS

LIST OF FIGURES

FIGURE Page

LIST OF TABLES

INTRODUCTION

The Late Pennsylvanian was a critical period of transition for the earth-atmosphere system. This time marked a pivotal waypoint along the long-term progression in central equatorial Pangea from dominantly everwet conditions in the Middle Pennsylvanian to more arid climates in the Permian (Parrish, 1993; Tabor and Poulsen, 2008, and sources cited therein). Tectonic mechanisms, such as the growth and northward drift of Pangea, fueled this 30 million year transformation (e.g. Parrish, 1993). Superimposed on this long-term trend were short- and intermediate-term oscillations in ice volume responsible for generating repetitive lithologic successions ("cyclothems") that span the Permo-Carboniferous interval in many parts of the world (e.g. Wanless and Shepard, 1936; Heckel, 1977; Miller et al., 1996; Olszewski and Patzkowsky, 2003; Davydov et al., 2010). These changes in ice volume and sea level were driven by Milankovitch cyclicity (Busch and Rollins, 1984; Crowley et al., 1993; Heckel, 1986; Tabor and Poulsen, 2008) and were likely coupled to systematic changes in climate (Cecil, 1990; Tandon and Gibling, 1994; West et al., 1997; Cecil et al., 2003; Olszewski and Patzkowsky, 2003; Falcon-Lang and DiMichele, 2010; Eros et al., 2012). However, the nature of this climate-eustatic connection at low latitudes remains disputed (e.g. Tabor and Poulsen, 2008).

Wanless and Shepard (1936) initially proposed that late Paleozoic glaciations were associated with relatively arid climate regimes, while interglacials represented more humid times. Many more recent studies based on palynological analyses, stratigraphic succession, and/or sedimentology support this conclusion (e.g. Tandon and

Gibling, 1994; Yang, 1996; Rankey, 1997; Olszewski and Patzkowsky, 2003, 2008; Falcon-Lang and DiMichele, 2010); however, others, (e.g. Miller and West, 1993; West et al., 1997; Cecil et al., 2003; Feldman et al., 2005; Eros et al., 2012) have favored humid glacial phases and arid interglacial times. Some of this disagreement may arise from the nature of "far-field" low-latitude sedimentological and palynological evidence for climate change, evidence commonly associated with facies (e.g. coals, paleosols) whose precise position in the transgressive-regressive cycle is debated or ambiguous. For instance, coals have alternatively been interpreted as either late lowstand systems tract or middle to late trangressive systems tract deposits (Falcon-Lang and DiMichele, 2010). Massive limestone has been interpreted by some (e.g. Miller and West, 1993; Olszewski and Patzkowsky, 2003) as a transgressive deposit, and by others (e.g. Cecil et al., 2003) as a regressive deposit. Meanwhile, some authors (e.g. Heckel 1977) have associated black phosphatic shale with highstands, while others (e.g. Cecil et al., 2003) have associated similar shales with early transgressive times. A further potential complication is that this climate relationship may have reversed (i.e. from moist highstands to arid highstands) between the Carboniferous and early Permian (e.g. Miller et al., 1996). Resolving this controversy will necessitate the application of climate proxies to intervals with unambiguous stratigraphic significance.

Geochemical proxies are a rigorous means of testing the implications of paleoclimate models. Stable oxygen and carbon isotope analyses have arguably been the lynchpin in quantifying environmental changes associated with the more recent ice ages (e.g. Zachos et al., 2001) and have been applied extensively to the Paleozoic as well (e.g.

Adlis et al., 1988; Grossman et al., 1993, 2008; Tabor and Montañez, 2002). This study presents new stable isotope and trace element analyses of well-preserved brachiopod shells from the Appalachian Basin documenting the degree of seasonal environmental change in the low-latitude Late Pennsylvanian epicontinental sea of North America (LPES) during an early Virgilian highstand, as well as additional analyses examining the potential for cycle-scale temporal changes. The stratigraphic record of the LPES preserves many classic cyclothemic successions (e.g. Wanless and Shepard, 1936; Heckel, 1977; Olszewski and Patzkowsky, 2003), and is thus an ideal setting to test climate predictions based on these deposits; moreover, the paleogeographic and paleoenvironmental setting of the Appalachian Basin during the early Virgilian allows maximum highstand deposits to be clearly identified based on faunal assemblages (Lebold and Kammer, 2006; see below).

Brachiopods are an ideal proxy for high-resolution environmental change in marine settings: brachiopod shells precipitate in equilibrium with seawater (Lowenstam, 1961; Parkinson et al., 2005; Yamamoto et al., 2010a, 2010b; Takayangi et al., 2013) and are highly resistant to diagenesis (Popp et al., 1986; Grossman et al., 1993; Samtleben et al., 2001). Geochemical records of seasonality have been identified in both modern (e.g. Buening and Spero, 1996) and ancient (e.g. Mii and Grossman, 1994; Wang, 1998; Powell et al., 2009; Nielson et al., 2013) specimens. This approach can be used to test conceptual models of low-latitude climate. The most common model suggesting an arid highstand association involves enhanced monsoonal circulation during interglacial periods. Melting the southern icecap presumably would diminish the

south polar high pressure atmospheric circulation cell, allowing the intertropical convergence zone (ITCZ) to migrate over a larger area annually and resulting in significant seasonal drying even at equatorial latitudes (Fig. 1; e.g. Miller and West, 1993; Cecil et al., 2003). This condition would exacerbate the Pangean "megamonsoon," a massive seasonal climatic shift associated with the supercontinent's large land area and symmetry about the equator (e.g. Kutzbach and Gallimore, 1989; Parrish, 1993). In a highly restricted portion of the LPES such as the Appalachian Basin, this type of seasonality would result in significant annual fluctuations of the seawater chemistry, changes that should be reflected in the isotopic composition of brachiopod shells deposited in the region. Modern gastropod shells in equatorial marine environments show a clear isotopic record of seasonal drying associated with the much weaker present-day tropical monsoon (Tao et al., 2013) If, on the other hand, everwet conditions prevailed during glacial times, the isotopic records of seasonality should show relatively little variability.

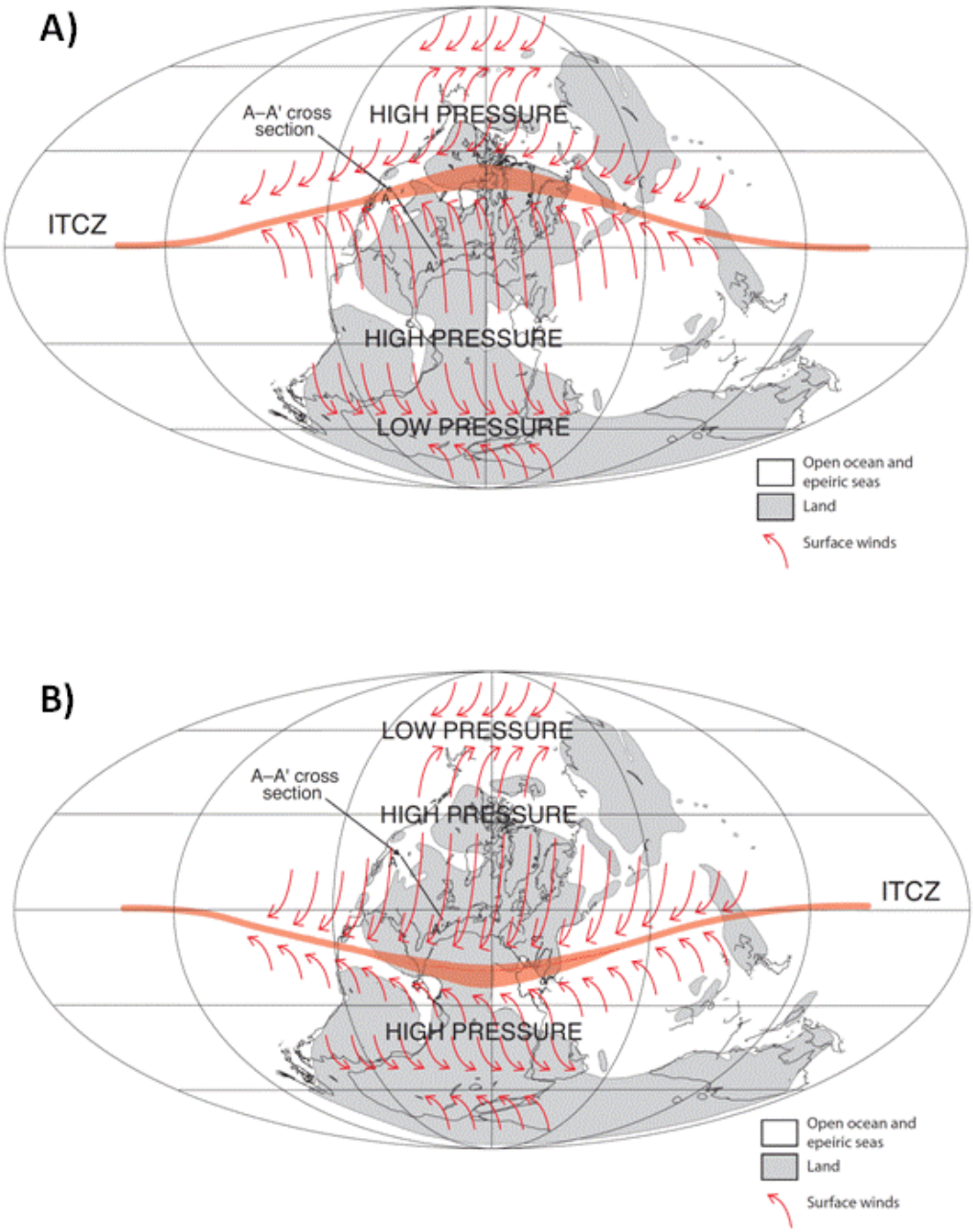

Figure 1 The Pangean "megamonsoon" in action. **A)** Northern Hemishpere summer; the ITCZ swings north to accommodate a large low pressure area created by heating of northern Pangea. **B)** Southern hemisphere summer; heating of southern Pangea creates a large low pressure zone over southern Pangea, causing the ITCZ to swing south. The region affected by these ITCZ swings will have a strongly seasonal climate, alternating between humid and arid conditions; Cecil et al. (2003) argued that these effects were exaggerated during interglacials. Figure modified from Cecil et al. (2003).

SAMPLES AND GEOLOGIC SETTING

Samples for this study were collected from the Virgilian (latest Pennsylvanian) Ames Member of the Conemaugh Group in the Appalachian Basin (Fig. 2). The Ames Member reflects the largest global transgression of the late Carboniferous, a time when marine waters breached the main foreland basin to the proto-Appalachian Mountains, a region typically dominated by fluvial systems and coal swamps (Al-Qayim, 1983; Fahrer, 1996). The Ames typically consists of a thin (cm-scale) bed of coal or carbonaceous shale overlain by marine limestsone and shale (Al-Qayim, 1983). On the western (Ohio) side of the basin, the Ames is about 1 m thick and is primarily skeletal limestone reflecting deposition in clear, shallow shelf conditions (Al-Qayim, 1983; Saltsman, 1986). To the east (West Virginia, Pennsylvania), the Ames thickens to about 2-3 m and consists mostly of marine shale with thin beds of argillaceous limestone, indicating greater clastic influx and subsidence approaching the Appalachians (Al-Qayim, 1983; Saltsman, 1986; Lebold and Kammer, 2006). A vertic paleosol complex immediately underlies the Ames (Joeckel, 1995) while the nonmarine Grafton Sandstone caps the Ames (Al-Qayim, 1983). The Ames contains at least two short-term (i.e. fifth order) transgressive-regressive pulses nested within one intermediate-term (fourth order) transgressive regressive cycle. Assuming that fourth order cycles were driven by changes in Earth's orbital eccentricity, analogous to the effects of orbital variations during the Quaternary, deposition of the entire Ames took place within ~400 kyr (Lebold and Kammer, 2006; Heckel, 1986; Heckel, 2002).

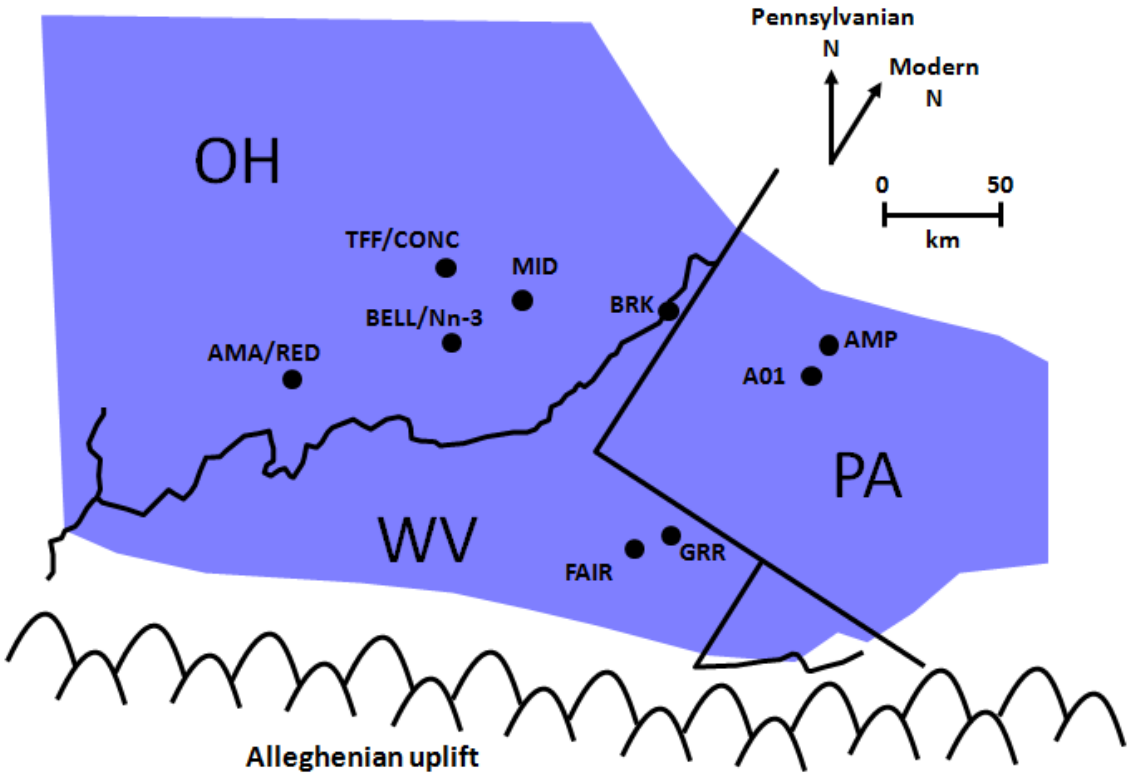

Figure 2. Site locations for specimens used in this study. Samples were collected from throughout the basin to constrain spatial variability. See Table 1 for detailed locality information. Paleogeography modified from Algeo and Heckel (2008).

This study utilizes two types of sampling strategies. First, specimens of the thick-shelled brachiopod *Neospirifer dunbari* have been selected for seasonality studies (Fig. 3). These shells are thick enough to permit serial sampling of stable isotopes and trace elements along transects perpendicular to the shell's growth bands (cf. Mii and Grossman, 1994; Wang, 1998; Nielson et al., 2013), revealing the degree of seasonal change. *Neospirifer* is generally indicative of fully marine environments: the species preferred low turbidity conditions and stable marine salinities and is typically found with other fully stenohaline fauna such as crinoids and bryozoans (Stevens, 1971; Donahue

and Rollins, 1977; Brezinski, 1983; Lebold and Kammer, 2006). During the Carboniferous, such conditions were only achieved in the Appalachian Basin during the maximum or near-maximum highstand (Lebold and Kammer, 2006). Horizons in the Ames associated with rising or falling sea level, on the other hand, are typically dominated by bivalves or thin-shelled brachiopods (Donahue and Rollins, 1977; Brezinski, 1983; Lebold and Kammer, 2006). Thus, seasonality studies based on *Neospirifer* offer a direct proxy for seasonal variability during a well-identified highstand. This type of proxy is unique and stands in contrast to other indicators such as paleosol geochemistry, tree rings, or floral assemblages that record conditions during lowstands or intermediate phases in the transgressive-regressive cycle.

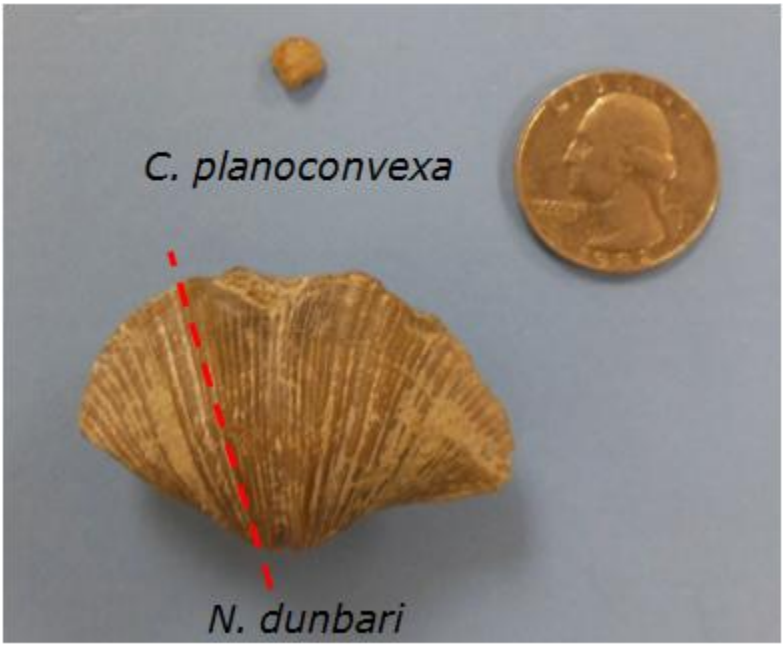

Figure 3 Representative *C. planoconvexa* and *N. dunbari* specimens. The dashed red line indicates approximate orientation along which *N. dunbari* shells were sectioned for seasonality studies.

Secondly, this report presents individual analyses of the smaller-shelled brachiopod *Crurithyris planoconvexa* (Fig. 3). *Crurithyris* specimens commonly have a well-preserved beak area greater than 1 mm thick (Adlis et al., 1988). These shells are too small for serial sampling, but are large enough to provide sufficient material for two or three isotopic analyses of the well-preserved portion. Due to their environmental preferences, *Crurithyris* specimens offer additional areal and temporal constraint on environmental conditions during the Ames transgression. *Neospirifer*, because of its need for stable stenohaline conditions, is largely confined to stratigraphic horizons in the Ames associated with the maximum highstand and is relatively uncommon in the eastern portion of the basin, where freshwater influence was strongest (Brezinski, 1983; Lebold and Kammer, 2006). *Crurithyris*, in contrast, was tolerant of moderate salinity fluctuations; specimens are common in the Ames interval throughout the basin and are associated with unstable environmental conditions, including times of changing sea level (Donahue and Rollins, 1977; Brezinski, 1983; Lebold and Kammer, 2006). This wider distribution permitted sampling from multiple stratigraphic horizons within the Ames to examine the potential for longer-scale temporal changes in the balance between freshwater input and evapotranspiration throughout the T-R cycle.

METHODS

Sample collection and preparation

Samples were collected from outcrops of the Ames Member of the Glenshaw Formation in Pennsylvania, West Virginia, and Ohio (Fig. 2). Localities were marked using a handheld GPS device. Additional specimens were gathered from collections housed at the Carnegie Museum (Pittsburgh, PA); West Virginia University (Morgantown) and Ohio State University (Columbus). For these samples, the sampling site coordinates were estimated based on the brief written locality descriptions included with the collections. In a few cases, samples were collected decades earlier and the actual outcrop location is vaguely described, no longer exists, or is referenced to ephemeral landmarks that no longer exist. To minimize ambiguity, Table 1 lists the written locality descriptions for museum specimens. Brachiopod species were identified based on Sturgeon and Hoare (1968).

Table 1 Sampling localities.

Locality	Locality description	County	State	Latitude	Longitude	Source*
A01	Monroeville, PA; more specific location not given	Allegheny	PA	40.421181(*i*)	-79.788103(*i*)	CMP
AMA	n/a	Athens	OH	39.317219	-82.101883	WVU
AMP	n/a	Allegheny	PA	40.571936	-79.790094	WVU
BELL	Belle Valley	Noble	OH	39.780917	-81.553303	WVU
BRK	PA and WV RR cut near mouth of Cross Creek	Brooke	WV	40.309850(*i*)	-80.599458(*i*)	CMP
CONC	New Concord	Guernsey	OH	39.982814	-81.693358	WVU
FAIR	near Fairmont, WV	Marion	WV	40.383517	-80.6279	FC, F, WVU
GRR	along Green Bag Road, Morgantown, WV	Monogalia	WV	39.197667	-79.933267	FC, F, WVU

Table 1 continued

Locality	Locality description	County	State	Latitude	Longitude	Source*
MID	I70 roadcut, 1 mile east of Middlebourne, Oxford Township	Guernsey	OH	40.054075(*i*)	-81.320381(*i*)	OSU
Nn-3	West side of rt. 77 approx. 0.5 mi south of 821 exit SE of Belle Valley, SW1/4 SE1/4 sec 20 Noble township	Noble	OH	39.780917(*i*)	-81.553303(*i*)	OSU
TFF	Tony Fasekas Farm, 1.5 mi south of New Concord, Union Township	Guernsey	OH	39.975977(*i*)	-81.727061(*i*)	OSU

*Sample source: FC= collected in the field by author; F= collected by Flake (2011); CMP= from collections housed at the Carnegie Museum, Pittsburgh; WVU= from collection housed at West Virginia University; OSU= collection housed at Ohio State University

i= coordinates inferred from locality description

Shells were examined visually for evidence of alteration. Specimens showing obvious pitting, severe oxidation staining, or large fractures were excluded. Samples that passed this initial screening were rinsed in deionized water and scrubbed clean with a firm-bristled toothbrush to remove dirt and encrusting materials when feasible (*Crurithyris* specimens were too thin to scrub vigorously without breaking the shell). Clean samples were placed in a glass desiccator for at least twelve hours to remove moisture and then embedded in Struers Epofix epoxy. The epoxy was allowed to cure for three days and then the shell was cut longitudinally using an Isomet saw. One of the resulting billets was roughened using 600 grit sandpaper and then mounted to a frosted petrographic slide using Struers EpoFix epoxy. Slides were cured for at least three days and then the excess billet was cut off using an Isomet saw. Thin sections were polished using successively finer grits down to 0.3 μm deaglommerated alpha alumina. For

Neospirifer specimens, the corresponding billets were also polished under 0.3 μm alumina to make growth banding more visible during sampling.

Preservation evaluation and trace element analysis

To eliminate the possibility of diagenetic alteration, samples were subjected to a three-part screening procedure (cf. Adlis et al., 1988; Grossman et al., 1996). First, thin sections of each shell were examined under standard optical microscopy for disruptions of the primary crystal fabric, such as filled fractures, secondary mineral phases, or anomalous extinction patterns under crossed polarizers. Specimens showing such features were excluded from paleoenvironmental analysis.

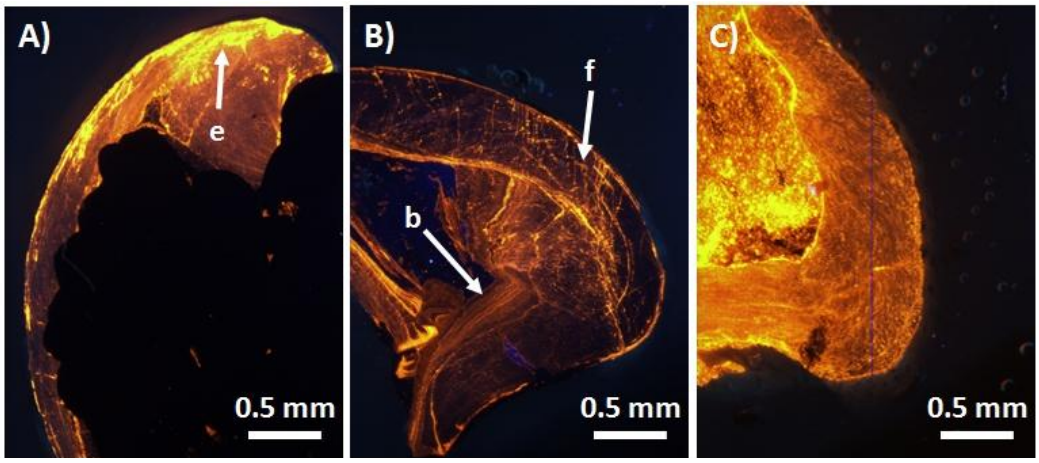

Figure 4 Luminescence patterns of altered shells. **A)** Pervasive recrystallization migrating inwards from the anterior shell edge, e; **B)** Recrystallization along small fractures (f) that served as fluid conduits and luminescent bands (b) parallel to the shell edge that likely formed as diagenetic fluids diffused into the shell; **C)** Pervasive recrystallization throughout the shell along a network of microfractures. **A)**, **B)**, and **C)** are *C. planoconvexa* specimens. **D)** Luminescent "splotches" (s) indicating patchy recrystallization inside the shell; **E)** Luminescence along fracture networks (f). **D)** and **E)** are *N. dunbari* specimens. Note that all of these alteration textures are easily distinguishable from primary luminescence, which forms strictly along growth bands (cf. Barbin and Gaspard, 1995). Exposure time in all images is 60 s.

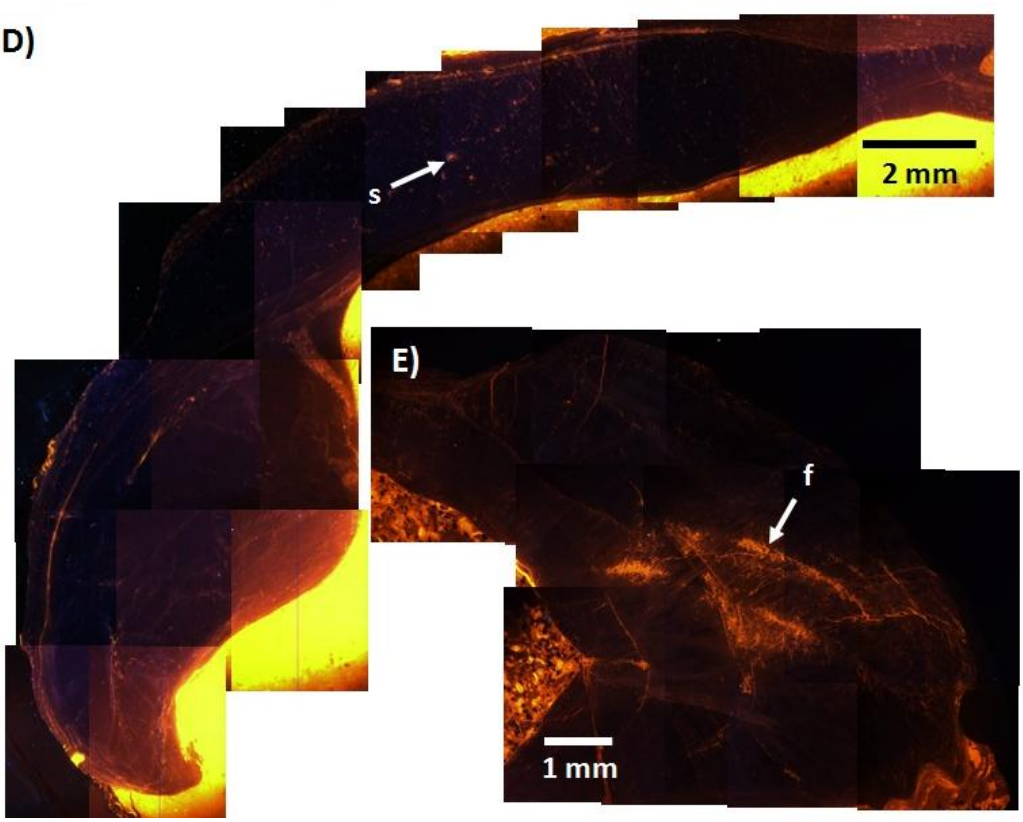

Figure 4 Continued.

Secondly, samples were analyzed under cathodoluminescence microscopy (CL) using a Technosyn 8200 MKII cold cathode luminoscope. Following the methods of Flake (2011), samples were exposed to a beam current and voltage of 200-300 nA and 10-15 kV, respectively, for 60 s. Orange luminescence in calcite is caused by Mn^{2+} in the crystal lattice (Machel, 1985; Machel et al., 1991) and is generally considered to be a good indicator of diagenetic alteration in brachiopod shells (Popp et al., 1986; Grossman et al., 1996; Samtleben et al., 2001). CL is particularly useful for screening ancient brachiopod shells due to its high spatial resolution and low detection limit for

diagenetically emplaced Mn^{2+} (~30 ppm; Machel et al., 1985), far below the range of concentrations typically resolved on electron microprobes or XRF scanners. The high spatial resolution permits identification of partial alteration fabrics and small recrystallized areas commonly rimming veins or fractures (Fig. 4), features that would not be detected through bulk trace element sampling techniques (e.g. solution-based ICP-MS) that average a relatively large volume of shell material. Shells from studies that utilized CL (e.g. Mii et al., 1999; Flake, 2011) typically have concentrations of the diagenetic metals Fe and Mn far below the levels tolerated by studies that rely solely on bulk trace element sampling (e.g. Bruckschen et al., 1999; Brand, 2004; cf. Denison et al., 1994); CL-screened samples also tend to yield isotopic ratios closer to predicted marine values than samples screened by trace element techniques alone (Grossman et al., 2008). Moreover, CL has been demonstrated to effectively identify alteration in shells that appeared pristine under SEM analysis (Angiolini et al., 2009).

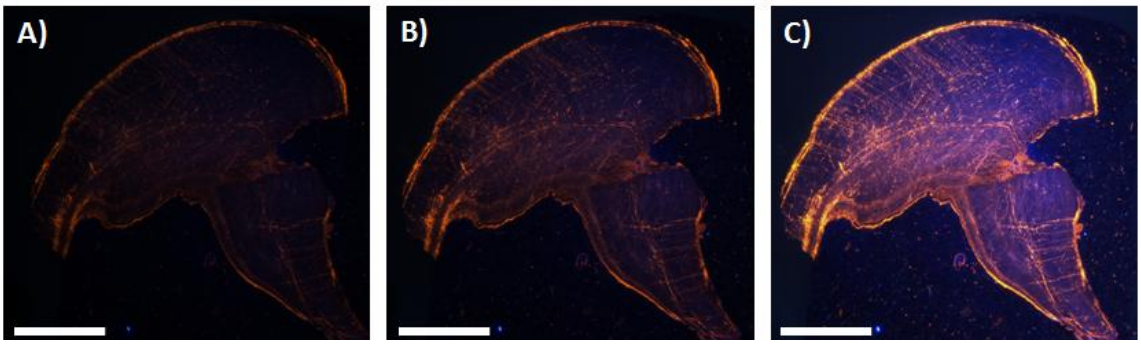

Figure 5 Cathodoluminescence images of an altered *C. planoconvexa* shell with varying exposure times. Exposure times are **A)** 10 s, **B)** 20 s, and **C)** 60 s. Inadequate exposure times may prevent detection of alteration; the luminescent features in this shell are difficult to resolve with 10 s exposure, even though such exposure times may be adequate for capturing images of more luminescent carbonates; however, secondary luminescence is clearly visible after exposing for 60 s. For this study, 60 s was the standard exposure time used for screening shells. Scale bar is 0.5 mm.

Despite these advantages, it is important to note that CL is a qualitative technique whose sensitivity depends heavily on the beam conditions and camera exposure time used. As there are currently no standard cathode beam operating conditions for brachiopod diagenesis screening, it is important for studies relying on CL to clearly state the beam current and voltage used (Flake, 2011). Equally important is camera exposure time. Brachiopod shells typically resist alteration more effectively than the carbonate matrix and cement materials (e.g. Popp et al., 1986), and thus tend to luminesce much more faintly. Brachiopod shells that initially appear nonluminescent, especially when juxtaposed against highly luminescent sparry cements, often show dull luminescence under further inspection. For instance, shells deemed "nonluminescent" by Angiolini et al. (2012; their Figure 4) and Laya et al. (2013; their Figure 3b) in fact show dull luminescence and would likely have been excluded from this study by the criteria established below. Failure to exclude luminescent specimens may be responsible for the anomalously high Fe and Mn brachiopod concentrations reported in Laya et al. (2013). Exposure times of 5-10 s, which may be adequate for some carbonate petrology applications, are insufficient to reveal the dull luminescence associated with some altered brachiopod shells (Fig. 5). This study used an exposure time of 60 s to ensure detection of faint luminescence. For shells occurring in a luminescent matrix, the matrix portion of the thin section was coated with SPI conductive carbon paint (colloidal graphite) to prevent matrix luminescence from "bleeding" over and obscuring the luminescence character of the shell during the long exposure time (Fig. 6). It is thus critically important for studies involving CL to explicitly state the camera exposure time

used. Many studies evaluating the efficacy of CL (e.g. Rush and Chafetz, 1990; Samtleben et al., 2001) have not specified CL exposure time, making comparison of results difficult. To avoid ambiguity, shells in this study were classified on a gradational scale from nonluminescent (NL) to luminescent (L; Fig. 7); only samples falling into the NL or NL/SL categories were used for paleoenvironmental analysis (cf. Flake, 2011).

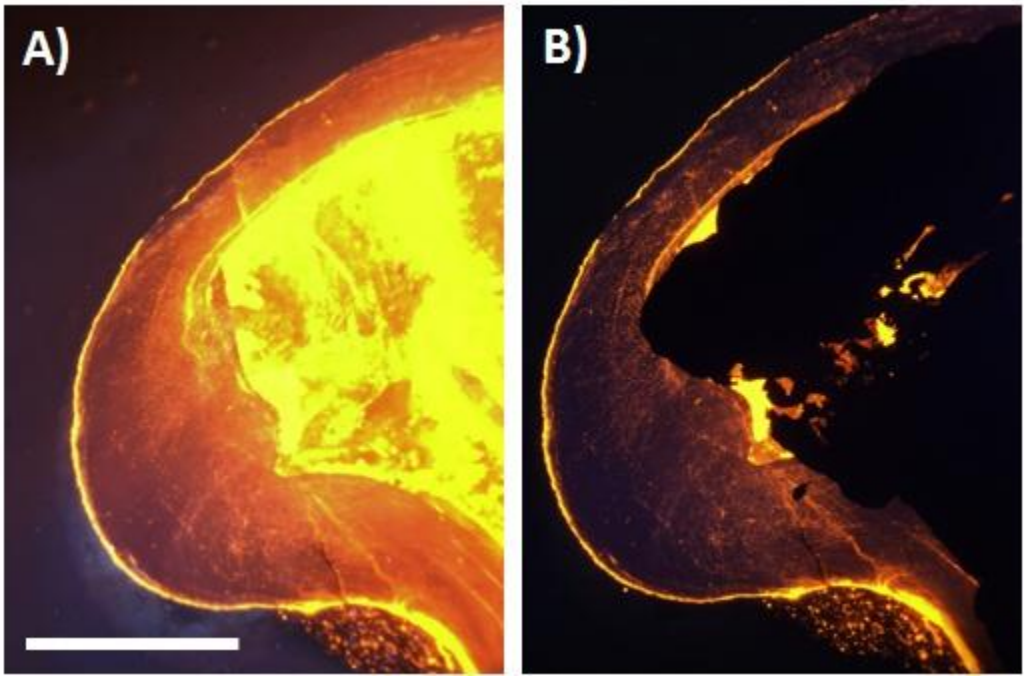

Figure 6 Luminescence "bleed over." Cathodoluminescence image of sample A01-3 **A)** without and **B)** with the highly luminescent matrix covered with conductive carbon paint. Without the coating, luminescence from the matrix "washes out" and obscures the luminescent character of the shell. In **A)**, it is impossible to tell whether the shell is luminescing brightly or just appearing to glow as luminescence "bleeds over" during the long exposure time. Exposure time in both images is 60 s. Scale bar is 1 mm.

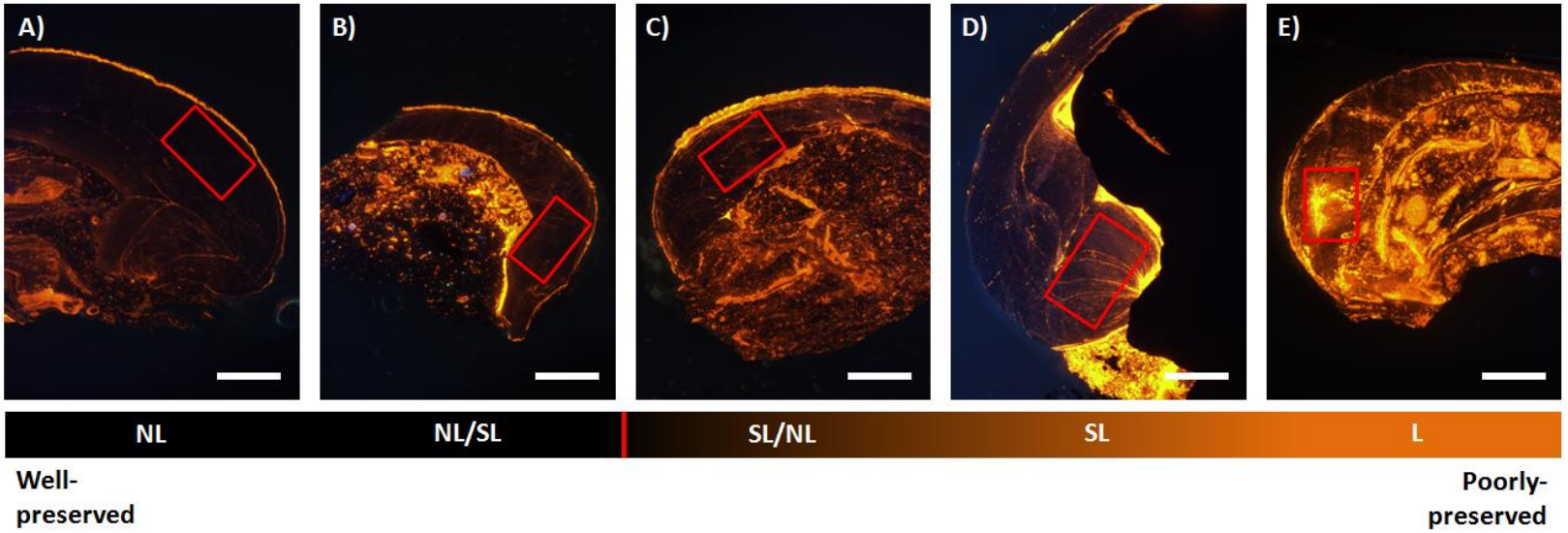

Figure 7 A gradient of cathodoluminescence. This spectrum of *C. planoconvexa* specimens illustrates the luminescence ranking scheme used in this study: **A)** nonluminescent (NL); **B)** nonluminescent/ slightly luminescent (NL/SL); **C)** slightly luminescent/ nonluminsecent (SL/NL); **D)** slightly luminescent (SL); **E)** luminescent (L). The red box outlines the relevant portion of the shell. Samples or portions of samples with greater luminescence than NL/SL were excluded from paleoenvironmental analysis. Exposure time is 60 s for **A)** through **D)** and 20 s for **E)**. Scale bar is 0.5 mm.

Barbin and Gaspard (1995) and Barbin (2000) have criticized the use of CL as a diagenetic screening mechanism on the grounds that modern brachiopod shells are not completely nonluminescent. However, these studies utilized hot CL, a technology distinct from the cold CL used in this study. Hot CL generates a cathode beam via a heated filament rather than an electron gun and is more effective at producing visible luminescence in weakly luminescent minerals than cold CL (Götze, 2002; Götze and Kempe, 2008). Consequently, hot CL is able to detect minor amounts of primary Mn^{2+} incorporated into the shell during its growth (Barbin and Gaspard, 1995; Barbin, 2000). These concentrations are likely below the amounts relevant to diagenetic alteration, which are generally detected on cold CL (cf. Grossman et al., 1996). Moreover, the patterns of primary luminescence described by Barbin and Gaspard (1995, their Plate 1) and Barbin (2000), which are generally parallel to the shell growth bands, are easily distinguishable from secondary luminescence patterns associated with diagenesis, such as "splotchy" or mottled textures and fracture fills (Fig. 4; cf. Fig. 4 of Angiolini et al., 2009). The possibility of primary luminescence thus does little to erode the utility of CL as a screening tool for diagenesis. One specimen in this study, TFF2, shows very faint luminescent lines paralleling growth bands (Fig. 8), similar to the type of growth-parallel primary luminescence of Barbin and Gaspard (1995) and Barbin (2000). Because of the distinct character of this luminescence, reasonable trace element concentrations (see below), the shell's pristine appearance under optical microscopy, and the absence of additional luminescence associated with secondary alteration features, isotopic data from this shell are incorporated into the study.

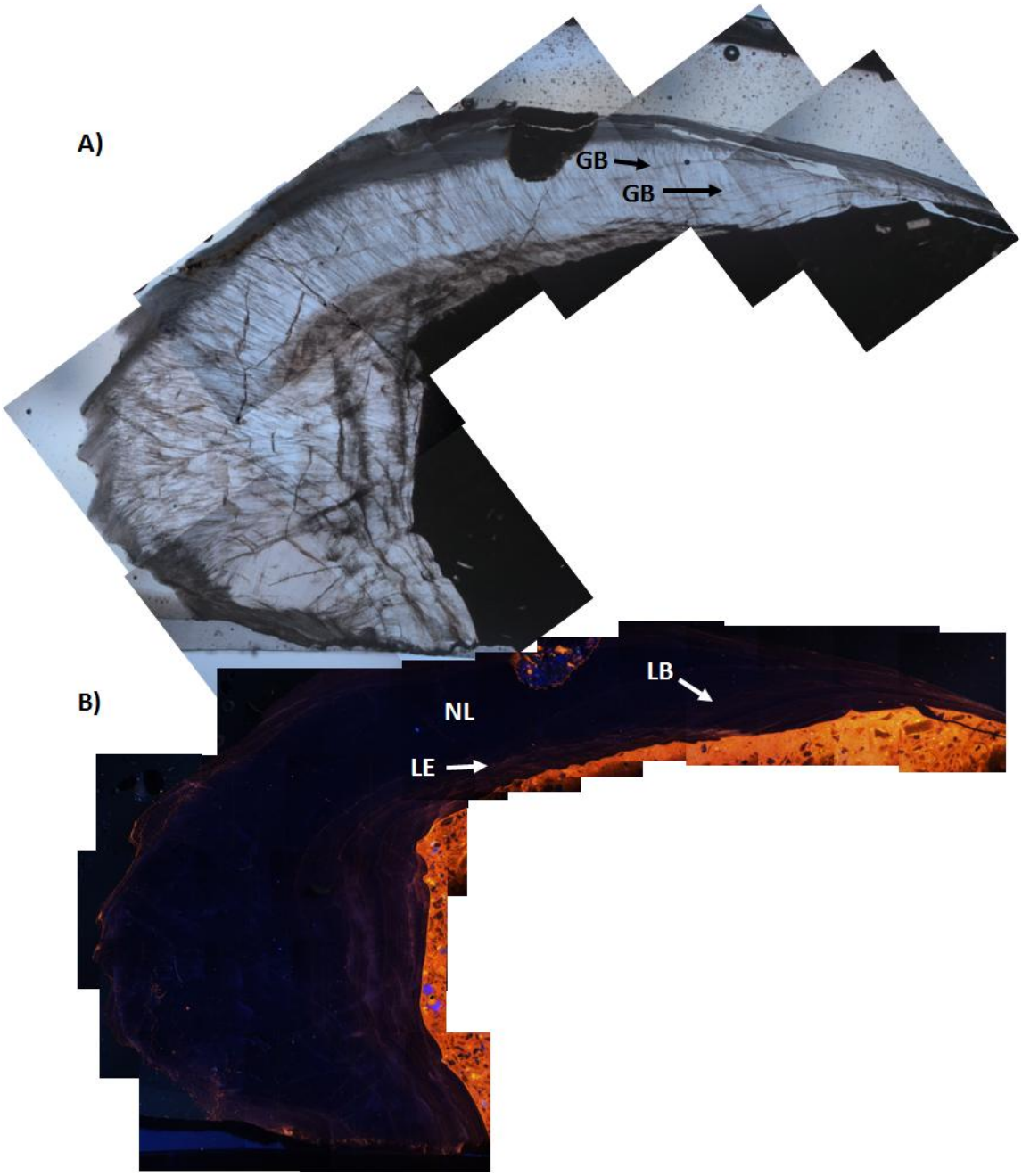

Figure 8 Possible primary luminescence. *N. dunbari* sample TFF 2 is displayed in **A)** plane light, showing growth band (GB) orientation, and **B)** cathodoluminescence microscopy, showing very faint, possibly primary luminescence along growth bands (LB). This luminescence pattern is distinct from typical patterns associated with diagenesis (Fig. 7) in that it parallels growth bands and is almost undetectable even with long exposure times. NL indicates completely nonluminescent portion of the shell; LE indicates faint secondary luminescence near the shell edge. Over all, the shell is generally nonluminescent. Exposure time in **B)** is 60 s.

As a final precaution, select *C. planconvexa* from each site and stratigraphic horizon were analyzed for Ca, Mg, Mn, Fe, Sr, Na, S, Al, and Si via wavelength dispersive spectroscopy on a Cameca SX50 microprobe. Analyses used a 20 μm-diameter, 15 kV beam. Detection limits are reported in Table 2. Mn and Fe concentrations systematically increase while Na and S concentrations systematically decrease during meteoric and burial diagenesis (Brand and Veizer, 1980). Anomalous concentrations of these elements relative to unaltered specimens may indicate alteration. Well-preserved *Crurithyris* specimens typically show Na/Ca concentrations of 4-12 mmol/mol and S/Ca concentrations of 8-26 mmol/mol (Grossman et al., 1996); samples with concentrations below these ranges were not included in the study. Although CL is generally capable of detecting lower Mn concentrations than electron microprobe, high Fe^{2+} concentrations may quench luminescence in calcite (Machel, 1985). Unaltered brachiopod shells typically have Fe and Mn concentrations of less than 0.7 mmol/mol Ca (Grossman et al., 1996); consequently, specimens with Fe or Mn concentrations greater than this amount were not sampled. Significant amounts of Al or Si would indicate secondary silicate inclusions, so concentrations of these elements exceeding trace levels (i.e. >1 mmol/mol Ca) were also used as a criterion for culling samples.

For *Neospirifer* specimens, trace elements were sampled along transects perpendicular to growth banding, corresponding to the isotope sampling track(s) in the billet (see discussion below on growth band orientation). In this case, trace element analyses serve an added purpose of helping to elucidate seasonal environmental changes. Mii and Grossman (1994), Wang (1998) and Powell et al. (2009) have documented

fluctuations in Na, S, and/or Mg concentrations in serially sampled brachiopod shells corresponding to seasonal cyclicity. Similar fluctuations also occur in the shells of modern marine invertebrates (e.g. Tao et al., 2013). These changes may reflect differences in temperature, seawater chemistry, precipitation rate, or metabolism of the organism (Mii and Grossman, 1994; Wang, 1998; Powell et al., 2009).

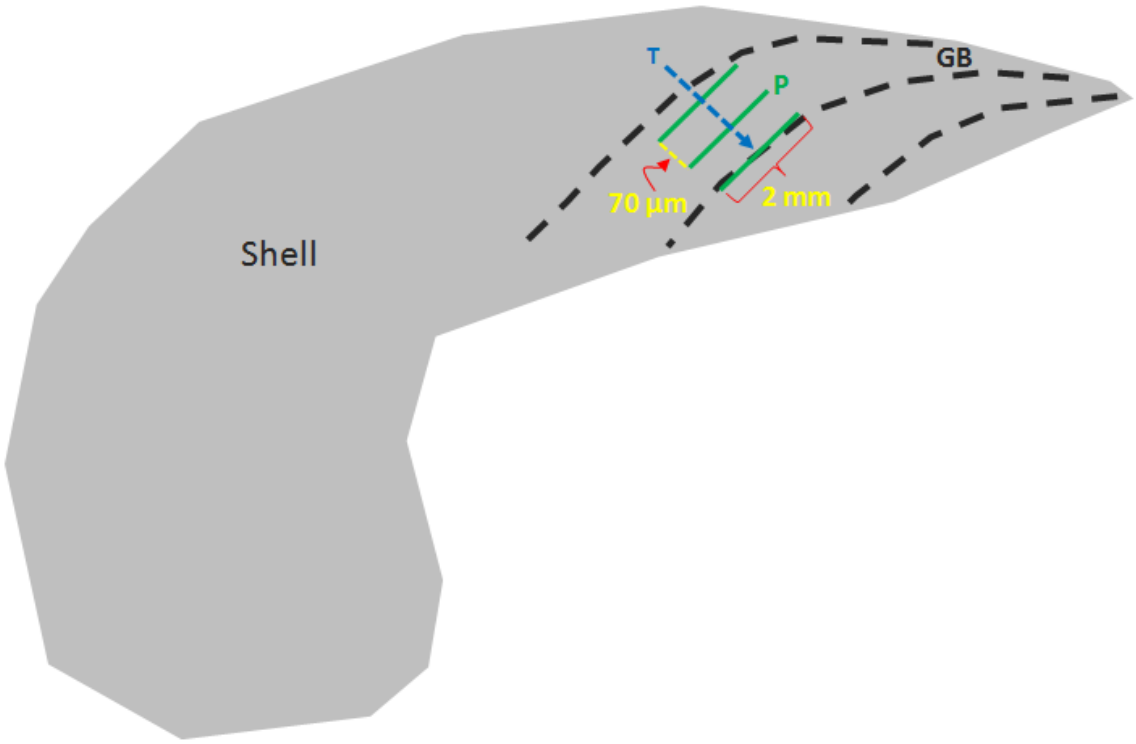

Figure 9 Schematic diagram illustrating the microsampling pattern for a hypothetical *N. dunbari* shell (drawing not to scale). Drilling paths (P) are oriented parallel to growth bands (GB) and spaced about 70 µm apart. One path is drilled at a time and the resultant powder collected. Drilling depth is approximately 500 µm. The drill is subsequently moved to the next path, and so on, creating a profile of the isotopic variation along a transect (T) perpendicular to growth bands.

Isotopic sampling and analytical methods

Seasonality studies on *Neospirifer* specimens followed the microsampling technique of Dettman and Lohmann (1995). Using a New Wave micromill equipped with a 0.5 mm diameter carbide-tipped drill bit, a series of tracks were drilled on a shell billet. These tracks were parallel to shell growth banding and arranged along a transect perpendicular to growth bands (Fig. 9). Each track was drilled individually, and the resulting powder was removed using a paintbrush trimmed to have only about five bristles and dumped into a glass reaction vial prior to drilling the next track. Tracks were approximately 2 mm long, 250 μm deep, and spaced 70 μm apart. About 60 μg of powder was recovered from each track. These methods were also used to mill transects through two *Crurithyris* specimens into subsequent generations of void-filling cement to investigate chemical trends during diagenesis.

Many shells sectioned in this study contain two intersecting sets of periodic, linear growth features, rather than one simple set of growth bands (Fig. 10). This situation is unusual and there is scant literature documenting such structures (Alberto Perez-Huerta, 2014, personal commun.; Thomas Yancey, 2014, personal commun.; Lucia Angiolini, 2014, personal commun.) True growth lines in brachiopods represent the shell surface during periodic lulls in growth (Williams and Rowell, 1965; Williams, 1968; Hiller, 1988) and thus cannot intersect. The orientation of line set II (Fig. 10) subparallel to the anterior edge of the shell and the fact that this set of lines crosses the boundary between secondary and tertiary calcite layers in the shell suggests that this set represents the true growth lines, although this interpretation is not conclusive (Alberto

Perez-Huerta, 2014, personal commun.; Lucia Angiolini, 2014, personal commun.; cf. Hiller, 1988; Williams, 1990). Brachiopod shells grow by both lateral extension and thickening (Williams and Rowell, 1965; Williams, 1968). One possible explanation for line set I is that these features formed as artifacts of crystal defects that were propagated through subsequent growth episodes as a result of shell thickening and do not represent time surfaces that would be relevant for sclerochronology (Perez-Huerta, 2014, personal commun.). This provisional explanation is incomplete and far from satisfactory; more research is necessary to clarify the significance of these structures. To ensure that this study captured the full range of seasonal environmental variability, separate isotope and trace element transects across both sets of structures were taken and compared for several shells.

Crurithyris specimens and matrix material from some sites were sampled manually using a dental pick whose tip had been filed to a sharp point. Resulting powders were weighed for a sample size of 30-100 μg and transferred directly to glass reaction vials. Powders from *Neospirifer*, *Crurithyris*, and rock matrix were reacted in "100%" orthophosphoric acid in a Kiel IV carbonate device and the evolved CO_2 was analyzed on a Thermo Finnigan MAT 253 mass spectrometer. Average analytical precision was 0.03‰ for $\delta^{13}C$ and 0.07‰ for $\delta^{18}O$.

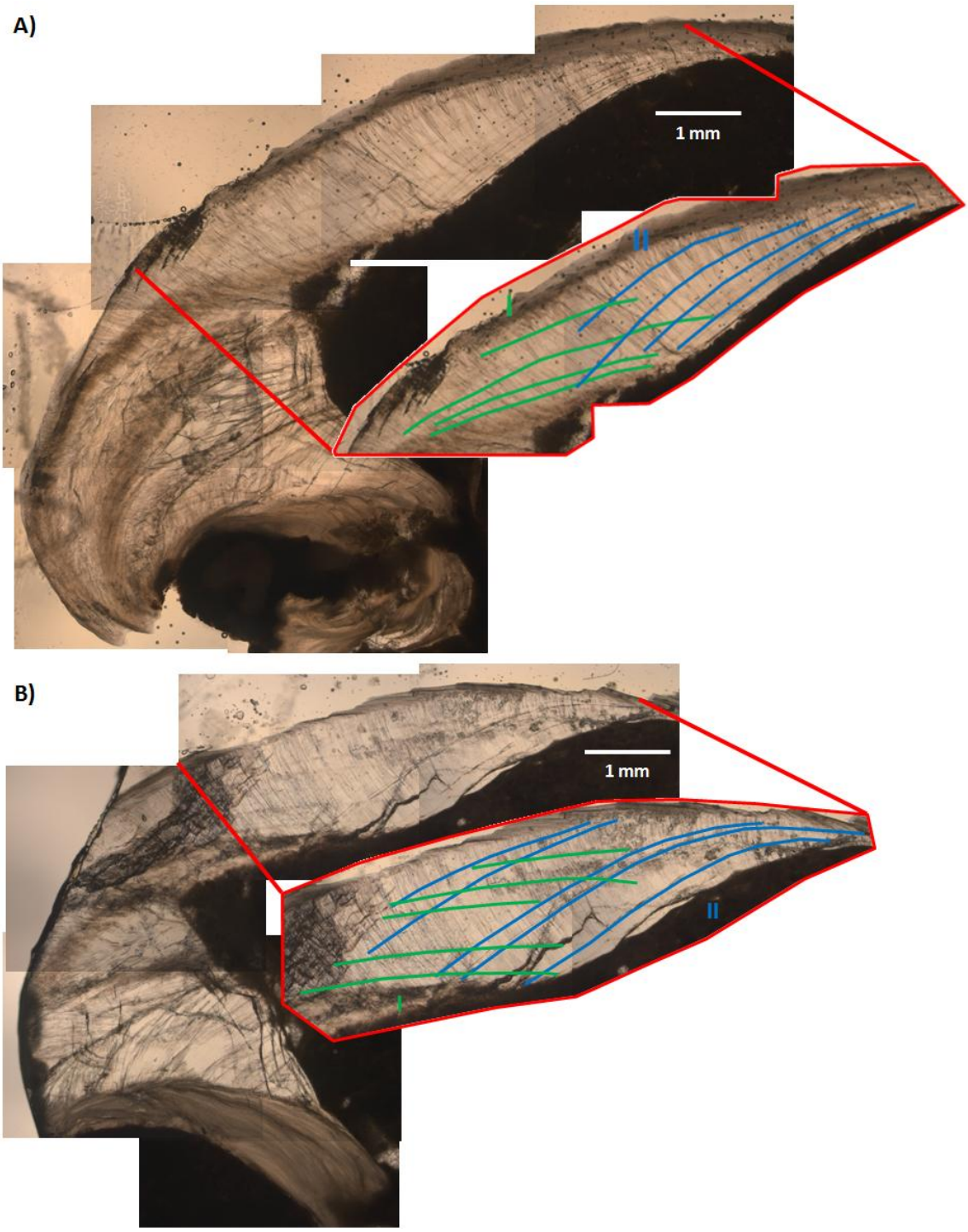

Figure 10 Conflicting growth structures. These plane light images show of the two intersecting sets of growth structures *N. dunbari* specimens **A)** MID2 and **B)** Nn-3; only one of the sets represents true "growth bands" in the sense of a time-significant surface. Transects parallel to both sets of structures were sampled for stable isotopes and trace elements in several samples for comparison.

RESULTS

Figure 11a displays the average isotopic compositions of well-preserved *Crurithyris* from this study by site location; Figure 11b graphs the results of all isotopic analyses of *Crurithyris* from this study and selected results from Flake (2011). Figure 11c illustrates isotope stratigraphies for two sites where specimens were collected from multiple horizons. $\delta^{13}C$ and $\delta^{18}O$ of well-preserved specimens show a slight (~0.6‰) increase moving from the present-day northeast to southwest side of the basin with two exceptions. Site A01 has significantly higher isotopic values than all other sites despite its location on the far northeast margin of the basin, and the FAIR locality reported by Flake (2011) has much higher values than either of the two FAIR horizons reported in this study. Flake (2011) did not report the specific stratigraphic interval sampled at FAIR. With the exception of the Flake (2011) samples from the FAIR locality, intra-site variability is generally minor. Isotopic values from poorly preserved shells frequently overlap with those of well-preserved specimens; however, luminescent samples account for all highly depleted (<0‰) $\delta^{13}C$ values (Fig. 11b). All specimens analyzed contained Na and S concentrations within expected limits for chemically-preserved Paleozoic brachiopods (Table 2; cf. Grossman et al., 1996). Fe and Mn concentrations were either very low or undetectable, and never exceeded the prescribed limit of 0.7 mmol/mol; Al and Si were only present in trace amounts as well, and never exceeded 0.3 mmol/mol in nonluminescent specimens (Table 2). Consequently, no samples were excluded based on trace element analyses.

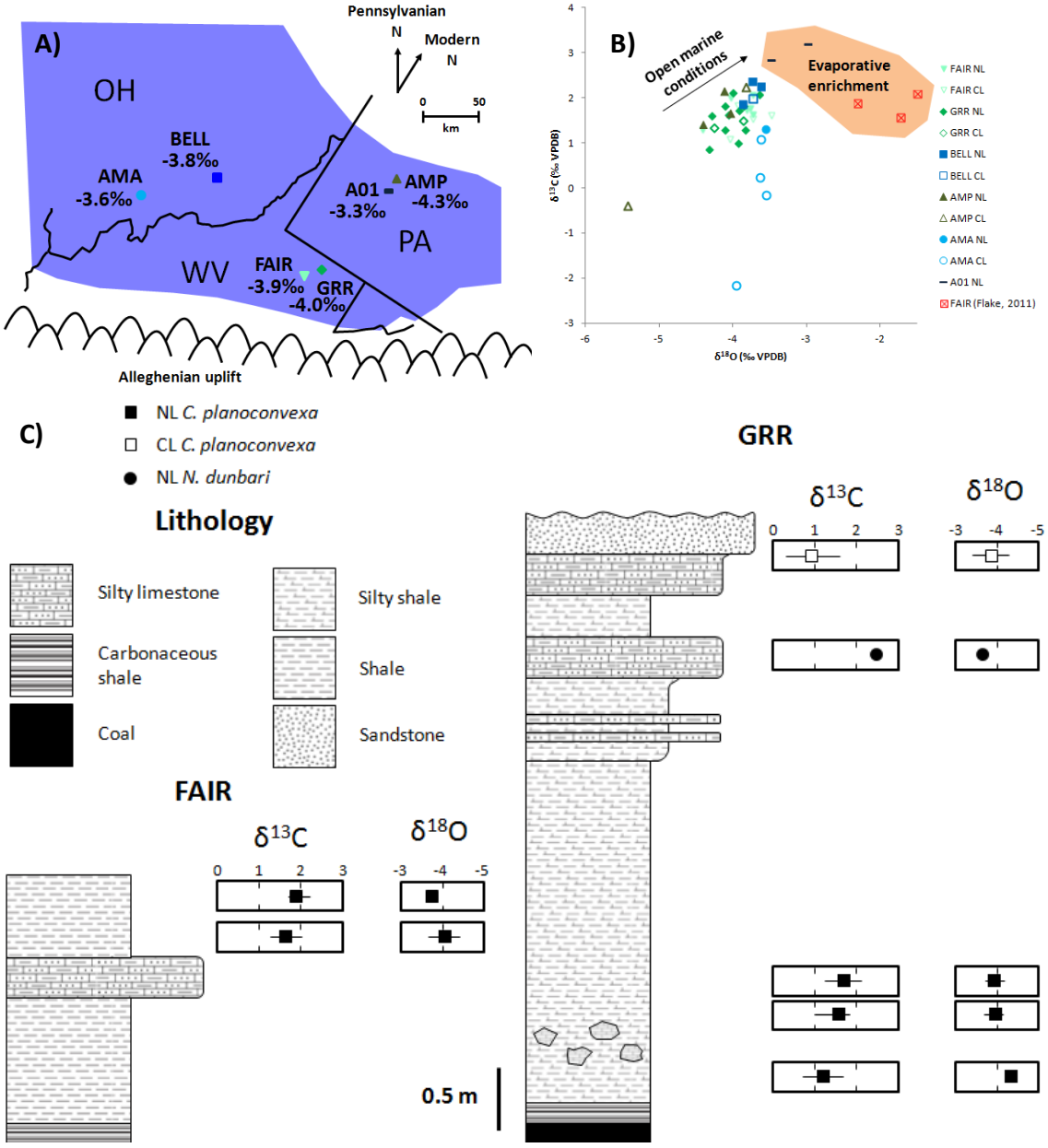

Figure 11 *C. planoconvexa* data. **A)** Average $\delta^{18}O$ for well-preserved *C. planoconvexa* specimens by sampling site; with the exception of site A01, values generally decrease moving from east to west. **B)** Plot illustrating the isotopic composition of all *C. planoconvexa* specimens in this study as well as samples from the FAIR locality reported by Flake (2011). Generally, values increase to the west reflecting decreased freshwater influence; anomalously high values are interpreted to represent episodes of aridity in the basin. **C)** Isotopic variability within the Ames at two sites where samples were collected from multiple horizons. In the uppermost horizon at GRR, no well-preserved specimens were recovered, so values from poorly preserved (CL) samples are included as an additional reference point. These poorly preserved specimens are not included in site averages in **A)**.

Table 2 Averaged isotopic and trace element data for *Crurithyris* specimens

Sample	Species	Fabric	L.C.	$\delta^{13}C$	±1σ	$\delta^{18}O$	±1σ	# of isotopic analyses	Trace element concentration (mmol/mol)								# of trace element analyses
									Mg	Fe	Mn	Sr	S	Na	Al	Si	
A01-1	*Crurithyris planoconvexa*	w	NL/SL	2.8	0.13	-3.5	0.05	2	7.1	0.3	-	1.4	16.1	12.3	-	-	4
A01-2	*Crurithyris planoconvexa*	p	SL/NL	2.2	n/a	-3.8	n/a	1	5.8	-	0.4	1.4	17.3	10.2	-	-	4
A01-6	*Crurithyris planoconvexa*	w	NL/SL	3.2	0.13	-3.0	0.14	2	x	x	x	x	x	x	x	x	x
AMA3-1	*Crurithyris planoconvexa*	w	NL/SL	1.3	0.46	-3.6	0.09	3	6.0	-	0.3	1.2	17.7	10.3	0.3	-	4
AMA3-2	*Crurithyris planoconvexa*	w	SL/L	-2.2	1.65	-4.0	0.09	2	x	x	x	x	x	x	x	x	x
AMA3-3	*Crurithyris planoconvexa*	w	SL/L	-0.2	0.18	-3.6	0.04	2	6.4	-	0.7	1.2	20.4	10.0	0.2	-	4
AMA5-1	*Crurithyris planoconvexa*	p	SL	0.5	1.52	-3.6	0.27	3	6.9	-	0.4	1.3	20.3	12.1	0.6	0.2	4
AMP1B-1	*Crurithyris planoconvexa*	w	NL/SL	1.7	0.84	-4.0	0.36	2	x	x	x	x	x	x	x	x	x
AMP1B-2	*Crurithyris planoconvexa*	w	SL/L	2.3	n/a	-3.8	n/a	1	x	x	x	x	x	x	x	x	x
AMP1B-3	*Crurithyris planoconvexa*	w	SL	-0.4	n/a	-5.4	n/a	1	7.7	-	0.5	1.2	20.4	11.6	0.7	-	3
AMP1B-4	*Crurithyris planoconvexa*	w	NL	2.1	0.21	-4.1	0.16	3	5.0	-	-	1.6	16.7	10.6	-	-	4
AMP1B-5	*Crurithyris planoconvexa*	w	NL/SL	1.4	n/a	-4.4	n/a	1	x	x	x	x	x	x	x	x	x
BELL5-1	*Crurithyris planoconvexa*	w	SL/L	2.0	0.44	-3.7	0.08	2	x	x	x	x	x	x	x	x	x
BELL5-4	*Crurithyris planoconvexa*	w	NL/SL	2.4	0.06	-3.7	0.08	2	x	x	x	x	x	x	x	x	x
BELL5-5	*Crurithyris planoconvexa*	w	NL/SL	2.3	0.10	-3.6	0.09	3	6.4	-	0.4	1.4	21.8	12.9	0.3	-	4

L. C. = luminescence character; samples other than NL or NL/SL were excluded from paleoevnironmental analysis (see Fig. 7)
Fabric: w= well-preserved; P= poorly preserved
x=specimen not analyzed; -=below detection limit
Approximate detection limits (mmol/mol Ca): Mg=0.18; Fe=0.19; Mn=0.18; Sr=0.31; S=0.25; Na=0.22; Al=0.16; Si=0.16

Table 2 continued

Sample	Species	Fabric	L.C.	$\delta^{13}C$	±1σ	$\delta^{18}O$	±1σ	# of isotopic analyses	Trace element concentration (mmol/mol)								# of trace element analyses
									Mg	Fe	Mn	Sr	S	Na	Al	Si	
BELL5-6	*Crurithyris planoconvexa*	w	NL/SL	1.9	1.04	-3.9	0.39	2	6.7	-	-	1.7	16.0	11.9	0.2	-	4
FAIR4a-1	*Crurithyris planoconvexa*	w	NL/SL	1.6	0.35	-3.7	0.10	3	4.8	-	0.3	1.4	20.1	11.8	-	-	4
FAIR4a-2	*Crurithyris planoconvexa*	w	NL/SL	2.0	0.07	-4.0	0.13	3	7.4	0.4	-	1.6	15.2	11.2	0.3	-	4
FAIR4a-3	*Crurithyris planoconvexa*	w	SL/NL	2.1	0.14	-3.7	0.03	3	x	x	x	x	x	x	x	x	x
FAIR4a-4	*Crurithyris planoconvexa*	w	SL/NL	1.5	n/a	-3.7	n/a	1	10.3	-	-	1.4	17.1	11.4	-	0.2	4
FAIR4a-6	*Crurithyris planoconvexa*	w	NL	1.3	n/a	-4.4	n/a	1	10.2	-	0.5	1.3	13.8	9.6	-	0.1	4
FAIR5-1	*Crurithyris planoconvexa*	w	NL/SL	1.8	n/a	-3.8	n/a	1	x	x	x	x	x	x	x	x	x
FAIR5-3	*Crurithyris planoconvexa*	w	NL/SL	2.1	0.19	-3.7	0.08	3	x	x	x	x	x	x	x	x	x
FAIR5-4	*Crurithyris planoconvexa*	w	SL	1.8	n/a	-3.9	n/a	1	x	x	x	x	x	x	x	x	x
FAIR5-5	*Crurithyris planoconvexa*	w	NL	1.7	0.23	-3.8	0.14	3	5.3	-	0.3	1.3	11.3	9.6	0.2	-	4
FAIR5-6	*Crurithyris planoconvexa*	w	SL/L	1.6	n/a	-3.5	n/a	1	10.5	-	0.5	1.3	14.9	11.4	-	-	4
GRR5A-1	*Crurithyris planoconvexa*	p	SL/NL	0.9	0.58	-4.3	0.05	2	6.9	-	0.3	1.2	21.6	12.8	0.2	-	4
GRR5A-2	*Crurithyris planoconvexa*	w	SL	1.5	n/a	-3.9	n/a	1	x	x	x	x	x	x	x	x	x
GRR5A-3	*Crurithyris planoconvexa*	w	SL	1.3	n/a	-4.3	n/a	1	7.1	-	0.4	1.4	15.3	11.2	0.9	0.3	4
GRR5A-4	*Crurithyris planoconvexa*	w	NL/SL	1.6	n/a	-4.3	n/a	1	5.6	-	0.4	1.6	15.4	12.7	0.2	0.3	4
GRRId-1	*Crurithyris planoconvexa*	w	NL/SL	1.3	0.22	-3.8	0.12	2	6.4	-	-	1.2	17.9	9.8	-	-	3
GRRId-2	*Crurithyris planoconvexa*	w	NL	1.7	0.02	-3.9	0.04	3	10.4	-	0.4	1.4	17.1	10.0	-	-	4
GRRId-3	*Crurithyris planoconvexa*	w	SL/NL	0.4	n/a	-4.7	n/a	1	x	x	x	x	x	x	x	x	x

Table 2 continued

Sample	Species	Fabric	L.C.	$\delta^{13}C$	±1σ	$\delta^{18}O$	±1σ	# of isotopic analyses	Trace element concentration (mmol/mol)								# of trace element analyses
									Mg	Fe	Mn	Sr	S	Na	Al	Si	
GRRId-5	*Crurithyris planoconvexa*	w	NL/SL	1.0	0.64	-3.9	0.46	3	8.8	-	-	1.7	14.6	10.9	-	-	4
GRRId-6	*Crurithyris planoconvexa*	p	NL/SL	1.5	n/a	-3.9	n/a	1	x	x	x	x	x	x	x	x	x
GRRId-7	*Crurithyris planoconvexa*	w	NL/SL	1.8	0.10	-4.1	0.02	3	6.6	-	0.3	1.6	13.9	11.0	-	0.2	4
GRRId-8	*Crurithyris planoconvexa*	w	NL/SL	2.1	n/a	-4.1	n/a	1	8.8	-	0.5	0.9	17.5	12.0	-	-	4
GRRId-9	*Crurithyris planoconvexa*	p	NL/SL	0.7	n/a	-4.7	n/a	1	x	x	x	x	x	x	x	x	x
GRRId-10	*Crurithyris planoconvexa*	w	SL	1.5	n/a	-3.8	n/a	1	x	x	x	x	x	x	x	x	x
GRRIIa-1	*Crurithyris planoconvexa*	w	NL/SL	1.6	0.05	-4.1	0.07	2	x	x	x	x	x	x	x	x	x
GRRIIa-4	*Crurithyris planoconvexa*	w	SL/NL	1.7	n/a	-4.3	n/a	1	x	x	x	x	x	x	x	x	x
GRRIIa-5	*Crurithyris planoconvexa*	w	SL/NL	1.3	n/a	-4.1	n/a	1	4.9	-	0.4	0.9	16.3	9.9	0.3	0.1	4
GRRIIa-8	*Crurithyris planoconvexa*	w	NL/SL	1.3	0.04	-4.2	0.12	3	7.6	-	-	1.2	17.2	8.9	0.2	-	4
GRRIIa-12	*Crurithyris planoconvexa*	w	NL/SL	1.8	n/a	-3.9	n/a	1	5.4	-	-	1.7	15.0	11.6	0.2	0.2	4
GRRVI-10	*Crurithyris planoconvexa*	w	L	0.3	0.50	-4.3	0.04	2	x	x	x	x	x	x	x	x	x

Matrix material is highly depleted and shows much greater variability in both $\delta^{13}C$ and $\delta^{18}O$ relative to shell specimens (Fig. 12). Two sampling transects were taken moving from the shell edge through successive generations of void-filling cement in specimens from the northeastern portion of the basin (western PA) to investigate trends in the isotopic composition of pore fluids through time (Fig. 13). Both transects show a systematic evolution from relatively heavy isotopic values within and near the shells, similar to those of other *Crurithyris* specimens, to very low $\delta^{13}C$ and $\delta^{18}O$ values.

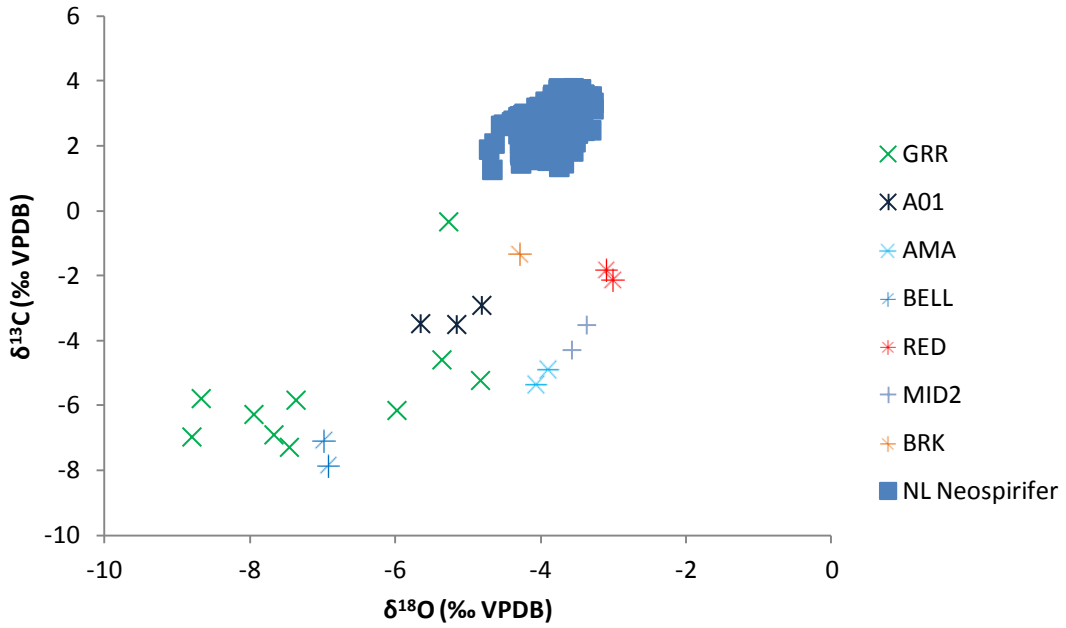

Figure 12 Isotopic composition of matrix material. Matrix $\delta^{13}C$ and $\delta^{18}O$ values are generally much lower and show a much greater degree of scatter than those of well-preserved ("NL") brachiopods. *Neospirifer* values are shown for comparison.

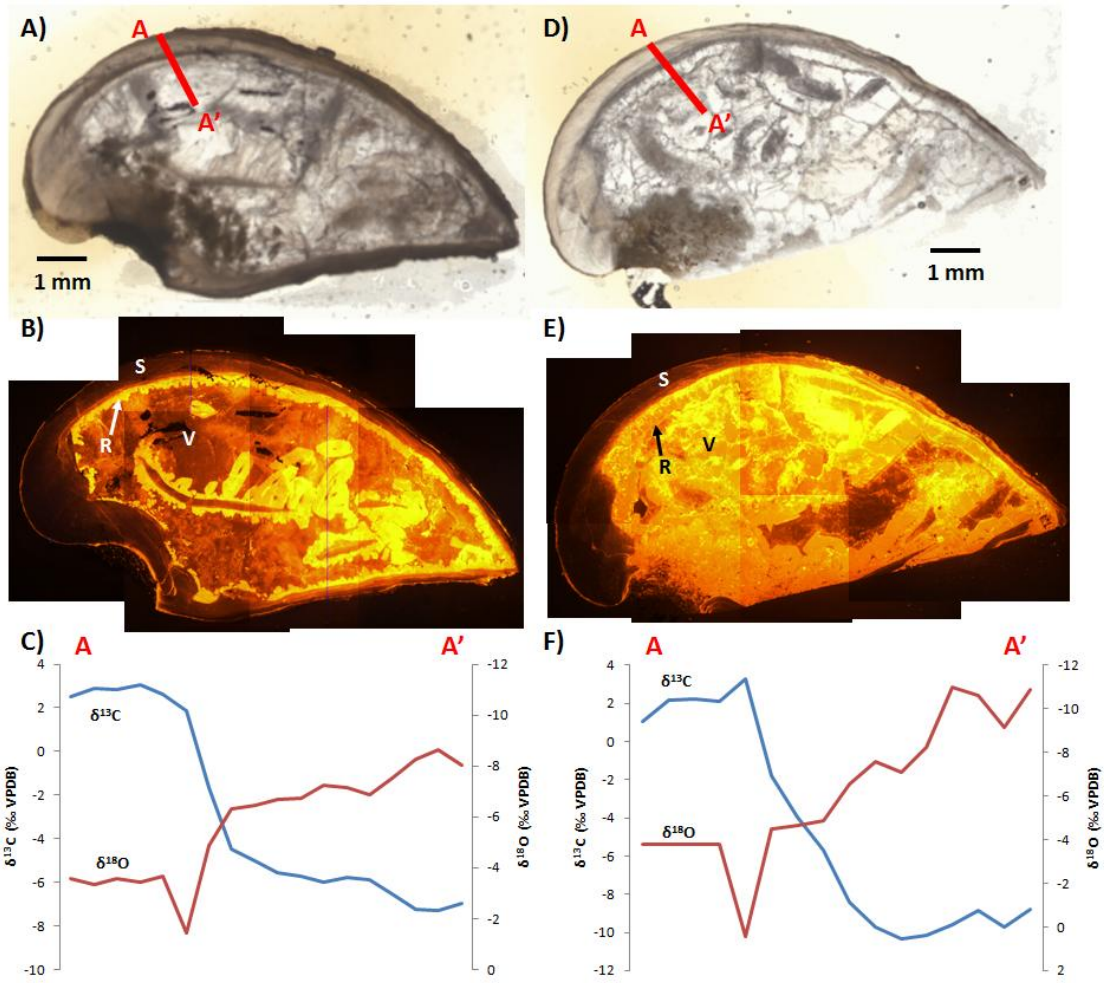

Figure 13 Chemical evolution of cement composition. **A)**, **D)** plane light and **B)**, **E)** cathodoluminescence images and **C)**, **F)** isotopic profiles through samples A01-3 and E01-3, respectively. $\delta^{13}C$ and $\delta^{18}O$ decrease progressively moving from the shell (S) through void-rimming cement (R) and finally into later-stage blocky void-filling cement (V). Exposure time on **B)** and **E)** is 10 s.

Figures 14-22 display the results of isotopic and trace element transects through several *Neospirifer* specimens. $\delta^{18}O$ of nonluminescent portions is essentially invariant within individual shells, generally changing by less than 0.5‰ and showing no systematic fluctuations. $\delta^{13}C$ varies by less than 1‰ in the well-preserved portions of

most specimens. All isotopic analyses of well-preserved portions of shells fall within a relatively narrow range of ~1‰ $\delta^{18}O$ and ~2‰ $\delta^{13}C$. $\delta^{18}O$ values are similar to those of *Crurithyris* but $\delta^{13}C$ values are on average 1-1.5‰ higher in *Neospirifer*. Unlike *Crurithyris*, *Neospirifer* specimens show no systematic regional trends in $\delta^{18}O$ across the basin. Fe, Mn, Al, and Si were generally below detection limits. S/Ca shows the greatest variability and highest concentrations of any trace element, with concentrations fluctuating by more than 4 mmol/mol within each sample. Na/Ca and Mg/Ca fluctuate by about 2 mmol/mol within individual samples, while Sr concentrations remain relatively constant near the detection limit. Na concentrations show a strong positive correlation with S; Mg shows no significant correlation with Na or S. There is no significant covariation between isotopic and trace element values except in the GRR 9 sample, where S concentrations correlate positively with $\delta^{13}C$.

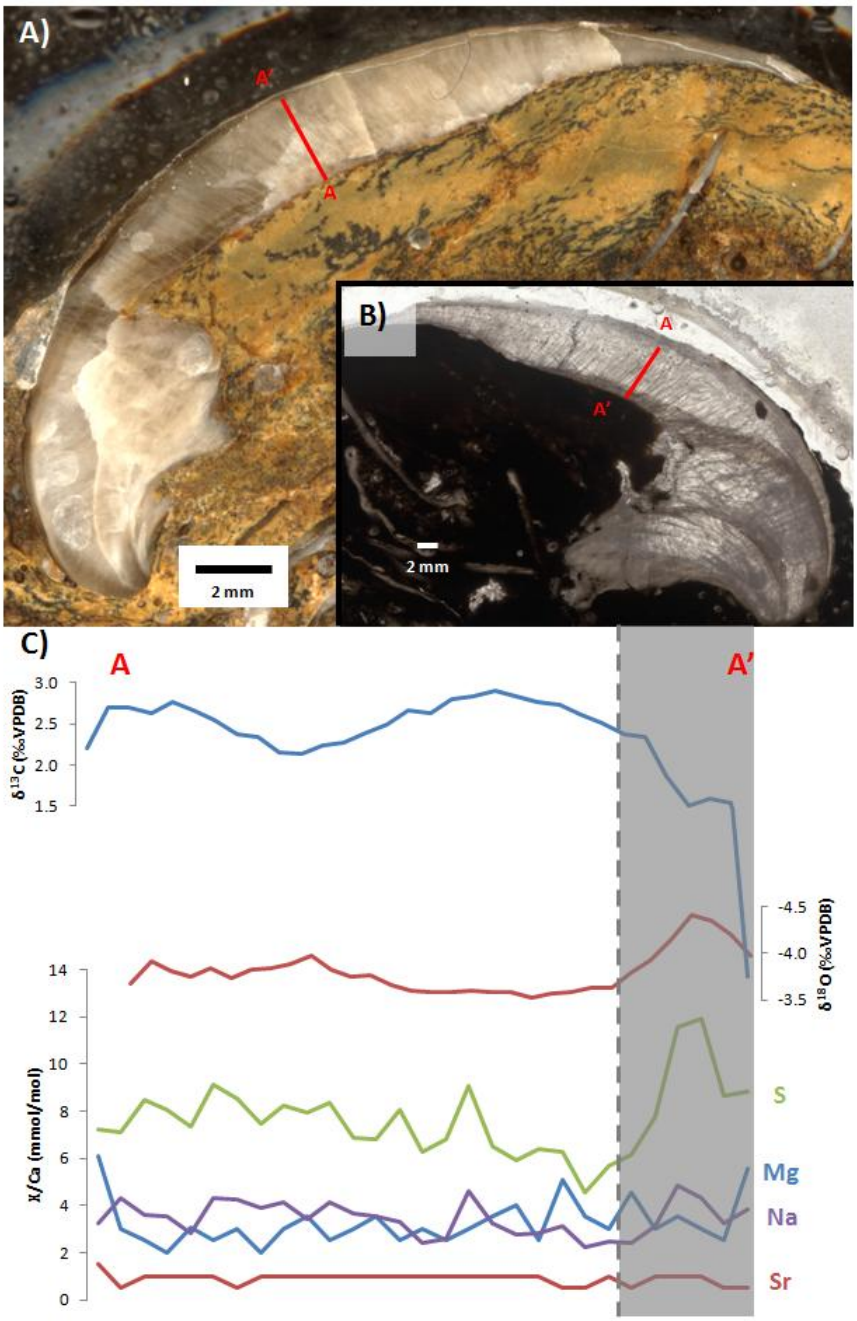

Figure 14 Geochemical seasonality data for sample GRR-1. **A)** is an image of the shell billet illustrating orientation of isotopic sampling transect; **B)** is a thin section image indicating the orientation of the corresponding trace element transect. **C)** shows plots of the data. The gray shaded region is slightly luminescent.

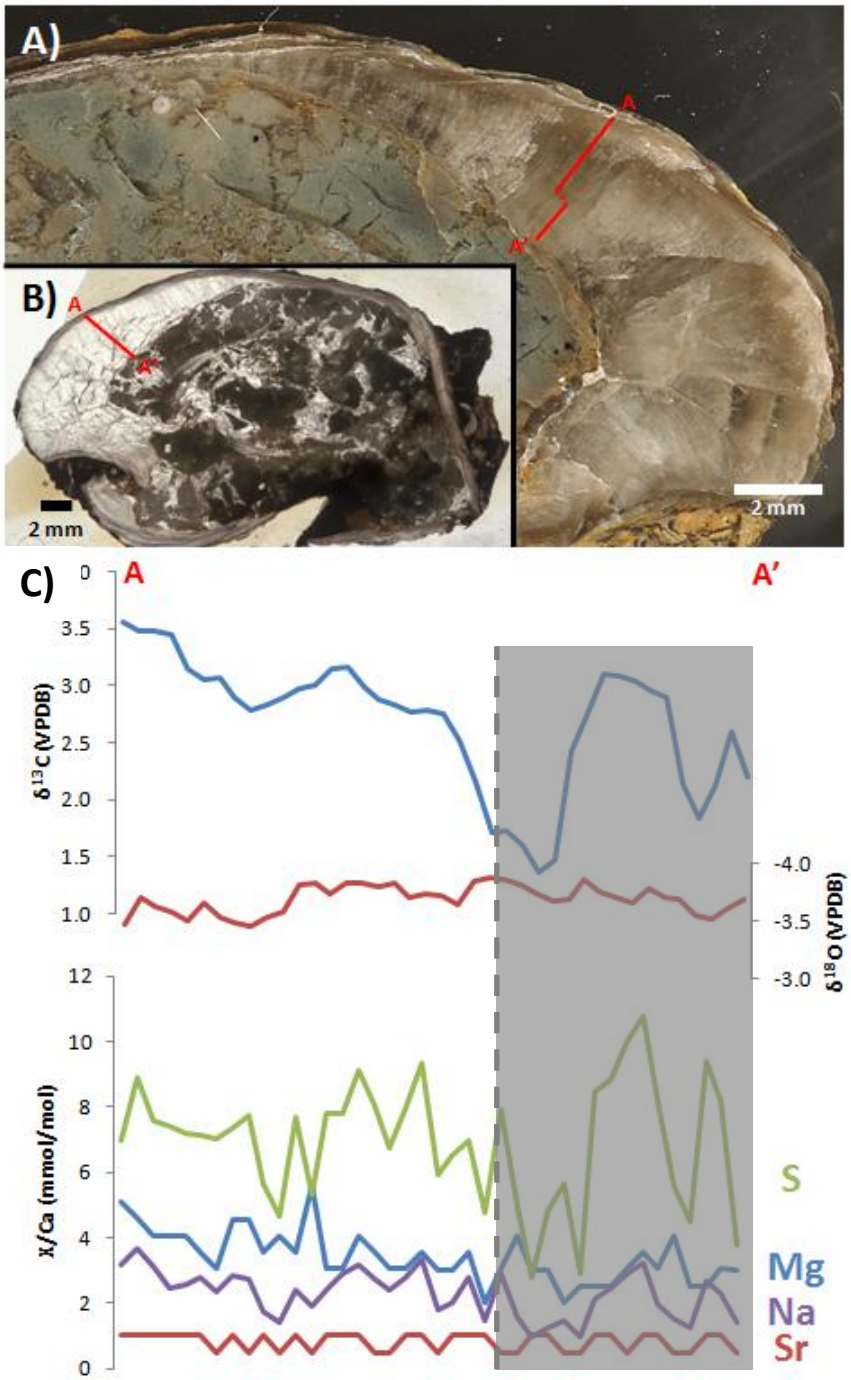

Figure 15 Geochemical seasonality data for sample GRR-9. **A)** is an image of the shell billet illustrating orientation of isotopic sampling transect; **B)** is a thin section image indicating the orientation of the corresponding trace element transect. **C)** shows plots of the data. Gray shaded region is slightly luminescent.

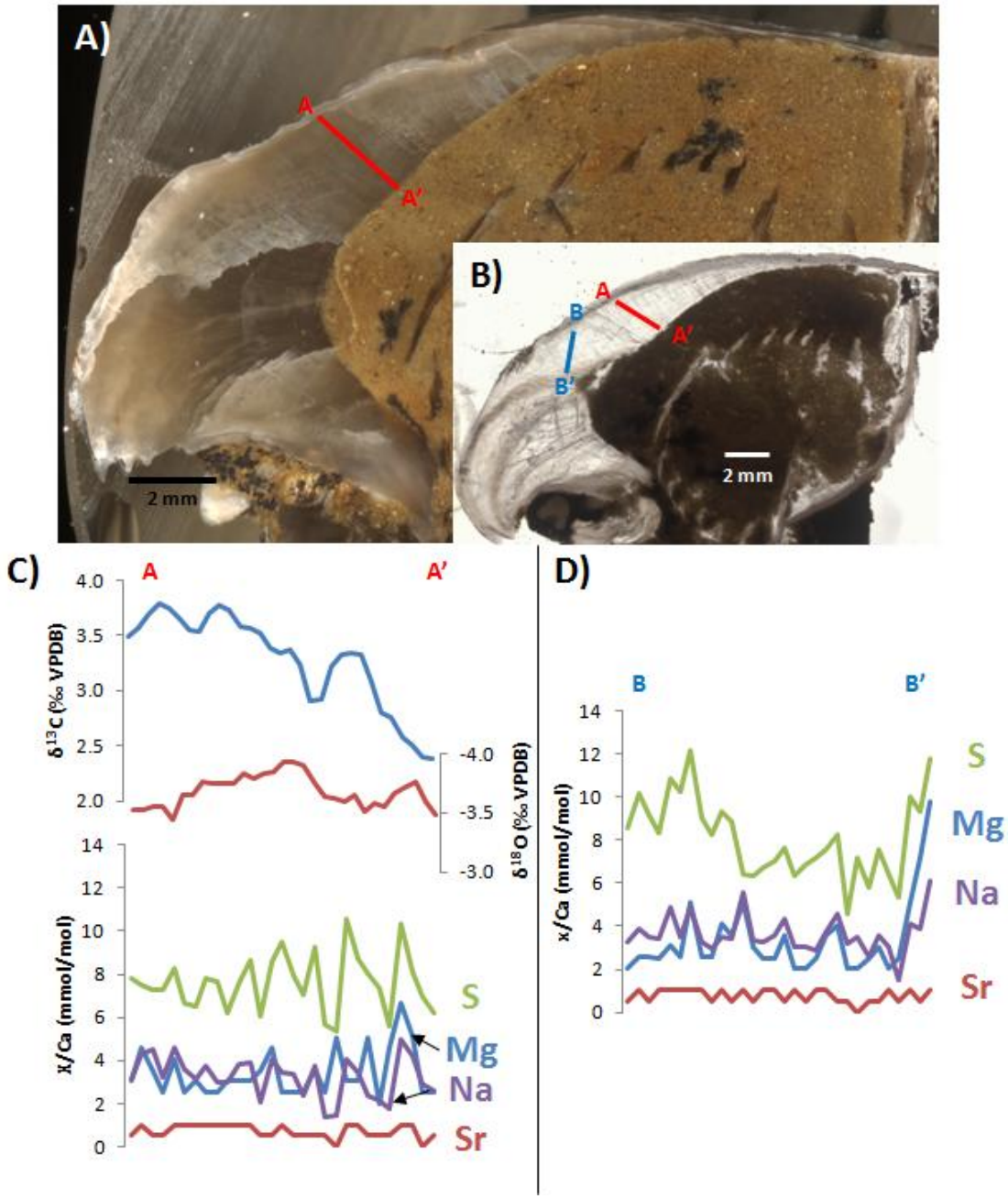

Figure 16 Geochemical seasonality data for sample MID2. **A)** is an image of the shell billet illustrating orientation of isotopic sampling transect. Two trace element transects were measured in the shell thin section, shown in **B)**. Transect A-A' corresponds to the isotopic sampling transect and is perpendicular to growth line set II; transect B-B' corresponds to growth line set I (see Fig. 10). **C)** and **D)** show plots of the data.

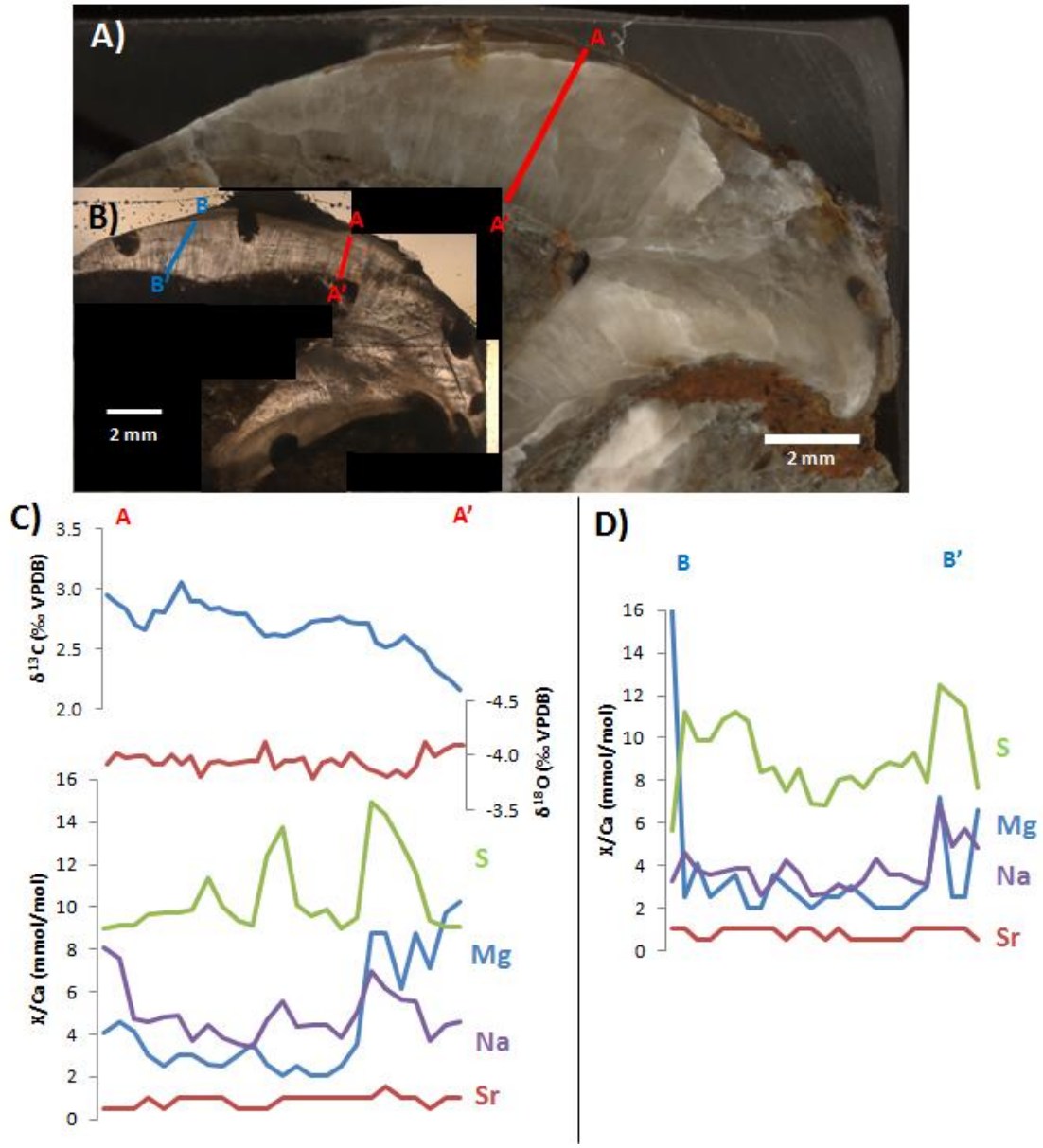

Figure 17 Geochemical seasonality data for sample BRK. **A)** is an image of the shell billet illustrating orientation of isotopic sampling transect. Two trace element transects were measured in the shell thin section, shown in **B)**. Transect A-A' corresponds most closely to the isotopic sampling transect and is growth line set I, although the line sets appear to have a different orientation in the billet and may have merged; transect B-B' corresponds most closely to growth line set II (see Fig. 10). **C)** and **D)** show plots of the data.

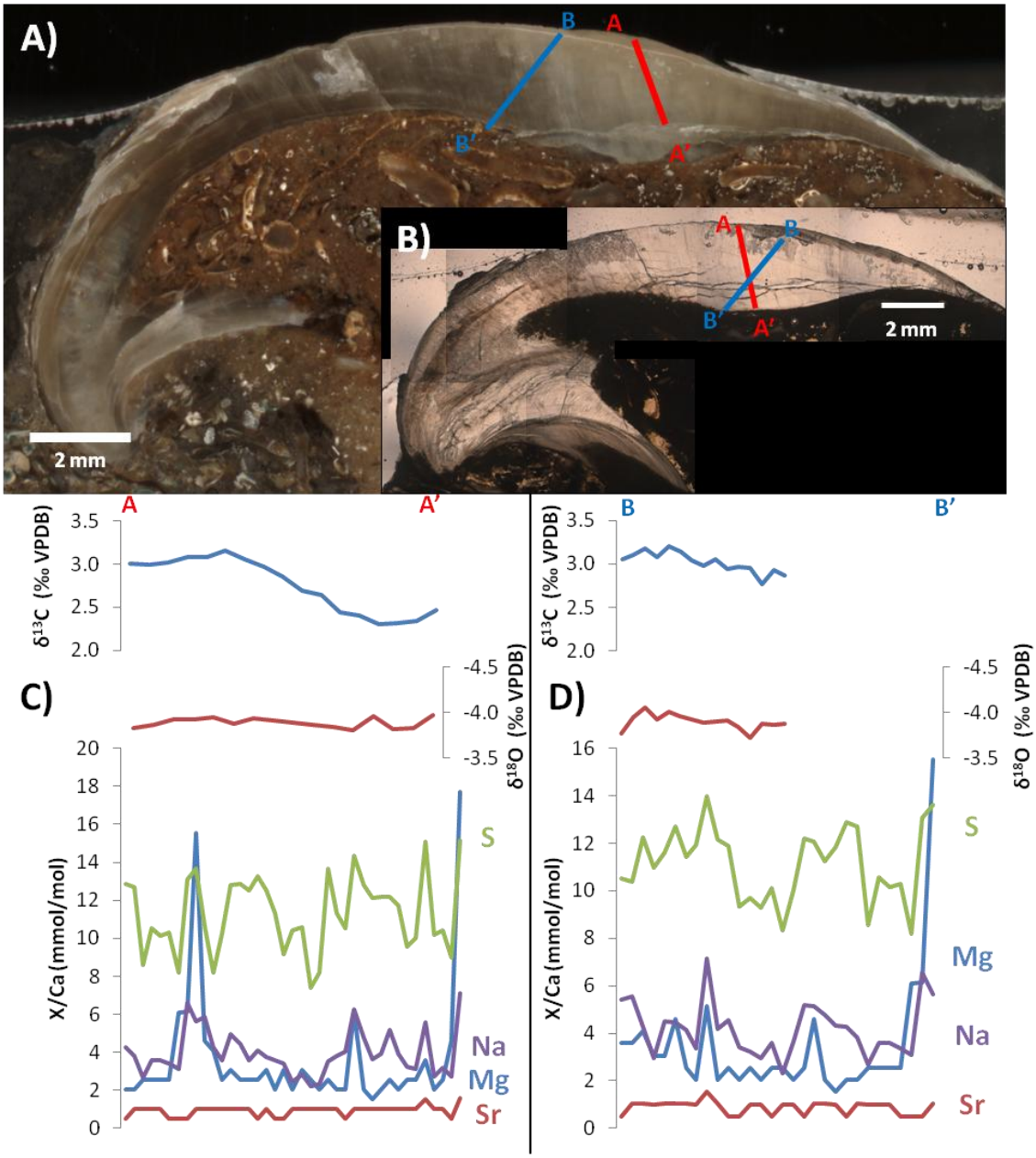

Figure 18 Geochemical seasonality data for sample TFF1. **A)** is an image of the shell billet illustrating orientation of the two isotopic sampling transects; **B)** shows the corresponding trace element transects in thin section. Transects A-A' and B-B' correspond to growth line sets II and I, respectively (see Fig. 10). **C)** and **D)** show plots of the data. Isotopic data were not reported for a portion of transect B-B' due to an instrument error.

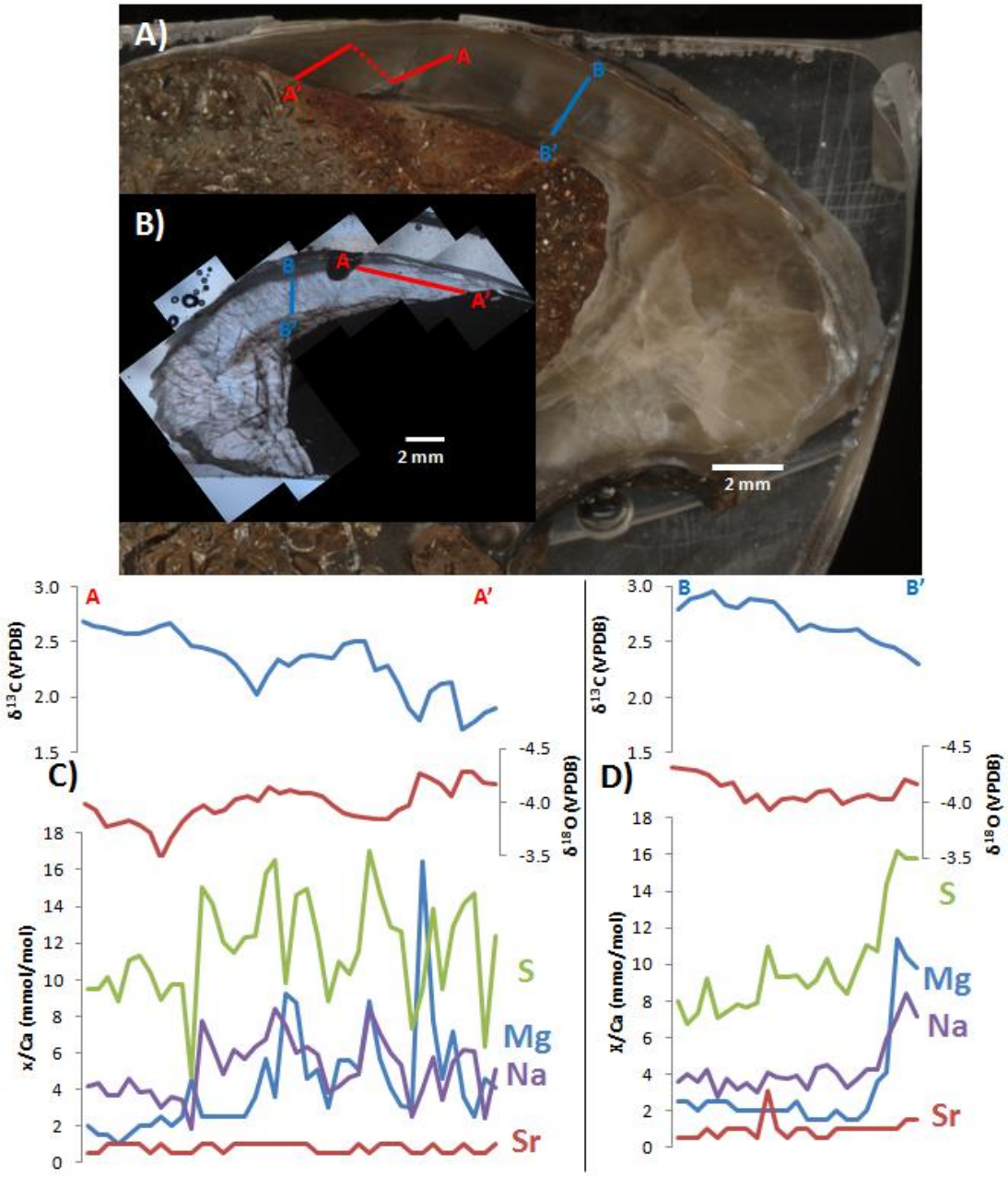

Figure 19 Geochemical seasonality data for sample TFF 2. **A)** is an image of the shell billet illustrating orientation of the two isotopic sampling transects; **B)** shows the corresponding trace element transects in thin section. Transects A-A' and B-B' correspond to growth line sets II and I, respectively (see Fig. 10). **C)** and **D)** show plots of the data.

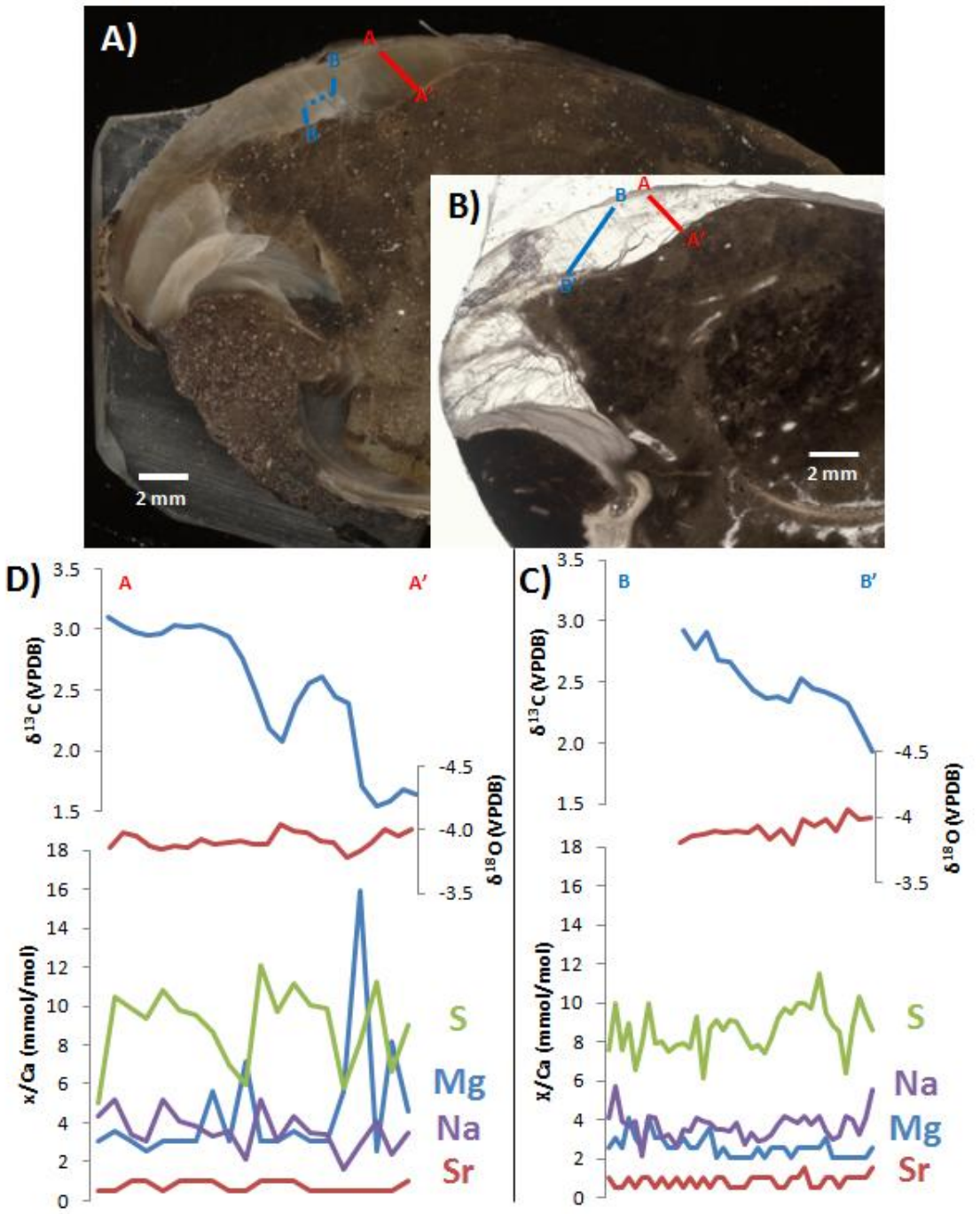

Figure 20 Geochemical seasonality data for sample Nn-3. **A)** is an image of the shell billet illustrating orientation of the two isotopic sampling transects; **B)** shows the corresponding trace element transects in thin section. Transects A-A' and B-B' correspond to growth line sets II and I, respectively (see Fig. 10). **C)** and **D)** show plots of the data. Isotopic data were not reported for part of the B-B' transect due to an instrument error.

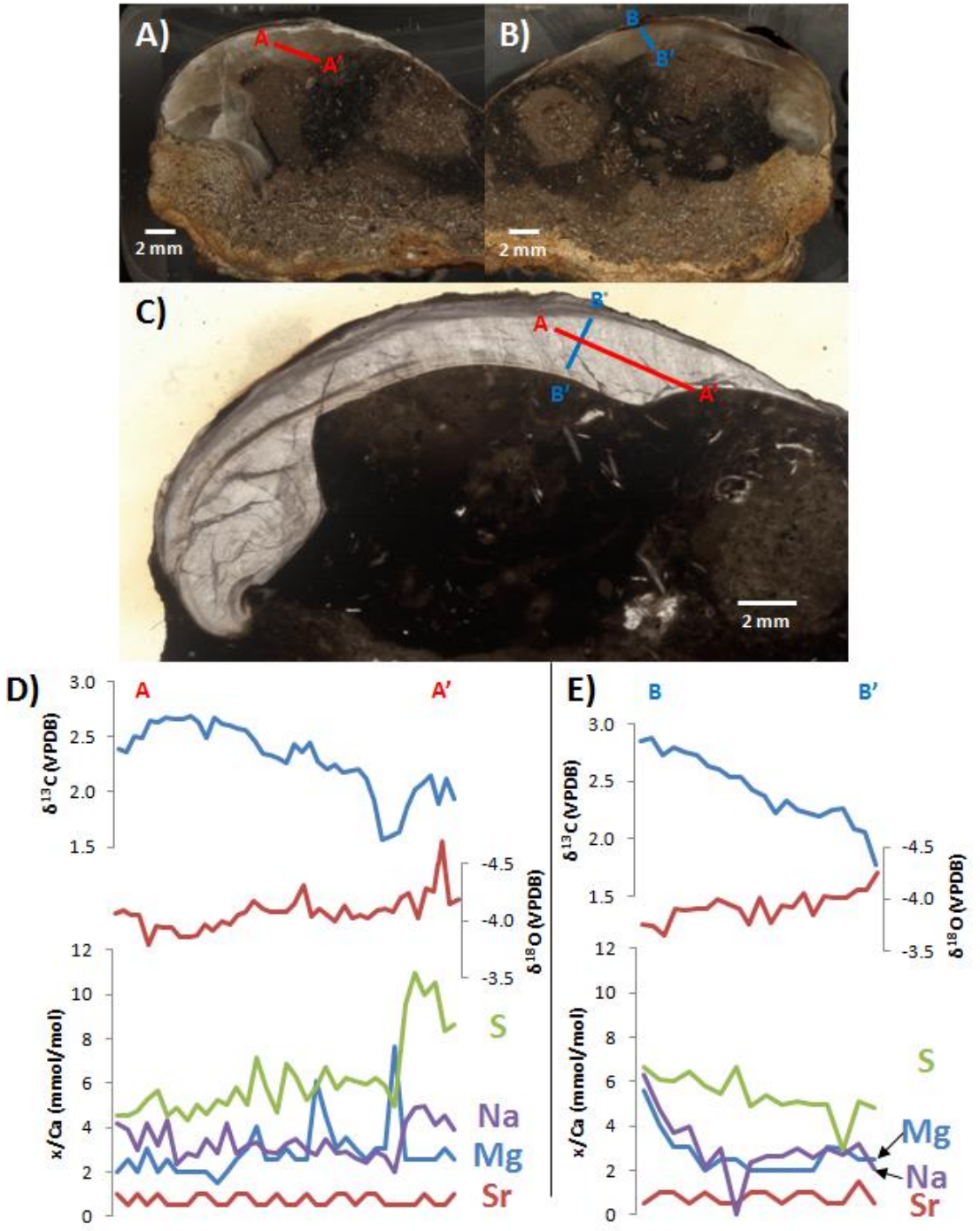

Figure 21 Geochemical seasonality data for sample CONC. **A)** and **B)** are images of the two opposing shell billet illustrating orientation of the two isotopic sampling transects; **C)** shows the corresponding trace element transects in thin section. Transects A-A' and B-B' correspond to growth line sets II and I, respectively (see Fig. 10). **D)** and **E)** show plots of the data.

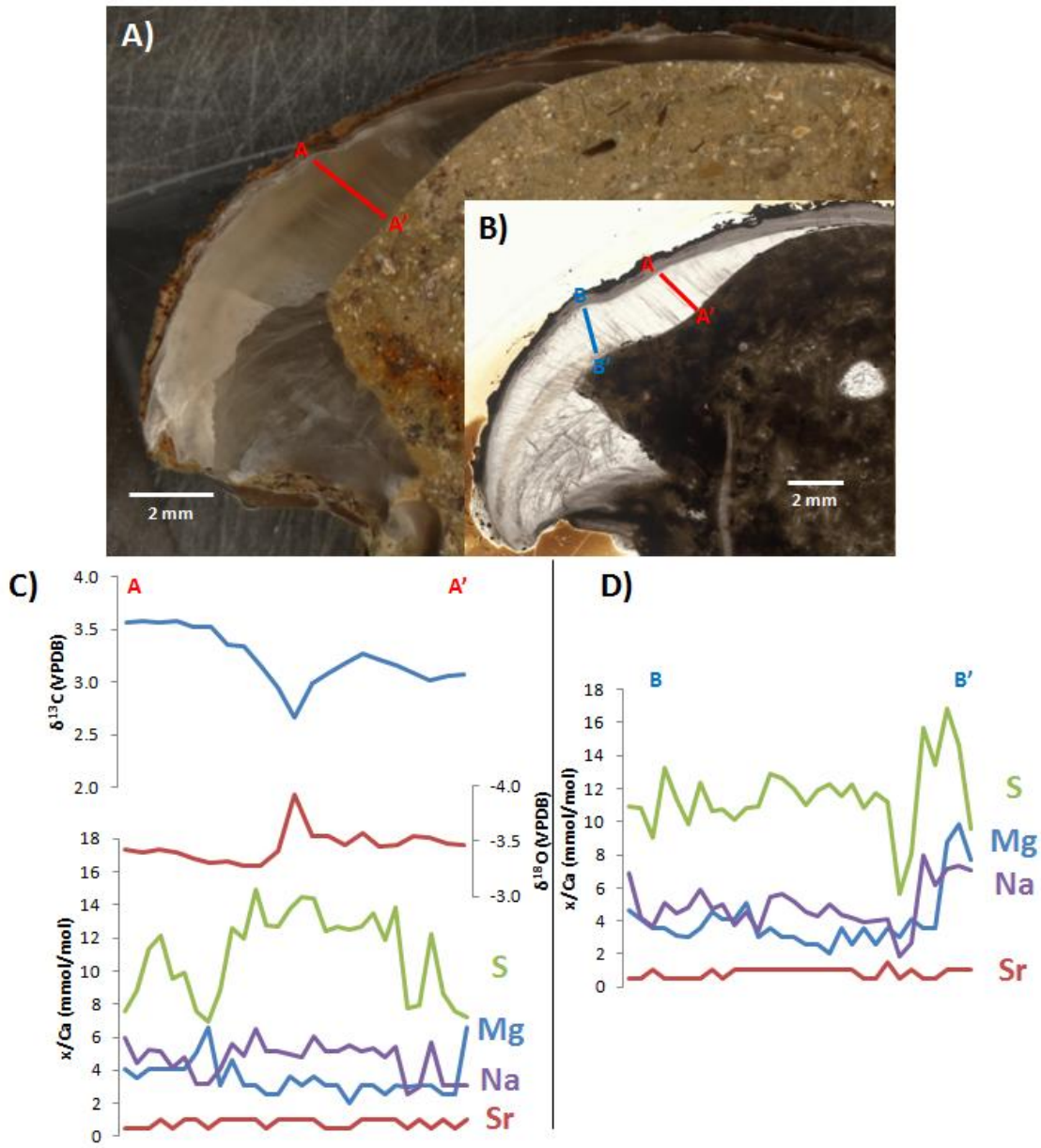

Figure 22 Geochemical seasonality data for sample RED. **A)** is an image of the shell billet illustrating orientation of the isotopic sampling transect. Two trace element transects were measured in the shell thin section, shown in **B)**. Transect A-A' corresponds to the isotopic sampling transect and growth line set II; transect B-B' corresponds most closely to growth line set II (see Fig. 10). **C)** and **D)** show plots of the data.

DISCUSSION

Spatial and temporal variability

The general trend toward lower $\delta^{13}C$ and $\delta^{18}O$ in well-preserved *Crurithyris* specimens approaching the eastern edge of the Appalachian Basin is consistent with a regional salinity gradient in the LPES resulting from Appalachian freshwater runoff, similar to the larger-scale gradient that Flake (2011) identified across the North American continent. This finding suggests the operation of a normal zonal climate regime, with the greatest rainfall along the equator (i.e. the low isotopic values on the eastern side of the basin). Additionally, the relatively low $\delta^{18}O$ variability throughout the GRR sections (Fig. 11c) indicates relatively homogeneous environmental conditions throughout the Ames interval. However, the anomalous values from site A01 hint at a more complicated picture. Interestingly, Flake (2011) documented similarly anomalous values in *Crurithyris* specimens from the FAIR locality. These samples are >1.5 ‰ higher in $\delta^{18}O$ than samples from either of the two horizons at the FAIR outcrop from which samples were recovered for this study (Fig. 11) and were likely collected from a different horizon. Flake (2011) attributed these values to evaporative enrichment during deposition, implying localized events of aridity. Evaporative influence is also the most probable explanation for the data from site A01 in this study. The universally low $\delta^{13}C$ and $\delta^{18}O$ values reported for luminescent matrix material (Fig. 12) and the general trend toward progressively lower isotopic values for subsequent generations of post-depositional cement (Fig. 13) demonstrate that it is highly unlikely that these anomalously high isotopic values are a product of diagenesis. Thus, the anomalously

high values reported in the A01 site in this study and at the FAIR site in Flake (2011) provide evidence for rare, episodic periods of net evaporation during the Ames interval, differing from the more typical dominance of everwet conditions during the maximum highstand (see discussion below on *Neospirifer* seasonality data). *Crurithyris* was an opportunistic species, colonizing the region during times of environmental flux or stress, such as varying salinity, and is clearly more widespread spatially in the basin than *Neospirifer* (Lebold and Kammer, 2006). Consequently, it is possible that *Crurithyris* populated the region during times of rapidly changing sea level and that these episodes of aridity may not reflect conditions during the highstand. Regardless, the majority of the regional data reflect a relatively moist climate in the Appalachian Basin region with few significant environmental perturbations.

Interannual variability

I contend that the isotopic and trace element data gathered from *Neospirifer* specimens represent an authentic paleoenvironmental signal. Diagenetic alteration is exceedingly unlikely due to the careful selection of nonluminescent, fabric-preserved, thick-shelled specimens and because serial sampling was conducted in tertiary layer prismatic calcite, the part of brachiopod shells most resistant to diagenesis (Grossman et al., 1996). Moreover, diagenesis generally increases chemical heterogeneity within individual shells (e.g. Grossman et al., 1996; Grossman et al., 2008), inconsistent with the nearly constant $\delta^{18}O$ record of these specimens. Although it is possible that the ~70 μm sample spacing was too coarse and aliased a much more variable signal, Mii and Grossman (1994) were able to identify well-defined seasonal cyclicity in a *Neospirifer*

specimen from the U. S. midcontinent using a much more widely-spaced grid of points, suggesting that this possibility is unlikely.

Serially-sampled *Neospirifer* shells show little systematic isotopic variation. Intra-shell $\delta^{18}O$ variability generally ranges from ~0.2‰ (RED, CONC, Nn-3, TFF1, BRK) to ~0.4‰ (MID2, GRR1, GRR9), with the TFF2 specimen showing a slightly greater range of 0.6‰, excluding the one aberrantly high (~-3.5‰) point. These variations are significant, much more than twice the average precision of 0.07‰, but are relatively minor, equivalent to fluctuations of less than 0.6‰ in seawater $\delta^{18}O$ or temperature variations of 1°C-3°C assuming constant seawater $\delta^{18}O$ using the paleotemperature equation of Hays and Grossman (1991, quadratic approximation of O'Neil et al., 1969). Oxygen isotope data thus suggest relatively little seasonal variability in the Appalachian Basin region during the Ames highstand. Moreover, there is no overall significant correlation between isotope and trace element signals (with the exception of $\delta^{13}C$ and S in the GRR 9 shell), further suggesting a lack of systematic seasonal changes in seawater chemistry. Similarly, Mg shows relatively low variability and no meaningful correlation with isotopic or other trace element values. Mg concentrations in biogenic calcite often co-vary with temperature (e.g. Klein et al., 1996; Rosenthal et al., 1997;), although admittedly the Mg/Ca paleothermometer is not clearly established in brachiopods (e.g. Perez-Huerta et al., 2008; Flake, 2011). Nevertheless, the relatively minor variability of Mg/Ca in these shells relative to specimens showing well-documented seasonality (cf. Mii and Grossman, 1994; Wang, 1998; Powell et al., 2009) supports a lack of significant intra-annual environmental change. Since it is

impossible to definitively identify seasonal cycles by correlating isotopic and trace element cyclicity, the total within-shell $\delta^{18}O$ range likely represents variability over several years rather than a single season. Consequently, the typical $\delta^{18}O$ seasonality may be less than the 0.2‰ to 0.4‰ total ranges, suggesting nearly invariant environmental conditions within a single year.

In contrast to Mg, S and Na concentrations in many shells show irregular fluctuations of similar magnitude to some of the smaller seasonal oscillations reported in Mii and Grossman (1994) and Wang (1998); additionally, Na and S are strongly positively correlated, a potential indication of seasonality (Grossman et al., 1996). However, neither Na nor S concentrations correlate with $\delta^{18}O$ or Mg/Ca, as would be expected if these patterns resulted from major changes in seawater temperature or chemistry during deposition (cf. Mii and Grossman, 1994; Grossman et al., 1996; Wang, 1998). Apparent covariation of Na and S could result from the presence of small, randomly distributed marine fluid inclusions in the shell matrix, similar to the Na^+ and SO_4^{2-}-rich inclusions in marine evaporates that are used to reconstruct ancient ocean chemistry (e.g. Brennan et al., 2013). Sulfur concentrations may also increase with increasing amounts of organic matrix in the shell structure (e.g. England et al., 2007). The lack of correlation with $\delta^{18}O$ and Mg suggests that fluctuations in the Na and S content of *Neospirifer* specimens were not caused by seasonal environmental change. If there was a seasonal component to this variability, the seasonality was too minor to affect the temperature (indicated by $\delta^{18}O$ and Mg/Ca) or the balance between freshwater input and evaporation in the basin (indicated by $\delta^{18}O$ and $\delta^{13}C$).

Combined with the lack of seasonality, relatively light $\delta^{18}O$ and $\delta^{13}C$ values suggest that everwet conditions prevailed year-round in the Appalachian Basin during this early Virgilian highstand. On average, $\delta^{18}O$ of well-preserved *Neospirifer* specimens in this study is over 1.5‰ less than that of coeval specimens from the Texas shelf, which experienced more direct exchange of water with the open ocean (cf. Grossman et al., 1993). Average $\delta^{13}C$ from this study is also somewhat lighter than the Texas values reported in Grossman et al. (1993). This finding is consistent with Flake (2011); that study documented a regional salinity gradient in the LPES, moving from the Midcontinent Basin (closest proximity to open ocean; near-marine $\delta^{18}O$, $\delta^{13}C$, and salinity) to the Appalachian Basin (greatest freshwater influence; lower $\delta^{18}O$, $\delta^{13}C$, and salinity; Flake, 2011). The salinity reduction was likely relatively minor, as the presence of *Neospirifer* indicates near-stenohaline conditions (e.g. Stevens, 1971), but was nevertheless sufficient to affect the isotopic composition of the water, reflecting a net surplus of precipitation and freshwater discharge entering this highly restricted basin throughout the year. If year-round evaporative conditions prevailed in such a setting, $\delta^{18}O$ of the water would be heavier than that of the open ocean, as in the modern Red Sea (e.g. Ganssen and Kroon, 1991). Taken together, the best explanation for this isotopic and trace element data is that this portion of central equatorial Pangea experienced little deviation from a tropical everwet climate throughout the Ames highstand, with minimal changes in the amount or source of rainfall throughout the year.

Paleoclimatic implications

The prevalence of moist equatorial climates during Carboniferous highstands is consistent with several independent lines of geological evidence. For instance, Falcon-Lang et al. (2009) and Falcon-Lang and DiMichele (2010) documented expansions of evermoist coal swamp floras during Pennsylvanian interglacial periods; in contrast, coniferous plants preferring seasonally dry conditions are more common in deposits associated with glacial periods. Sur et al. (2010) demonstrated a decrease in the silicate mineral fraction of low-latitude North American carbonates during interpreted interglacial periods, suggesting a diminished amount of airborne dust, an indicator of aridity, relative to glacial phases. Additionally, Kabanov et al. (2010) report numerous paleosols, interpreted to have formed during lowstand, with clear aridity indicators including calcrete in the Pennsylvanian cyclothems on the Russian Platform, implying that glacial phases were the most arid portions of the T-R cycle. Similarly, Olszewski and Patzkowsky (2003, 2008) support humid highstand systems tract intervals but more widely spread aridity during lowstand and transgressive systems tracts based on chemical evolution of paleosols towards increasingly calcic compositions at sequence boundaries (e. g. Miller et al., 1996) and alternations between carbonate and clastic depositional patterns in late Pennsylvanian cyclothems from the North American midcontinent. However, this climate association is disputed. Numerous other analyses of cyclothemic successions (e.g. Miller and West, 1993; Cecil et al., 2003) have suggested an arid highstand association. Eros et al. (2012), in particular, convincingly demonstrate that thick, laterally extensive coal deposits in the Donets Basin, Ukraine, formed during the late lowstand phase of fourth-order glacial cycles, indicating a humid-

lowstand association. To synthesize and interpret these seemingly divergent paleoenvironmental indicators, it is important to discuss the theoretical models for climatic-eustatic linkages.

The most prominent model for an arid-highstand teleconnection (e.g. Miller and West, 1993; Cecil et al., 2003) involves systematic changes in the strength of the Pangean monsoon coupled to variations in ice volume. There is a general consensus that large-scale monsoonal circulation ensued following the assembly of Pangea due to the supercontinent's large land area and relative symmetry about the equator (e.g. Kutzbach and Gallimore, 1989; Patzkowsky et al., 1991; Parrish, 1993; Tabor and Poulsen, 2008). Heating of the northern part of Pangea during northern hemisphere summer would create a large area of low pressure over this region, drawing the ITCZ northward; during southern hemisphere summer, the heating of the southern part of Pangea would pull the ITCZ southward by a similar process (Fig. 1; Parrish, 1993; Cecil et al., 2003; Tabor and Poulsen, 2008). This situation would break down normal Hadley-cell zonal circulation and result in seasonal aridity even near the equator (Parrish, 1993; Tabor and Poulsen, 2008). Miller and West (1993) and Cecil et al (2003) argue, though, that during Carboniferous glacial epochs, a large high pressure circulation cell above the southern hemisphere ice sheet would prevent these excursions by confining the ITCZ to a relatively narrow band around the equator. During interglacial times, the southern high pressure zone would be much smaller and weaker, permitting a climax of monsoonal conditions as the ITCZ undertook massive swings to the north and south. Data presented in this study, however, show that equatorial Pangea did not undergo the massive

seasonal changes that this conceptual model predicts during the early Virgilian highstand. Instead, conditions in the Appalachian Basin remained relatively moist throughout the year. Consequently, a different model is necessary to explain climate during this time.

One potential explanation for the absence of monsoonal conditions during the Late Pennsylvanian is the presence of the Central Pangean Mountains (CPM). Global climate model (GCM) simulations (Otto-Bleisner, 1993, 1998, 2003) indicate that Himalayan-scale equator-parallel mountains would have limited seasonal migration of the ITCZ by blocking cross-equatorial airflow, a major component of the monsoon (cf. Parrish, 1993). If the CPM were sufficiently high in the late Pennsylvanian, as some have suggested (e.g. Ziegler et al., 1985), they could have played an important role in maintaining year-round stability. Furthermore, their subsequent erosion may have helped establish more widespread arid, monsoonal conditions in the Permian (e.g. Tabor and Montañez, 2002). However, the hypothesis of the CPM acting as the primary control of fixing the ITCZ near the equator during highstands fails to account for evidence of seasonal or periodic aridity in this region during other parts of the T-R cycle, such as the well-documented desiccation structures in the paleosol immediately underlying the Ames (Joeckel, 1995) as well as the isotopic evidence of evaporative enrichment based on analyses of *Crurithyris* shells in this study and Flake (2011). The CPM likely played a role in limiting monsoonal circulation prior to the Permian, but these mountains did not completely prevent monsoonal conditions throughout all parts of the glacial-interglacial cycle.

Miller et al. (1996) proposed an alternative explanation for humid climate indicators during late Carboniferous interglacial periods, suggesting that monsoonal circulation was actually stronger during the late Pennsylvanian than in the early Permian. According to Miller et al. (1996), following the strong interglacial monsoon model of Miller and West (1993), late Pennsylvanian interglacial monsoons were strong enough to completely reverse the normal easterly trade wind flow and draw moisture in from the western margin of the supercontinent. This effect would have resulted in more humid conditions during interglacial times than during glacial maximums, when monsoons were somewhat weaker but still strong enough to produce seasonal aridity. Miller et al. (1996) further suggest that monsoon weakened in the Permian, resulting in a reversal of this pattern (i.e. glacial monsoons became so weak that they did not result in significant movement of the ITCZ and thus maintained humid tropics during lowstands). This explanation is an attempt to account for the fact that many cyclothemic studies promoting humid highstands (e.g. Tandon and Gibling, 1994) focus on Pennsylvanian strata, while others promoting an arid highstand association (e.g. Miller and West, 1993) are based on Permian sections. However, this hypothesis fails to account for the monsoon-retarding effect of the CPM, an effect that would have presumably weakened, not strengthened, into the Permian as the mountains eroded (e.g. Tabor and Montañez, 2002). Moreover, a comprehensive suite of paleoclimate indicators generally point to a progressively strengthening monsoonal regime moving from the late Carboniferous to the Triassic (e.g. Witzke, 1990; Parrish, 1993). Additionally, deposits from western Pangea show evidence for continued, and perhaps increased, aridity in the late

Pennsylvanian (e.g. Bishop et al., 2010), not the humid conditions that this model predicts. Even if a radically energized monsoon did provide year-round moisture to the region, the source and distance travelled by the precipitation would change when the monsoon reversed course annually. Such changes cause up to 2‰ fluctuations in $\delta^{18}O$ in modern meteoric watersheds of the Himalayas (Maurya et al., 2010) and likely would have influenced the isotopic composition of the restricted Ames seaway. Seasonal $\delta^{18}O$ data reported in this study, though, show no evidence for such a change. Finally, the regional freshwater gradient across the LPES during this highstand documented by Flake (2011) strongly suggests the prevalence of normal zonal atmospheric circulation. Freshwater influence decreased moving from the tropical Appalachian Basin further north into the then-subtropical latitudes of the Midcontinent Basin (Flake, 2011), consistent with normally-positioned Hadley circulation cells causing precipitation near the equator and net evaporation in the subtropics. Thus, the overall weight of paleoclimatic evidence suggests that Pangean monsoons were weakened, not strengthened, during the early Virgilian highstand.

A more conventional model is derived from the more recent analog of the last glacial maximum (LGM). During the LGM, increased ice volume caused the high pressure atmospheric circulation cells above the poles to expand, forcing the ITCZ to contract to a relatively narrow band around the equator and producing globally more arid conditions (Perlmutter and Matthews, 1992). Central equatorial Africa, which experiences a continental monsoon analogous to (albeit much weaker than) that inferred for Pangea, had a much drier climate during the LGM relative to the present due to a

weakened hydrologic cycle associated with lower temperatures and a greater portion of moisture being locked up as ice (Gasse, 2000). Applying this model to the late Carboniferous suggests that equatorial Pangea would have been more arid during glacial times and moister during interglacial times regardless of any orographic effects. This model is consistent with the data presented in this study, but fails to account for other lines of evidence suggesting arid highstands (e.g. Eros et al., 2012).

Olszweski and Patzkowsky (2003, 2008) invoked a related argument involving ITCZ contraction along with a rain shadow effect of the CPM to explain aridity during fifth-order lowstands in late Pennsylvanian cyclothems in the U.S. midcontinent. According to this scheme, expansion of the ITCZ during interglacials (following the LGM analog of Perlmutter and Matthews, 1992) allowed tropical moisture to flow around the eastern flank of the CPM, delivering moisture to central Pangea; during glacial periods, though, the eastern CPM entirely blocked the much narrower ITCZ at the edge of the continent (Fig. 23; Olszewski and Patzkowsky, 2003, 2008). A key feature of this model is that it implies only regional, not global, climate changes. The moist tropical airmass associated with the expanded ITCZ could have potentially bypassed more eastern regions of Pangea and allowed arid conditions to prevail during highstands in, for example, the Ukrainian region studied in Eros et al. (2012), while still producing the moist highstand association seen in this study for the Appalachian Basin region.

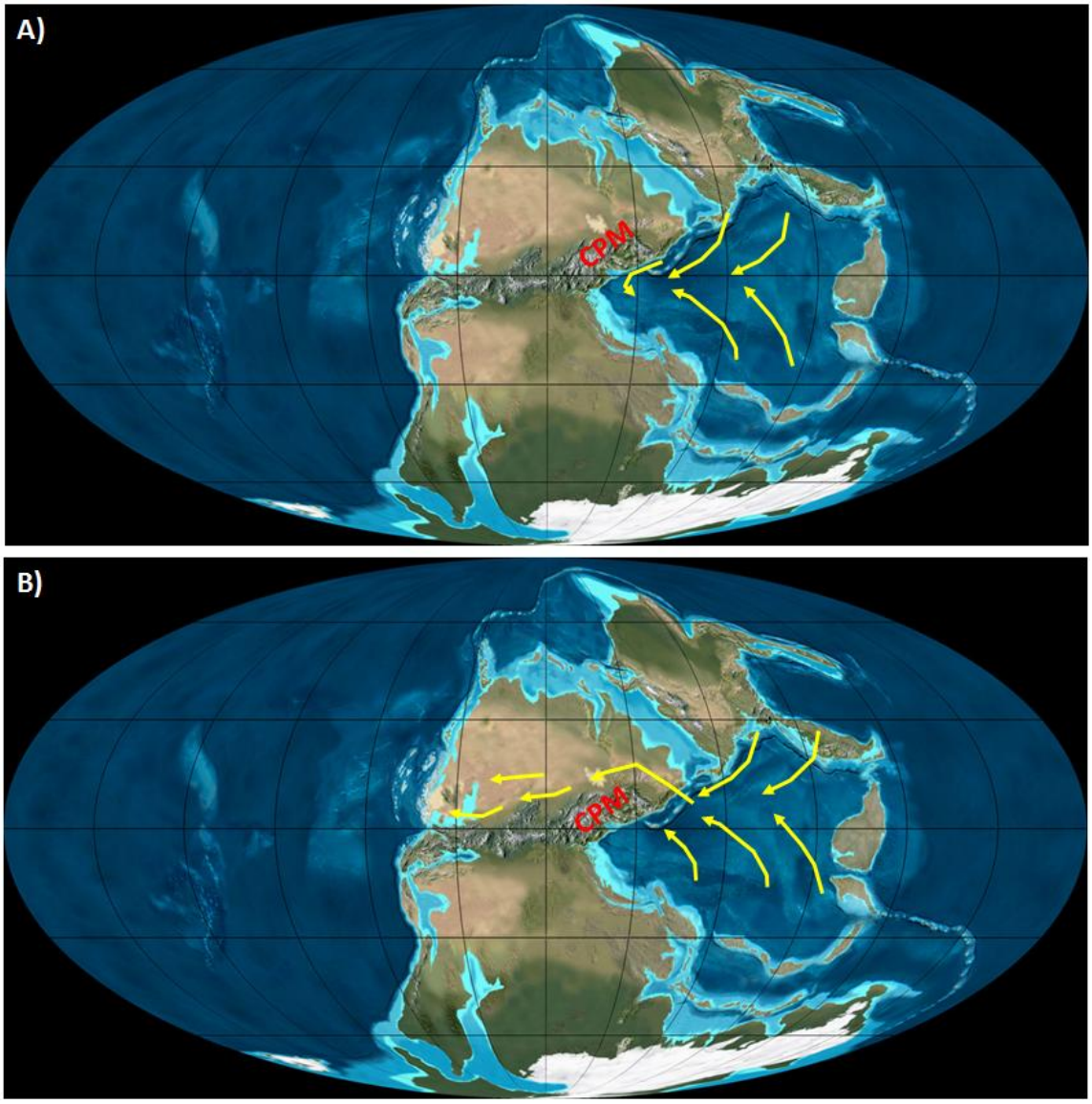

Figure 23 Model for late Carboniferous glacial-interglacial climate fluctuations proposed by Olszewski and Patzkowsky (2008). **A)** During glacial times, the ITCZ would contract, creating a rain shadow effect; the NE-SW trending arm of the Central Pangean Mountains (CPM) would block Tethyan moisture from reaching the continental interior. **B)** During interglacials, an expanded ITCZ would carry equatorial moisture around the CPM, bringing moist conditions to central Pangea. Figure concept modified from Olszewski and Patzkowsky (2008); paleogeographic background modified from Blakey (2013).

However, GCM simulations of early Permian times have suggested that any reduction in global ice volume would have led to drier conditions in central Pangea by reducing the pole-to-equator temperature gradient and leading to sluggish Hadley cell atmospheric circulation (Peyser and Poulsen, 2008). Given this suggestion's inconsistency with evidence presented in this study for everwet highstands and with the LGM analog, it is possible that the GCM improperly weighted the strength of this atmospheric sluggishness against other effects such as an invigorated hydrologic cycle driven by warmer temperatures (cf. Gasse, 2000).

Another possibility, though, is that there was a major changeover in the nature of climate-eustatic teleconnections between Carboniferous and Permian times, reversing the moist highstand association of the Late Pennsylvanian. Although the Miller et al. (1996) model for this change is inconsistent with the data reported in this study (see discussion above), other factors could have triggered such a reversal. Montañez et al. (2007), for instance, argued for rapidly rising CO_2 levels in the early Permian based on stable isotope analyses of soil and shallow marine carbonates and organic matter. GCM simulations in Peyser and Poulsen (2008) indicated that elevated CO_2 levels could exacerbate Pangean aridity. Montañez et al. (2007) suggest even further elevated pCO_2 during early Permian highstands relative to lowstand periods; furthermore, Montañez et al. (2007) documented trends toward more aridity-tolerant floral assemblages during early Permian interglacials, opposite of moist highstand flora association during the Pennsylvanian (e.g. Falcon-Lang et al., 2009; Falcon-Lang and DiMichele, 2010). Conceivably, these large-scale secular shifts in atmospheric pCO_2 moving into the

Permian could have altered the balance of mechanisms governing Earth's climatic response to Milankovitch forcing, although it is beyond the scope of this study to fully investigate this possibility. Such a change could potentially explain the direct evidence presented in this study for everwet tropical climates during Late Carboniferous interglacials without invalidating interpretations of arid highstands based on Permian sections (e.g. Miller and West, 1993; Miller et al., 1996). If such a climate reversal occurred, the late Pennsylvanian likely straddled these two climate regimes and thus could represent a key period of transition.

One final consideration is interaction between different orders of cyclicity. Cyclic changes in sea level have been documented on multiple timescales during the Permo-Carboniferous (Busch and Rollins, 1984), ranging from short-term (<100 kyr; Olszewski and Patzkowsky, 2003, 2008) to intermediate term (100 kyr- 400 kyr; Heckel, 1986; Eros et al., 2012) to longer-intermediate term (600 kyr – 1 myr) to long term (>1 myr; e.g. Eros et al., 2012) on top of the even longer-term, multi-myr tectonically driven cycles (e.g. Parrish, 1993; Tabor and Poulsen, 2008). Through time, these cycles may have interacted with each other, interfering constructively or destructively. In one potential manifestation of this effect, Bishop et al. (2010) used sedimentological evidence to argue that the late Carboniferous southern hemisphere glacier system did not behave as a single, unified ice sheet but rather as multiple independent ice bodies that waxed and waned asynchronously. Such a model implies that different glaciers responded with different intensities to the same climate forcing mechanisms. At any given time, for example, a smaller ice sheet might be melting while a larger glacier was

expanding; these processes would have competed for control of the overall global climate. Due to these types of interactions, cycles at different time scales may have presented radically different climate regimes. Thus, it may be possible that fifth order highstands, such as the Ames highstand of this study or the highstands associated with the meter-scale cycles of Olszewski and Patzkowsky (2003; 2008), were relatively humid while fourth-order highstands remained arid (e.g. Feldman et al., 2005; Eros et al., 2012).

Implications for sea circulation models

Extensive black shale deposits are a ubiquitous yet somewhat enigmatic feature of late Pennsylvanian cyclothems in North America. These strata record frequent episodes of dysoxic to anoxic conditions in the LPES (Algeo and Maynard, 2004; Algeo and Heckel, 2008) and were interpreted as deep water, offshore "core shales" by Heckel (1977). However, subsequent research has demonstrated that these deposits actually formed in relatively shallow water depths (10s of meters; e.g. Miller and West, 1993; Olszewski and Patzkowsky, 2003, 2008; Algeo and Heckel, 2008). Algeo et al. (2008) proposed the superestuarine circulation model to explain how the LPES was able to maintain low oxygen conditions despite its relatively shallow water depths and connection to the open ocean. According to this model, large volumes of tropical moisture entered the LPES as rainfall and runoff from the then-equatorial proto-Appalachian uplift. This influx of water formed a tongue of warm, reduced-salinity surface water above cooler, saline waters which advected into the LPES from the open ocean through two limited passageways to the west (Fig. 24; Algeo et al., 2008).

Westerly trade winds presumably caused upwelling and a resultant productivity boom along the west coast of Pangea, ultimately leading to an elevated oxygen minimum zone. Waters passing into the LPES from this area were thus "preconditioned" to low-oxygen conditions (Algeo and Heckel, 2008; Algeo et al., 2008). Density stratification resulting from the temperature and salinity differences between the upper and lower water masses in the LPES prevented the sea from overturning and mixing, ensuring that the underlying waters remained dysoxic (Algeo and Heckel, 2008; Algeo et al., 2008).

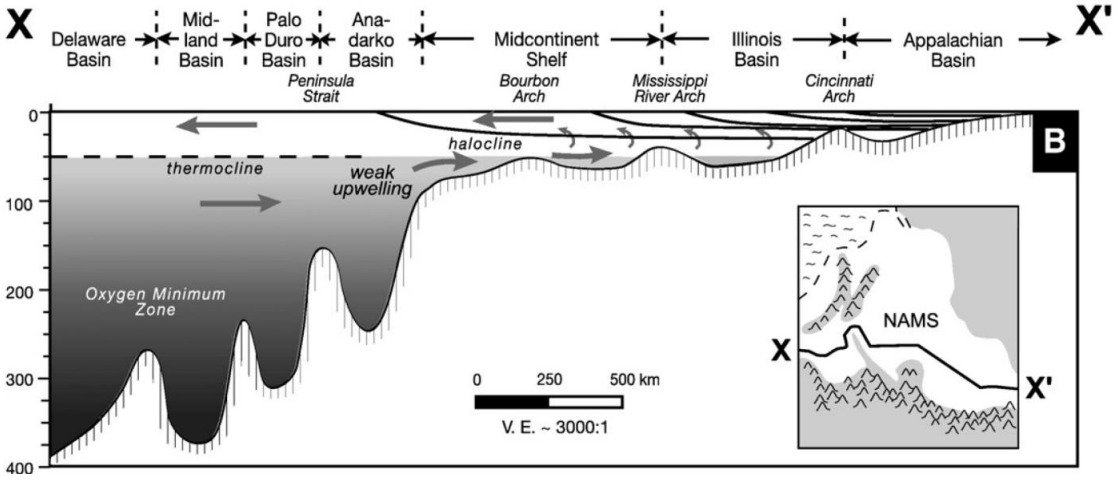

Figure 24 The superestuarine circulation model for maintaining anoxia in the LPES: large amounts of freshwater runoff from the proto-Appalachian mountains supposedly formed a warm, low-salinity tongue over saltier, cooler waters advecting in from the west. This effect created a stratified water column and prevented oxic surface waters from mixing with the lower, low-oxygen watermass. Figure from Algeo and Heckel (2008).

The superestuarine model faces some significant uncertainties. An inherent problem with superestuarine circulation is that there is no complete modern analog (Algeo et al., 2008), so it is essential to apply a variety of geologic tests and proxies to evaluate the model's feasibility. Another major criticism of this type of model has been

whether climate conditions could have sustained long-term water column stratification in the LPES. Tyson and Pearson (1991) argued that, over a sea the size of the LPES, winds would have had enough fetch to overturn the relatively shallow waters regardless of density stratification. Furthermore, Tyson and Pearson (1991) questioned whether estuarine-type models were even necessary to explain black shale in continental settings. Modern epicontinental seas can develop seasonal anoxia due to yearly phytoplankton blooms and seasonal lulls in wind strength and then later revert to oxic conditions in the winter when wind patterns become more vigorous and cause the sea to overturn and mix again. Such a situation could still result in high preservation of organic matter and an absence of benthic fauna, which would not have enough time to recolonize the seafloor between episodes of anoxia (Tyson and Pearson, 1991).

The lack of seasonality reported in this study has major implications for the viability of the superestuarine model. These data show no evidence of significant annual upwelling or turnover events, like those suggested by Tyson and Pearson (1991), and indicate a stable, high level of freshwater input throughout the year. Such conditions near the coastline could potentially have sustained a well-stratified water column and low oxygen conditions further offshore in the North American midcontinent. Furthermore, these results pinpoint fifth-order highstands as the most optimal time to establish such conditions, implying that black shales in the midcontinent were most likely deposited during these times. Heightened monsoonal conditions, including fluctuations in rainfall and wind patterns, would have made it more difficult to maintain this type of stratification during off-highstand times.

CONCLUSIONS

Serially sampled isotopic and trace element analyses of *Neospirifer* brachiopod shells from the Virgilian Ames Member in the Appalachian Basin provide direct evidence for a year-round moist climate in this paleo-tropical region during a Late Carboniferous highstand. $\delta^{18}O$ and $\delta^{13}C$ in well-preserved shells is >1‰ lighter than that of coeval specimens deposited in the open ocean, indicating relatively high levels of freshwater influence in this region, and neither isotope nor trace element data show evidence of major seasonal cyclicity, suggesting that this high freshwater influence was relatively constant throughout the year. Because of its environmental preferences, *Neospirifer* only colonized this marginal basin during the maximum highstand, when stenohaline conditions were established (Lebold and Kammer, 2006). This proxy is unique in that it provides a direct record of paleoclimate during highstand conditions, unlike other climate proxies such as coal, paleosols, or evaporites whose precise position in the transgressive-regressive cycle may be ambiguous. Analyses of *Crurithyris*, an opportunistic brachiopod that populated the basin during times of environmental variability, occasionally show anomalously high $\delta^{18}O$ and $\delta^{13}C$ values, likely reflecting episodic periods of net evaporation. Combined with evidence of seasonal aridity recorded in the paleosol directly underlying the Ames Member that formed during the early stages of this transgression (Joeckel, 1995), these results suggest that the climate of this paleo-equatorial region was most consistently moist during fifth-order highstands.

This conclusion contradicts some conceptual models of Pangean climate (e.g. Miller et al., 1993; Cecil et al., 2003) predicting that the supercontinental monsoon

reached its climax during highstands, resulting in widespread seasonal aridity. A moist highstand climatic association is also at odds with some GCM simulations (e.g. Peyser and Poulsen, 2008) which predict that diminished ice mass would lead to sluggish Hadley cell circulation and reduced rainfall over Pangea. The evidence of everwet conditions presented in this report indicates that the Pangean monsoon was either weak or completely not operating during the Ames highstand and further suggests that any reduction in atmospheric circulation due to decreases in ice volume was outweighed by a more energized interglacial hydrologic cycle, as is inferred to have occurred in equatorial Africa following the last glacial maximum (e.g. Gasse, 2000). The Central Pangean Mountains may have played a role in limiting monsoonal circulation by blocking cross-equatorial airflow (Otto-Bleisner, 1993, 1998, 2003), although the mountains clearly did not forestall monsoon development during all phases of the glacioeustatic cycle. Viable models for explaining this set of conditions include an expansion of the ITCZ during interglacial times, a partial modern analog based on climate following the last glacial maximum (e.g. Perlmutter and Matthews, 1991), as well as the related argument of Olszewski and Patzkowsky (2003, 2008) that expansion of the ITCZ during Carboniferous interglacials allowed tropical moisture to flow around the eastern flank of CPM, circumventing a rain shadow effect that prevailed during glacial times. Further research is necessary in other basins to determine whether moist highstands were a global phenomenon or a more localized regional occurrence. These results do not preclude the possibility that the nature of climate-eustatic connections may have changed drastically or even reversed in the Permian (e.g. Miller et al., 1996), nor

can this study exclude the operation of additional variables, such as the out-of-phase growth of multiple southern hemisphere ice sheets or changes in pCO_2 (e.g. Bishop et al., 2010; Montañez et al., 2012) that may have complicated climate patterns over longer time scales. Nevertheless, this evidence unambiguously demonstrates that the potential for perennially moist equatorial climates in central Pangea during highstands persisted until at least the latest Pennsylvanian and will serve as one critical calibration point for climate reconstructions of this waning phase of the Carboniferous icehouse.

REFERENCES

Adlis, D. S., Grossman, E. L., Yancey, T. E., and McLerran, D., 1988, Isotope stratigraphy and paleodepth changes of Pennsylvanian cyclical sedimentary deposits: Palaios, v. 3, no. 5, p. 487-506.

Algeo, T. J., and Heckel, P. H., 2008, The Late Pennsylvanian Midcontinent Sea of North America: A review: Palaeogeography, Palaeoclimatology, Palaeoecology, v. 268, no. 3-4, p. 205–221.

Algeo, T. J., and Maynard, J. B., 2004, Trace-element behavior and redox facies in core shales of Upper Pennsylvanian Kansas-type cyclothems: Chemical Geology, v. 206, no. 3-4, p. 289-318.

Algeo, T. J., Heckel, P. H., Maynard, J. B., Blakey, R. C., and Rowe, H., 2008, Modern and ancient epeiric seas and the super-estuarine model of marine anoxia *in* Holmden, C., and Pratt, B. R., eds., Dynamics of epeiric seas: sedimentological, paleontological, and geochemical perspectives: Geological Association of Canada Special Publication, v. 48, p. 7-38.

Al-Qayim, B. A., 1983, Facies and depositional environment of the Ames marine member (Virgilian) of the Conemaugh Group (Pennsylvanian) in the Appalachian Basin [PhD. thesis]: University of Pittsburgh, 306 p.

Angiolini, L., Jadoul, F., Leng, M. J., Stephenson, M. H., Rushton, J., Chenery, S., and Crippa, Gaia, 2009, How cold were the Early Permian glacial tropics? Testing sea-surface temperature using the oxygen isotope composition of rigorously screened brachiopod shells: Journal of the Geological Society, v. 166, p. 933-945.

Angiolini, L., Stephenson, M., Leng, M., J., Jadoul, F., Millward, D., Aldridge, A., Andrews, J., Chenery, S., and Williams, G., 2012, Heterogeneity, cyclicity and diagenesis in a Mississippian brachiopod shell of palaeoequatorial Britain: Terra Nova, v. 24, v. 1, p. 16-26.

Barbin, V., 2000, Cathodoluminescence of carbonate shells: biochemical versus diagenetic process *in* Pagel, M., Barbin, V., Philippe, B., and Ohnenstetter, D., eds., Cathodoluminescence in Geosciences: Berlin, Springer, p. 303-329.

Barbin, V., and Gaspard, D., 1995, Cathodoluminescence of recent articulate brachiopod shells: Implications for growth stages and diagenesis evaluation: Journal Geobios, Mémoire Spécial, v. 18, p. 39-45.

Bishop, J. W., Montañez, I. P., and Osleger, D. A., 2010, Dynamic Carboniferous climate change, Arrow Canyon, Nevada: Geosphere, v. 6, no. 1, p. 1-34.

Brand, U. and Veizer, J., 1980, Chemical diagenesis of a multicomponent carbonate system: trace elements: Journal of Sedimentary Petrology, v. 50, no. 4, p. 1219-1236.

Brand, U., 2004, Carbon, oxygen, and strontium isotopes in Paleozoic carbonate components: an evaluation of original seawater-chemistry proxies: Chemical Geology, v. 204, no. 1-2, p. 23-44.

Brennan, S. T., Lowenstein, T. K., and Cendón, D. I., 2013, The major-ion composition of Cenozoic seawater: the past 36 million years from fluid inclusions in marine halite: American Journal of Science, v. 313, no. 8, p. 713-775.

Brezinski, D. K., 1983, Developmental model for an Appalachian Pennsylvanian marine incursion: Northeastern Geology, v. 5, no. 2, p. 92-99.

Bruckschen, P., Oesmann, S., and Veizer, J., 1999, Isotope stratigraphy of the European Carboniferous: proxy signals for ocean chemistry, climate, and tectonics: Chemical Geology, v. 161, no. 1-3, p. 127-163.

Buening, N., and Spero, H. J., 1996, Oxygen- and carbon-isotope analyses of the articulate brachiopod *Laqueus californianus*: a recorder of environmental changes in the subeuphotic zone: Marine Biology, v. 127, no. 1, p. 105-114.

Busch, R. M., and Rollins, H. B., 1984, Correlation of Carboniferous strata using a hierarchy of transgressive-regressive units: Geology, v. 12, no. 8, p. 471-474.

Cecil, B., 1990, Paleoclimate controls on stratigraphic repetition of chemical and siliciclastic rocks: Geology, v. 18, no. 6, p. 533-536.

Cecil, C. B., Dulong, F. T., West, R. R., Stamm, R., Wardlaw, B., Edgar, N. T., 2003, Climate controls on the stratigraphy of a Middle Pennsylvanian cyclothem in North America *in* Climate controls on stratigraphy, SEPM Special Publication, v. 77, p. 151-180.

Crowley, T. J., Yip, K. J., and Baum, S. K., 1993, Milankovitch cycles and Carboniferous climate: Geophysical Research Letters, v. 20, no. 12, p. 1175-1178.

Davydov, V. I., Crowley, J. L., Schmitz, M. D., and Poletaev, V. I., 2010, High-precision U-Pb zircon age calibration of the global Carboniferous time scale and Milankovitch band cyclicity in the Donets Basin, eastern Ukraine: Geochemistry, Geophysics, Geosystems, v. 11, no. 1, 22 p.

Denison, R. E., Koepnick, R. B., Fletcher, A., Howell, M. W., and Calloway, W. S., 1994, Criteria for retention of original seawater $^{87}Sr/^{86}Sr$ in ancient limestones: Chemical Geology, v. 140, no. 1-2, p. 132-143.

Dettman, D. L., and Lohmann, K. C., 1995, Microsampling carbonates for stable isotope and minor element analysis: Physical separation of samples on a 20 micrometer scale: Journal of Sedimentary Research, v. 65, no. 3, p. 566-569.

Donahue, J., and Rollins, H. B., 1977, Paleoecological anatomy of a Conemaugh (Pennsylvanian) marine incursion in Briggs, G., ed., Carboniferous of the southeastern United States: Geological Society of America Special Paper, v. 148, p. 153-170.

England, J., Cusack, M., and Lee, M. R., 2007, Magnesium and sulphur in the calcite shells of two brachiopods, *Terebratulina retusa* and *Novocrania anomala*: Lethaia, v. 40, no. 1, p. 2-10.

Eros, J. M., Montañez, I. P., Osleger, D. A., Davydov, V. I., Nemyrovska, T. I., Poletaev, V. I., and Zhykalyak, M. V., 2012, Sequence stratigraphy and onlap history of the Donets Basin, Ukraine: Insight into Carboniferous icehouse dynamics: Palaeogeography, Palaeoclimatology, Palaeoecology, v. 313-314, p. 1-25.

Fahrer, T. R., 1996, Stratigraphy, petrography and paleoecology of marine units within the Conemaugh Group (Upper Pennsylvanian) of the Appalachian Basin in Ohio, West Virginia, and Pennsylvania [PhD. Thesis]: Iowa City, The University of Iowa, 298 p.

Falcon-Lang, H. J., and DiMichele, W. A., 2010, What happened to the coal forests during Pennsylvanian glacial phases?: Palaios, v. 25, no. 9, p. 611-617.

Falcon-Lang, H. J., Nelson, W. J., Elrick, S., Looy, C. V., Ames, P. R., and DiMichele, W. A., 2009, Incised channel fills containing conifers indicate that seasonally dry

vegetation dominated Pennsylvanian tropical lowlands: Geology, v. 37, no. 10, p. 923-926.

Feldman, H. R., Franseen, E. K., Joeckel, R. M., and Heckel, P. H., 1995, Impact of longer-term modest climate shifts on architecture of high-frequency sequences (cyclothems), Pennsylvanian of the midcontinent, U.S.A.: Journal of Sedimentary Research, v. 75, no. 3, p. 350-368.

Flake, R. C., 2011, Circulation of North American epicontinental seas during the Carboniferous using stable isotope and trace element analyses of brachiopod shells [M.S. Thesis]: College Station, Texas A&M University, 63 p.

Ganseen, G., and Kroon, D, 1991, Evidence for Red Sea surface circulation from oxygen isotopes of modern surface waters and planktonic foraminiferal tests: Paleoceanography, v. 6, no. 1, p. 73-82.

Gasse, F., 2000, Hydrological changes in the African tropics since the Last Glacial Maximum: Quaternary Science Reviews, v. 19, no. 1-5, p. 189-211.

Götze, J., 2002, Potential of cathodoluminescence (CL) microscopy and spectroscopy for the analysis of minerals and materials: Analytical and Bioanalytical Chemistry, v. 374, no. 4, p. 703-708.

Götze, J., and Kempe, U., 2008, A comparison of optical microscope- and scanning electron microscope-based cathodoluminescence (CL) imaging and spectroscopy applied to geosciences: Mineralogical Magazine, v. 72, no. 4, p. 909-924.

Grossman, E. L., Mii, H. S., and Yancey, T. E., 1993, Stable isotopes in Late Pennsylvanian brachiopods from the United States: Implications for Carboniferous paleoceanography: Geological Society of America Bulletin, v. 105, no. 10, p. 1284-1296.

Grossman, E. L., Mii, H. S., Zhang, C., and Yancey, T. E., 1996, Chemical variation in Pennsylvanian brachiopod shells–diagenetic, taxonomic, microstructural, and seasonal effects: Journal of Sedimentary Research, v. 66, no. 5, p. 1011-1022.

Grossman, E. L., Yancey, T. E., Jones, T. E., Bruckschen, P., Chuvashov, B., Mazzullo, S. J., and Mii, H. S., 2008, Glaciation, aridification, and carbon sequestration in the Permo-Carboniferous: The isotopic record at low latitudes: Palaeogeography, Palaeoclimatology, Palaeoecology, v. 268, no. 3-4, p. 222-233.

Hays, P.D., and Grossman, E.L., 1991, Oxygen isotopes in meteoric and calcite cements and indicators of continental paleoclimate: Geology, v. 19, p. 441-444.

Heckel, P. H., 1977, Origin of phosphatic black shale facies in Pennsylvanian cyclothems of mid-continent North America: American Association of Petroleum Geologists Bulletin, v. 61, no. 7, p. 1045-1068.

Heckel, P. H., 1986, Sea-level curve for Pennsylvanian eustatic marine transgressive-regressive depositional cycles along midcontinent outcrop belt, North America: Geology, v. 14, no. 4, p. 330-334.

Heckel, P. H., 2002, Observations and constraints on radiometric dating of the Pennsylvanian succession in North America and its correlation with dates from Europe: Newsletter on Carboniferous Stratigraphy, v. 20, p. 10-14.

Hiller, N., 1988, The development of growth lines on articulate brachiopods: Lethaia, v. 21, no. 2, p. 177-188.

Joeckel, R. M., 1995, Paleosols below the Ames marine unit (Upper Pennsylvanian, Conemaugh Group) in the Appalachian Basin, U.S.A.: variability on an ancient depositional landscape: Journal of Sedimentary Research, v. A65, no. 2, p. 393-407.

Kabanov, P. B., Alekseeva, T. V., Alekseeva, V. A., Alekseev, A. O., and Gubin, S. V., 2010, Paleosols in late Moscovian (Carboniferous) marine carbonates of the east European craton revealing "great calcimagnesian plain" paleolandscapes: Journal of Sedimentary Research, v. 80, no. 3, p. 195-215.

Klein, R. T., Lohmann, K. C., and Thayer, C. W., 1996, Bivalve skeletons record sea-surface temperature and $\delta^{18}O$ via Mg/Ca and $^{18}O/^{16}O$ ratios: Geology, v. 24, no. 5, p. 415-418.

Kutzbach, J. E., and Gallimore, R. G., 1989, Pangaean Climates: Megamonsoons of the Megacontinent: Journal of Geophysical Research, v. 94, no. D3, p. 3341-3357.

Laya, J. C., Tucker, M. E., Gröcke, D. R., and Perez-Huerta, A., 2013, Carbon, oxygen, and strontium isotopic composition of low-latitude Permian carbonates (Venezuelan Andes): climate proxies of tropical Pangea: Geological Society, London, Special Publications, v. 376, p. 367-385.

Lebold, J. G., and Kammer, T. W., 2006, Gradient analysis of faunal distributions associated with rapid transgression and low accommodation space in a Late

Pennsylvanian marine embayment: Biofacies of the Ames Member (Glenshaw Formation, Conemaugh Group) in the northern Appalachian Basin, USA: Palaeogeography, Palaeoclimatology, Palaeoecology, v. 231, p. 291- 314.

Lowenstam, H. A., 1961, Mineralogy, O^{18}/O^{16} ratios, and strontium and magnesium contents of recent and fossil brachiopods and their bearing on the history of the oceans: The Journal of Geology, v. 69, no. 3, p. 241-260.

Machel, H. G., 1985, Cathodoluminescence in calcite and dolomite and its chemical interpretation: Geoscience Canada, v. 12, no. 4, p. 139-147.

Machel, H. G., Mason, R. A., Mariano, A. N., and Mucci, A., 1991, Causes and emission of luminescence in calcite and dolomite in Barker, C. E. and Kopp, O. C., eds., Luminescence Microscopy: Quantitative and qualitative aspects: SEPM Short Course 25, p. 9-25.

Maurya, A. S., Shah, M., Deshpande, R. D., Bhardwaj, R. M., Prasad, A., and Gupta, S. K., 2010, Hydrograph separation and precipitation source identification using stable water isotopes and conductivity: River Ganga at Himalayan foothills: Hydrological Processes, v. 25, no. 10, p. 1521-1530.

Mii, H. S., and Grossman, E. L., 1994, Late Pennsylvanian seasonality reflected in the 18O and elemental composition of a brachiopod shell: Geology, v. 22, no. 7, p. 661-664.

Mii, H. S., Grossman, E. L., and Yancey, T. E., 1999, Carboniferous isotope stratigraphies of North America: Implications for Carboniferous paleoceanography and Mississippian glaciation: Geological Society of America Bulletin, v. 111, no. 7, p. 960-973.

Miller, K. B., and West, R. R., 1993, Reevaluation of Wolfcampian cyclothems in northeastern Kansas: Significance of subaerial exposure and flooding surfaces *in* Current Research on Kansas Geology, Summer 1993: Kansas Geological Survey Bulletin, v. 235, p. 1-26.

Miller, K. B., McCahon, T. J., and West, R. R., 1996, Lower Permian (Wolfcampian) paleosol-bearing cycles of the U. S. midcontinent: evidence of climatic cyclicity: Journal of Sedimentary Research, v. 66, no. 1, p. 71-84.

Montañez, I. P., Tabor, N. J., Niemeier, D., DiMichele, W. A., Frank, T. D., Fielding, C. R., Isbell, J. L., Birgenheier, L. P., and Rygel, M. C., 2007, CO_2-forced climate

and vegetation instability during Late Paleozoic deglaciation: Science, v. 315, no. 87, p. 87-91.

Nielson, J. K., Blazejowski, B., Gieszcz, P., and Nielson, J. K., 2013, Carbon and oxygen isotope records of Permian brachiopods from relatively low and high palaeolatitudes: climatic seasonality and evaporation: Geological Society, London, Special Publications, v. 376, p. 387-406.

O'Neil, J. R.; Clayton, R. N.; and Mayeda, T. K., 1969, Oxygen isotope fractionation in divalent metal carbonates: Journal of Chemical Physics, v. 51, no.12, p. 5547-5558.

Olszewski, T. D., and Patzkowsky, M. E., 2003, From cyclothems to sequences: the record of eustasy and climate on an icehouse epeiric platform (Pennsylvanian-Permian, North American midcontinent): Journal of sedimentary research, v. 73, no. 1, p. 15-30.

Olszewski, T. D., and Patzkowsky, M. E., 2008, Icehouse climate and eustasy recorded in a low-latitude epeiric platform: Alternating climate regimes in the Pennsylvanian-Permian succession of the North American continent in Holmden, C., and Pratt, B. R., eds., Dynamics of epeiric seas: sedimentological, paleontological, and geochemical perspectives: Geological Association of Canada Special Publication 47, p. 229-245.

Otto-Bleisner, 1993, Tropical mountains and coal formation: a climate model study of the Westphalian (306 Ma): Geophysical Research Letters, v. 20, no. 18, p. 1947-1950.

Otto-Bleisner, 1998, Effects of tropical mountain elevations on climate of the Late Carboniferous: Climate Model Simulations *in* Crowley, T. J., and Burke, K. C., eds., Tectonic Boundary Conditions for Climate Reconstructions: New York, Oxford University Press, p. 100-115.

Otto-Bleisner, 2002, The role of mountains, polar ice, and vegetation in determining the tropical climate during the Middle Pennsylvanian: climate model simulations *in* Cecil, B. and Edgar, N. T., eds., Climate Controls on Stratigraphy: SEPM Special Publication 77, p. 227-237.

Parkinson, D., Curry, G. B., Cusach, M., and Fallick, A. E., 2005, Shell structure, patterns, and trends of oxygen and carbon stable isotopes in modern brachiopod shells: Chemical Geology, v. 219, no. 1-4, p. 387-406.

Parrish, J. T., 1993, Climate of the supercontinent Pangea: The Journal of Geology, v. 101, no. 2, p. 215-233.

Patzkowsky, M. E., Smith, L. H., Markwick, P. J., Engberts, C. J., and Gyllenhaal, E. D., 1991, Application of the Fujita-Ziegler paleoclimate model: Early Permian and Late Cretaceous examples: Palaeogeograhpy, Palaeoclimatology, Palaeoecology, v. 86, no. 1-2, p. 67-85.

Perez-Huerta, A., Cusack, M., Jeffries, T. E., and Williams, C. T., 2008, High resolution distribution of magnesium and strontium and the evaluation of Mg/Ca thermometry in Recent brachiopod shells: Chemical Geology, v. 247, no. 1-2, p. 229-241.

Perlmutter, M. A., and Matthews, M. D., 1992, Global cyclostratigraphy *in* Nierenberg, W. A., ed., Encyclopedia of Earth System Science, v. 2, p. 379-393.

Peyser, C. E., and Poulsen, C. J., 2008, Controls on Permo-Carboniferous precipitation over tropical Pangea: A GCM sensitivity study: Palaeogeograhpy, Palaeoclimatology, Palaeoecology, v. 268, no. 3-4, p. 181-192.

Popp, B. N., Anderson, T. F., and Sandberg, P. A., 1986, Brachiopods as indicators of original isotopic compositions in some Paleozoic limestones: Geological Society of America Bulletin, v. 97, no. 10, p. 1262-1269.

Powell, M. G., Schöne, B. R., and Jacob, D. E., 2009, Tropical marine climate during the late Paleozoic ice age using trace element analyses of brachiopods: Palaeogeography, Palaeoclimatology, Palaeoecology, v. 280, no. 1-2, p. 143-149.

Rankey, E., 1997, Relations between relative changes in sea level and climate shifts: Pennsylvanian-Permian mixed carbonate-siliciclastic strata, western United States: Geological Society of America Bulletin, v. 109, no. 9, p. 1089-1100.

Rosenthal, Y., Boyle, E. A., and Slowey, N., 1997, Temperature control on the incorporation of magnesium, strontium, fluorine, and cadmium into benthic foraminiferal shells from Little Bahama Bank: Prospects for thermocline paleoceanography: Geochimica et Cosmochimica Acta, v. 61, no. 17, p. 3633-3643.

Rush, P. F., and Chafetz, H. S., 1990, Fabric-retentive, non-luminescent brachiopods as indicators of original $\delta^{13}C$ and $\delta^{18}O$ composition: a test: Journal of Sedimentary Petrology, v. 60, no. 6, p. 968-981.

Saltsman, A. L., 1986, Paleoenvironments of the Upper Pennsylvanian Ames Limestone and associated rocks near Pittsburgh, Pennsylvania: Geological Society of America Bulletin, v. 97, no. 2, p. 222-231.

Samtleben, C., Munnecke, A., Bickert, T., and Pätzold, J., 2001, Shell succession, assemblage and species dependent effects on the C/O-isotopic composition of brachiopods — examples from the Silurian of Gotland: Chemical Geology, v. 175, no. 1-2, p. 61-107.

Stevens, C. H., 1971, Distribution and diversity of Pennsylvanian marine faunas relative to water depth and distance from shore: Lethaia, v. 4, no. 4., p. 403-412.

Sturgeon, M. T., and Hoare, R. D., 1968, Pennsylvanian brachiopods of Ohio: Geological Survey of Ohio Bulletin, v. 63, 95 p.

Sur, S., Soreghan, G. S., Soreghan, M. J., Yang, W., and Saller, A. H., 2010, A record of glacial aridity and Milankovitch-scale fluctuations in atmospheric dust from the Pennsylvanian tropics: Journal of Sedimentary Research, v. 80, no. 12, p. 1046-1067.

Tabor, N. J., and Montañez, I. P., 2002, Shifts in late Paleozoic atmospheric circulation over western equatorial Pangea: Insights from pedogenic mineral $\delta^{18}O$ compositions: Geology, v. 30, no. 12, p. 1127-1130.

Tabor, N. J., and Poulsen, C. J., 2008, Palaeoclimate across the Late Pennsylvanian-Early Permian tropical palaeolatitudes: A review of climate indicators, their distribution, and relation to palaeophysiographic climate factors: Palaeogeography, Palaeoclimatology, Palaeoecology: v. 268, no. 3-4, p. 293-310.

Takayanagi, H., Asami, R., Abe, O., Miyajima, T., Kitagawa, H., Sasaki, K., and Iryu, Y., 2013, Intraspecific variations in carbon-isotope and oxygen-isotope compositions of a brachiopod *Basiliola lucida* collected off Okinawa-Jima, southwestern Japan: Geochemica et Cosmochimica Acta, v. 115, p. 115-136.

Tandon, S. K., and Gibling, M. R., 1994, Calcrete and coal in late Carboniferous cyclothems of Nova Scotia, Canada: Climate and sea-level changes linked: Geology, v. 22, no. 8, p. 755-758.

Tao, K., Robbins, J. A., Grossman, E. L., and O'Dea, A., 2013, Quantifying upwelling and freshening in nearshore tropical American environments using stable isotopes in modern gastropods: Bulletin of Marine Science, v. 89, no. 4, p. 815-835.

Tyson, R. V., and Pearson, T. H., 1991, Modern and ancient continental shelf anoxia: an overview in Tyson, R. V., and Pearson, T. H., eds., Modern and ancient continental shelf anoxia: Geological Society Special Publication, v. 58, p. 1-24.

Wang, H., 1998, Oxygen isotope records of Carboniferous seasonality on the Russian Platform [M. S. thesis]: College Station, Texas A&M University, 51 p.

Wanless, H. R., and Shepard, F. P., 1936, Sea level and climatic changes related to Late Paleozoic cycles: Geological Society of America Bulletin, v. 47, no. 8, p. 1177-1206.

West, R. R., Archer, A. W., and Miller, K. B., 1997, The role of climate in stratigraphic patterns exhibited by late Paleozoic rocks exposed in Kansas: Palaeogeography, Palaeoclimatology, and Palaeoecology, v. 128, p. no. 1-4, p. 1-16.

Williams, A., 1968, Evolution of the shell structure of articulate brachiopods: The Paleontological Society of London Special Papers in Paleontology, v. 2, 55 p.

Williams, A., 1990, Biomineralization in the lophophorates *in* Carter, J. G., ed., Skeletal Biomineralization: Patterns, Processes, and Evolutionary Trends, Volume I: New York, Van Nostrand Reinhold, p. 67-82.

Williams, A., and Rowell, A., J., 1965, Morphology *in* Moore, R. C., ed., Treatise on Invertebrate Paleontology, Part H Brachiopoda: Lawrence, KS, Geological Society of America and University of Kansas Press, p. H57-H155.

Witzke, B. J., 1990, Palaeoclimatic constraints for Palaeozoic palaeolatitudes of Laurentian and Euramerica *in* McKerrow, W. S., and Scotese, C. R., eds., Palaeozoic Palaeogeography and Biogeography: Geological Society Memoir 12, p. 57-73.

Yamamoto, K., Asami, R., and Iryu, Y., 2010, Carbon and oxygen isotopic compositions of modern brachiopod shells from a warm-temperate shelf environment, Sagami Bay, central Japan: Palaeogeography, Palaeoclimatology, Palaeoecology, v. 291, no. 3-4, p. 348-359.

Yamamoto, K., Asami, R., and Iryu, Y., 2010, Within-shell variations in carbon and oxygen isotope compositions of two modern brachiopods from a subtropical shelf environment off Amami-o-shima, southwestern Japan: Geochemistry, Geophysics, Geosystems, v. 11, no. 10, 17 p.

Yang, W., 1996, Cycle symmetry and its causes, Cisco Group (Virgilian and Wolfcampian), Texas: Journal of Sedimentary Research, v. 66, no. 6, p. 1102-1121.

Zachos, J., Pagani, M., Sloan, L., Thomas, E., Billups, K, 2001, Trends, rhythms, and aberrations in global climate 65 Ma to present: Science, v. 292, no. 5517, p. 686-693.

Ziegler, A. M., Rowley, D. B., Lottes, A. L., Sahagian, D. L., Hulver, M. L., and Gierlowski, T. C., 1985, Paleogeographic interpretation: with an example from the Mid-Cretaceous: Annual Reviews in Earth and Planetary Sciences, v. 13, p.385-425.

APPENDIX I

RAW STABLE ISOTOPE DATA

Species: *N. dunbari=Neospirifer dunbari*; *C. planoconvexa=Crurithyris planoconvexa*
Material: s=secondary layer calcite; t= tertiary layer calcite; m=matrix; * sample may have included matrix
L.C.= luminescent character (see. Fig. 4)
Fabric: w= well-preserved; p=poorly preserved; f= fractured
Samples of material other than tertiary calcite, with L.C. worse than NL/CL, or fabric other than w were eliminated from paleoenvironmental considerations.

Specimen	Species	Transect	Sample #	$\delta^{13}C$	$\delta^{18}O$	Material	L.C.	Fabric
BRK	*N. dunbari*	A-A'	1	**1.46**	**-4.45**	s	SL/NL	w
BRK	*N. dunbari*	A-A'	2	**2.25**	**-4.22**	s	NL/SL	w
BRK	*N. dunbari*	A-A'	3	**2.60**	**-3.31**	s	NL/SL	w
BRK	*N. dunbari*	A-A'	4	**3.20**	**-3.70**	s	NL/SL	w
BRK	*N. dunbari*	A-A'	5	**3.21**	**-3.68**	s	NL/SL	w
BRK	*N. dunbari*	A-A'	6	**3.16**	**-3.60**	t	NL/SL	f
BRK	*N. dunbari*	A-A'	7	**3.11**	**-3.70**	t	NL/SL	f
BRK	*N. dunbari*	A-A'	8	**3.10**	**-3.76**	t	NL/SL	f
BRK	*N. dunbari*	A-A'	9	**3.00**	**-3.91**	t	NL/SL	f
BRK	*N. dunbari*	A-A'	10	**2.96**	**-3.93**	t	NL/SL	f
BRK	*N. dunbari*	A-A'	11	**2.89**	**-4.03**	t	NL/SL	w
BRK	*N. dunbari*	A-A'	12	**2.83**	**-3.98**	t	NL/SL	w
BRK	*N. dunbari*	A-A'	13	**2.70**	**-3.99**	t	NL/SL	w
BRK	*N. dunbari*	A-A'	14	**2.66**	**-4.00**	t	NL/SL	w
BRK	*N. dunbari*	A-A'	15	**2.82**	**-3.92**	t	NL/SL	w
BRK	*N. dunbari*	A-A'	16	**2.81**	**-3.91**	t	NL/SL	w
BRK	*N. dunbari*	A-A'	17	**2.91**	**-4.01**	t	NL/SL	w
BRK	*N. dunbari*	A-A'	18	**3.06**	**-3.92**	t	NL/SL	w
BRK	*N. dunbari*	A-A'	19	**2.91**	**-4.00**	t	NL/SL	w
BRK	*N. dunbari*	A-A'	20	**2.91**	**-3.80**	t	NL/SL	w
BRK	*N. dunbari*	A-A'	21	**2.83**	**-3.93**	t	NL/SL	w
BRK	*N. dunbari*	A-A'	22	**2.85**	**-3.94**	t	NL/SL	w
BRK	*N. dunbari*	A-A'	23	**2.81**	**-3.91**	t	NL/SL	w
BRK	*N. dunbari*	A-A'	24	**2.80**	**-3.93**	t	NL/SL	w
BRK	*N. dunbari*	A-A'	25	**2.80**	**-3.94**	t	NL/SL	w
BRK	*N. dunbari*	A-A'	26	**2.69**	**-3.94**	t	NL/SL	w
BRK	*N. dunbari*	A-A'	27	**2.61**	**-4.12**	t	NL/SL	w
BRK	*N. dunbari*	A-A'	28	**2.63**	**-3.87**	t	NL/SL	w
BRK	*N. dunbari*	A-A'	29	**2.61**	**-3.94**	t	NL/SL	w
BRK	*N. dunbari*	A-A'	30	**2.64**	**-3.94**	t	NL/SL	w
BRK	*N. dunbari*	A-A'	31	**2.68**	**-3.98**	t	NL/SL	w
BRK	*N. dunbari*	A-A'	32	**2.72**	**-3.79**	t	NL/SL	w

Specimen	Species	Transect	Sample #	$\delta^{13}C$	$\delta^{18}O$	Material	L.C.	Fabric
BRK	*N. dunbari*	A-A'	33	**2.74**	**-3.94**	t	NL/SL	w
BRK	*N. dunbari*	A-A'	34	**2.74**	**-3.96**	t	NL/SL	w
BRK	*N. dunbari*	A-A'	35	**2.77**	**-3.91**	t	NL/SL	w
BRK	*N. dunbari*	A-A'	36	**2.73**	**-4.02**	t	NL/SL	w
BRK	*N. dunbari*	A-A'	37	**2.72**	**-3.93**	t	NL/SL	w
BRK	*N. dunbari*	A-A'	38	**2.71**	**-3.88**	t	NL/SL	w
BRK	*N. dunbari*	A-A'	39	**2.55**	**-3.85**	t	NL/SL	w
BRK	*N. dunbari*	A-A'	40	**2.52**	**-3.81**	t	NL/SL	w
BRK	*N. dunbari*	A-A'	41	**2.55**	**-3.86**	t	NL/SL	w
BRK	*N. dunbari*	A-A'	42	**2.60**	**-3.80**	t	NL/SL	w
BRK	*N. dunbari*	A-A'	43	**2.53**	**-3.90**	t	NL/SL	w
BRK	*N. dunbari*	A-A'	44	**2.47**	**-4.12**	t	NL/SL	w
BRK	*N. dunbari*	A-A'	45	**2.35**	**-3.99**	t	NL/SL	w
BRK	*N. dunbari*	A-A'	46	**2.30**	**-4.06**	t	NL/SL	w
BRK	*N. dunbari*	A-A'	47	**2.25**	**-4.09**	t	NL/SL	w
BRK	*N. dunbari*	A-A'	48	**2.17**	**-4.10**	t	NL/SL	w
BRK	*N. dunbari*	A-A'	49	**0.67**	**-5.07**	m	SL/NL	w
BRK	*N. dunbari*	n/a	M1	**-1.32**	**-4.28**	m	L	n/a
GRR-1	*N. dunbari*	A-A'	1	**2.20**	**-3.68**	t	NL/SL	w
GRR-1	*N. dunbari*	A-A'	2	**2.69**	**-3.91**	t	NL/SL	w
GRR-1	*N. dunbari*	A-A'	3	**2.69**	**-3.81**	t	NL/SL	w
GRR-1	*N. dunbari*	A-A'	4	**2.64**	**-3.75**	t	NL/SL	w
GRR-1	*N. dunbari*	A-A'	5	**2.76**	**-3.83**	t	NL/SL	w
GRR-1	*N. dunbari*	A-A'	6	**2.66**	**-3.74**	t	NL/SL	w
GRR-1	*N. dunbari*	A-A'	7	**2.54**	**-3.82**	t	NL/SL	w
GRR-1	*N. dunbari*	A-A'	8	**2.38**	**-3.83**	t	NL/SL	w
GRR-1	*N. dunbari*	A-A'	9	**2.34**	**-3.89**	t	NL/SL	w
GRR-1	*N. dunbari*	A-A'	10	**2.15**	**-3.97**	t	NL/SL	w
GRR-1	*N. dunbari*	A-A'	11	**2.14**	**-3.82**	t	NL/SL	w
GRR-1	*N. dunbari*	A-A'	12	**2.24**	**-3.75**	t	NL/SL	w
GRR-1	*N. dunbari*	A-A'	13	**2.28**	**-3.77**	t	NL/SL	w
GRR-1	*N. dunbari*	A-A'	14	**2.38**	**-3.67**	t	NL/SL	w
GRR-1	*N. dunbari*	A-A'	15	**2.49**	**-3.59**	t	NL/SL	w
GRR-1	*N. dunbari*	A-A'	16	**2.67**	**-3.58**	t	NL/SL	w
GRR-1	*N. dunbari*	A-A'	17	**2.63**	**-3.58**	t	NL/SL	w
GRR-1	*N. dunbari*	A-A'	18	**2.80**	**-3.60**	t	NL/SL	w
GRR-1	*N. dunbari*	A-A'	19	**2.84**	**-3.59**	t	NL/SL	w
GRR-1	*N. dunbari*	A-A'	20	**2.90**	**-3.58**	t	NL/SL	w
GRR-1	*N. dunbari*	A-A'	21	**2.84**	**-3.52**	t	NL/SL	w

Specimen	Species	Transect	Sample #	$\delta^{13}C$	$\delta^{18}O$	Material	L.C.	Fabric
GRR-1	*N. dunbari*	A-A'	22	**2.76**	**-3.57**	t	NL/SL	w
GRR-1	*N. dunbari*	A-A'	23	**2.72**	**-3.58**	t	NL/SL	w
GRR-1	*N. dunbari*	A-A'	24	**2.61**	**-3.63**	t	NL/SL	w
GRR-1	*N. dunbari*	A-A'	25	**2.51**	**-3.63**	t	NL/SL	w
GRR-1	*N. dunbari*	A-A'	26	**2.37**	**-3.79**	t	NL/SL	w
GRR-1	*N. dunbari*	A-A'	27	**2.34**	**-3.92**	t	NL/SL	w
GRR-1	*N. dunbari*	A-A'	28	**1.86**	**-4.13**	t	SL/NL	w
GRR-1	*N. dunbari*	A-A'	29	**1.50**	**-4.41**	t	SL/NL	w
GRR-1	*N. dunbari*	A-A'	30	**1.59**	**-4.35**	t	SL/NL	w
GRR-1	*N. dunbari*	A-A'	31	**1.53**	**-4.20**	t	SL/NL	w
GRR-1	*N. dunbari*	A-A'	32	**-0.62**	**-3.98**	t	SL/NL	w
GRR-9	*N. dunbari*	A-A'	1	**3.55**	**-3.48**	t	NL/SL	w
GRR-9	*N. dunbari*	A-A'	2	**3.47**	**-3.71**	t	NL/SL	w
GRR-9	*N. dunbari*	A-A'	3	**3.48**	**-3.62**	t	NL/SL	w
GRR-9	*N. dunbari*	A-A'	4	**3.44**	**-3.58**	t	NL/SL	w
GRR-9	*N. dunbari*	A-A'	5	**3.15**	**-3.50**	t	NL/SL	w
GRR-9	*N. dunbari*	A-A'	6	**3.05**	**-3.66**	t	NL/SL	w
GRR-9	*N. dunbari*	A-A'	7	**3.07**	**-3.53**	t	NL/SL	w
GRR-9	*N. dunbari*	A-A'	8	**2.89**	**-3.49**	t	NL/SL	w
GRR-9	*N. dunbari*	A-A'	9	**2.78**	**-3.46**	t	NL/SL	w
GRR-9	*N. dunbari*	A-A'	10	**2.83**	**-3.53**	t	NL/SL	w
GRR-9	*N. dunbari*	A-A'	11	**2.89**	**-3.58**	t	NL/SL	w
GRR-9	*N. dunbari*	A-A'	12	**2.97**	**-3.81**	t	NL/SL	w
GRR-9	*N. dunbari*	A-A'	13	**3.01**	**-3.84**	t	NL/SL	w
GRR-9	*N. dunbari*	A-A'	14	**3.15**	**-3.74**	t	NL/SL	w
GRR-9	*N. dunbari*	A-A'	15	**3.16**	**-3.83**	t	NL/SL	w
GRR-9	*N. dunbari*	A-A'	16	**2.99**	**-3.83**	t	NL/SL	w
GRR-9	*N. dunbari*	A-A'	17	**2.88**	**-3.80**	t	NL/SL	w
GRR-9	*N. dunbari*	A-A'	18	**2.83**	**-3.83**	t	NL/SL	w
GRR-9	*N. dunbari*	A-A'	19	**2.77**	**-3.71**	t	NL/SL	w
GRR-9	*N. dunbari*	A-A'	20	**2.78**	**-3.74**	t	NL/SL	w
GRR-9	*N. dunbari*	A-A'	21	**2.76**	**-3.73**	t	NL/SL	w
GRR-9	*N. dunbari*	A-A'	22	**2.51**	**-3.65**	t	NL/SL	w
GRR-9	*N. dunbari*	A-A'	23	**2.15**	**-3.85**	t	NL/SL	w
GRR-9	*N. dunbari*	A-A'	24	**1.71**	**-3.88**	t	NL/SL	w
GRR-9	*N. dunbari*	A-A'	25	**1.73**	**-3.86**	t	SL/NL	w
GRR-9	*N. dunbari*	A-A'	26	**1.60**	**-3.81**	t	SL/NL	w
GRR-9	*N. dunbari*	A-A'	27	**1.36**	**-3.74**	t	SL/NL	w
GRR-9	*N. dunbari*	A-A'	28	**1.47**	**-3.68**	t	SL/NL	w

Specimen	Species	Transect	Sample #	$\delta^{13}C$	$\delta^{18}O$	Material	L.C.	Fabric
GRR-9	*N. dunbari*	A-A'	29	**2.42**	**-3.69**	t	SL/NL	w
GRR-9	*N. dunbari*	A-A'	30	**2.75**	**-3.86**	t	SL/NL	w
GRR-9	*N. dunbari*	A-A'	31	**3.09**	**-3.75**	t	SL/NL	w
GRR-9	*N. dunbari*	A-A'	32	**3.08**	**-3.71**	t	SL/NL	w
GRR-9	*N. dunbari*	A-A'	33	**3.03**	**-3.66**	t	SL/NL	w
GRR-9	*N. dunbari*	A-A'	34	**2.96**	**-3.78**	t	SL/NL	w
GRR-9	*N. dunbari*	A-A'	35	**2.90**	**-3.71**	t	SL/NL	w
GRR-9	*N. dunbari*	A-A'	36	**2.14**	**-3.70**	t	SL/NL	w
GRR-9	*N. dunbari*	A-A'	37	**1.83**	**-3.55**	t	SL/NL	w
GRR-9	*N. dunbari*	A-A'	38	**2.12**	**-3.52**	t	SL/NL	w
GRR-9	*N. dunbari*	A-A'	39	**2.59**	**-3.61**	t	SL/NL	w
GRR-9	*N. dunbari*	A-A'	40	**2.19**	**-3.69**	t	SL/NL	w
GRR-9	*N. dunbari*	n/a	M1	**-5.78**	**-8.67**	m	L	n/a
GRR-9	*N. dunbari*	n/a	M2	**-5.83**	**-7.37**	m	L	n/a
MID-2	*N. dunbari*	A-A'	1	**3.49**	**-3.53**	t	NL	w
MID-2	*N. dunbari*	A-A'	2	**3.57**	**-3.52**	t	NL	w
MID-2	*N. dunbari*	A-A'	3	**3.69**	**-3.55**	t	NL	w
MID-2	*N. dunbari*	A-A'	4	**3.78**	**-3.55**	t	NL	w
MID-2	*N. dunbari*	A-A'	5	**3.75**	**-3.45**	t	NL	w
MID-2	*N. dunbari*	A-A'	6	**3.66**	**-3.65**	t	NL	w
MID-2	*N. dunbari*	A-A'	7	**3.55**	**-3.65**	t	NL	w
MID-2	*N. dunbari*	A-A'	8	**3.54**	**-3.76**	t	NL	w
MID-2	*N. dunbari*	A-A'	9	**3.70**	**-3.74**	t	NL	w
MID-2	*N. dunbari*	A-A'	10	**3.78**	**-3.75**	t	NL	w
MID-2	*N. dunbari*	A-A'	11	**3.73**	**-3.75**	t	NL	w
MID-2	*N. dunbari*	A-A'	12	**3.58**	**-3.82**	t	NL	w
MID-2	*N. dunbari*	A-A'	13	**3.56**	**-3.79**	t	NL	w
MID-2	*N. dunbari*	A-A'	14	**3.52**	**-3.83**	t	NL	w
MID-2	*N. dunbari*	A-A'	15	**3.38**	**-3.84**	t	NL	w
MID-2	*N. dunbari*	A-A'	16	**3.35**	**-3.93**	t	NL	w
MID-2	*N. dunbari*	A-A'	17	**3.37**	**-3.93**	t	NL	w
MID-2	*N. dunbari*	A-A'	18	**3.24**	**-3.91**	t	NL	w
MID-2	*N. dunbari*	A-A'	19	**2.90**	**-3.75**	t	NL	w
MID-2	*N. dunbari*	A-A'	20	**2.92**	**-3.63**	t	NL	w
MID-2	*N. dunbari*	A-A'	21	**3.21**	**-3.63**	t	NL	w
MID-2	*N. dunbari*	A-A'	22	**3.32**	**-3.60**	t	NL	w
MID-2	*N. dunbari*	A-A'	23	**3.34**	**-3.65**	t	NL	w
MID-2	*N. dunbari*	A-A'	24	**3.32**	**-3.52**	t	NL	w
MID-2	*N. dunbari*	A-A'	25	**3.09**	**-3.58**	t	NL	w

Specimen	Species	Transect	Sample #	$\delta^{13}C$	$\delta^{18}O$	Material	L.C.	Fabric
MID-2	*N. dunbari*	A-A'	26	**2.80**	**-3.56**	t	NL	w
MID-2	*N. dunbari*	A-A'	27	**2.76**	**-3.66**	t	NL	w
MID-2	*N. dunbari*	A-A'	28	**2.57**	**-3.72**	t	NL	w
MID-2	*N. dunbari*	A-A'	28	**2.57**	**-3.72**	t	NL	w
MID-2	*N. dunbari*	A-A'	29	**2.50**	**-3.76**	t	NL	w
MID-2	*N. dunbari*	A-A'	30	**2.40**	**-3.59**	t	NL	w
MID-2	*N. dunbari*	A-A'	31	**2.38**	**-3.49**	t	NL	w
MID-2	*N. dunbari*	A-A'	33	**2.47**	**-3.40**	t	SL/NL	w
MID-2	*N. dunbari*	A-A'	34	**2.49**	**-3.30**	t	SL/NL	w
MID-2	*N. dunbari*	A-A'	36	**-1.60**	**-3.46**	m	L	n/a
MID-2	*N. dunbari*	A-A'	37	**-2.75**	**-3.96**	m	L	n/a
MID-2	*N. dunbari*	n/a	M1	**-3.52**	**-3.37**	m	L	n/a
MID-2	*N. dunbari*	n/a	M2	**-4.29**	**-3.57**	m	L	n/a
RED	*N. dunbari*	A-A'	06	**2.65**	**-3.77**	s	SL/NL	p
RED	*N. dunbari*	A-A'	07	**2.73**	**-3.73**	s	SL/NL	p
RED	*N. dunbari*	A-A'	08	**2.69**	**-4.22**	s	SL/NL	p
RED	*N. dunbari*	A-A'	09	**3.22**	**-3.60**	s	SL/NL	p
RED	*N. dunbari*	A-A'	10	**3.38**	**-3.55**	s	SL/NL	p
RED	*N. dunbari*	A-A'	11	**3.56**	**-3.43**	t	NL	w
RED	*N. dunbari*	A-A'	12	**3.58**	**-3.40**	t	NL	w
RED	*N. dunbari*	A-A'	13	**3.56**	**-3.42**	t	NL	w
RED	*N. dunbari*	A-A'	14	**3.58**	**-3.40**	t	NL	w
RED	*N. dunbari*	A-A'	15	**3.52**	**-3.34**	t	NL	w
RED	*N. dunbari*	A-A'	16	**3.53**	**-3.30**	t	NL	w
RED	*N. dunbari*	A-A'	17	**3.36**	**-3.31**	t	NL	w
RED	*N. dunbari*	A-A'	18	**3.33**	**-3.27**	t	NL	w
RED	*N. dunbari*	A-A'	19	**3.13**	**-3.27**	t	NL	w
RED	*N. dunbari*	A-A'	20	**2.94**	**-3.42**	t	NL	w
RED	*N. dunbari*	A-A'	21	**2.66**	**-3.92**	t	NL	w
RED	*N. dunbari*	A-A'	22	**2.99**	**-3.54**	t	NL	w
RED	*N. dunbari*	A-A'	24	**3.08**	**-3.55**	t	NL	w
RED	*N. dunbari*	A-A'	25	**3.18**	**-3.46**	t	NL	w
RED	*N. dunbari*	A-A'	26	**3.26**	**-3.57**	t	NL	w
RED	*N. dunbari*	A-A'	27	**3.20**	**-3.45**	t	NL	w
RED	*N. dunbari*	A-A'	28	**3.16**	**-3.46**	t	NL	w
RED	*N. dunbari*	A-A'	29	**3.08**	**-3.55**	t	NL	w
RED	*N. dunbari*	A-A'	30	**3.01**	**-3.53**	t	NL	w
RED	*N. dunbari*	A-A'	31	**3.05**	**-3.48**	t	NL	w
RED	*N. dunbari*	A-A'	32	**3.07**	**-3.46**	t	NL	w

Specimen	Species	Transect	Sample #	$\delta^{13}C$	$\delta^{18}O$	Material	L.C.	Fabric
RED	*N. dunbari*	A-A'	33	**2.37**	**-4.71**	t*	NL	w
RED	*N. dunbari*	A-A'	34	**2.44**	**-3.58**	t*	NL	w
RED	*N. dunbari*	n/a	M1	**-1.81**	**-3.09**	m	L	n/a
RED	*N. dunbari*	n/a	M2	**-2.12**	**-3.01**	m	L	n/a
TFF-1	*N. dunbari*	A-A'	1	**3.00**	**-3.83**	t	NL	w
TFF-1	*N. dunbari*	A-A'	2	**3.00**	**-3.87**	t	NL	w
TFF-1	*N. dunbari*	A-A'	3	**3.02**	**-3.93**	t	NL	w
TFF-1	*N. dunbari*	A-A'	4	**3.08**	**-3.92**	t	NL	w
TFF-1	*N. dunbari*	A-A'	5	**3.08**	**-3.95**	t	NL	w
TFF-1	*N. dunbari*	A-A'	6	**3.16**	**-3.87**	t	NL	w
TFF-1	*N. dunbari*	A-A'	7	**3.05**	**-3.94**	t	NL	w
TFF-1	*N. dunbari*	A-A'	8	**2.97**	**-3.92**	t	NL	w
TFF-1	*N. dunbari*	A-A'	9	**2.86**	**-3.89**	t	NL	w
TFF-1	*N. dunbari*	A-A'	10	**2.69**	**-3.87**	t	NL	w
TFF-1	*N. dunbari*	A-A'	11	**2.64**	**-3.84**	t	NL	w
TFF-1	*N. dunbari*	A-A'	12	**2.44**	**-3.81**	t	NL	w
TFF-1	*N. dunbari*	A-A'	13	**2.40**	**-3.96**	t	NL	w
TFF-1	*N. dunbari*	A-A'	15	**2.30**	**-3.82**	t	NL	w
TFF-1	*N. dunbari*	A-A'	16	**2.31**	**-3.83**	t	NL	w
TFF-1	*N. dunbari*	A-A'	17	**2.34**	**-3.98**	t	NL	w
TFF-1	*N. dunbari*	A-A'	18	**2.47**	**-4.01**	t	NL	w
TFF-1	*N. dunbari*	B-B'	1	**3.05**	**-3.77**	t	NL	w
TFF-1	*N. dunbari*	B-B'	2	**3.10**	**-3.96**	t	NL	w
TFF-1	*N. dunbari*	B-B'	3	**3.18**	**-4.06**	t	NL	w
TFF-1	*N. dunbari*	B-B'	4	**3.08**	**-3.93**	t	NL	w
TFF-1	*N. dunbari*	B-B'	5	**3.21**	**-4.01**	t	NL	w
TFF-1	*N. dunbari*	B-B'	6	**3.14**	**-3.96**	t	NL	w
TFF-1	*N. dunbari*	B-B'	7	**3.04**	**-3.92**	t	NL	w
TFF-1	*N. dunbari*	B-B'	8	**2.98**	**-3.90**	t	NL	w
TFF-1	*N. dunbari*	B-B'	9	**3.05**	**-3.90**	t	NL	w
TFF-1	*N. dunbari*	B-B'	10	**2.95**	**-3.91**	t	NL	w
TFF-1	*N. dunbari*	B-B'	11	**2.97**	**-3.85**	t	NL	w
TFF-1	*N. dunbari*	B-B'	13	**2.95**	**-3.73**	t	NL	w
TFF-1	*N. dunbari*	B-B'	14	**2.77**	**-3.88**	t	NL	w
TFF-1	*N. dunbari*	B-B'	15	**2.93**	**-3.87**	t	NL	w
TFF-1	*N. dunbari*	B-B'	16	**2.87**	**-3.88**	t	NL	w
TFF-2	*N. dunbari*	A-A'	01	**2.68**	**-3.98**	t	NL	w
TFF-2	*N. dunbari*	A-A'	02	**2.64**	**-3.93**	t	NL	w
TFF-2	*N. dunbari*	A-A'	03	**2.63**	**-3.77**	t	NL	w

Specimen	Species	Transect	Sample #	$\delta^{13}C$	$\delta^{18}O$	Material	L.C.	Fabric
TFF-2	*N. dunbari*	A-A'	04	**2.60**	**-3.80**	t	NL	w
TFF-2	*N. dunbari*	A-A'	05	**2.58**	**-3.83**	t	NL	w
TFF-2	*N. dunbari*	A-A'	06	**2.58**	**-3.78**	t	NL	w
TFF-2	*N. dunbari*	A-A'	07	**2.61**	**-3.72**	t	NL	w
TFF-2	*N. dunbari*	A-A'	08	**2.64**	**-3.47**	t	NL	w
TFF-2	*N. dunbari*	A-A'	09	**2.67**	**-3.68**	t	NL	w
TFF-2	*N. dunbari*	A-A'	10	**2.58**	**-3.81**	t	NL	w
TFF-2	*N. dunbari*	A-A'	11	**2.46**	**-3.91**	t	NL	w
TFF-2	*N. dunbari*	A-A'	12	**2.45**	**-3.97**	t	NL	w
TFF-2	*N. dunbari*	A-A'	13	**2.43**	**-3.90**	t	NL	w
TFF-2	*N. dunbari*	A-A'	14	**2.38**	**-3.93**	t	NL	w
TFF-2	*N. dunbari*	A-A'	15	**2.30**	**-4.02**	t	NL	w
TFF-2	*N. dunbari*	A-A'	16	**2.18**	**-4.06**	t	NL	w
TFF-2	*N. dunbari*	A-A'	17	**2.02**	**-4.01**	t	NL	w
TFF-2	*N. dunbari*	A-A'	19	**2.20**	**-4.14**	t	NL	w
TFF-2	*N. dunbari*	A-A'	20	**2.34**	**-4.08**	t	NL	w
TFF-2	*N. dunbari*	A-A'	21	**2.29**	**-4.12**	t	NL	w
TFF-2	*N. dunbari*	A-A'	22	**2.36**	**-4.08**	t	NL	w
TFF-2	*N. dunbari*	A-A'	23	**2.38**	**-4.08**	t	NL	w
TFF-2	*N. dunbari*	A-A'	24	**2.37**	**-4.06**	t	NL	w
TFF-2	*N. dunbari*	A-A'	25	**2.35**	**-3.97**	t	NL	w
TFF-2	*N. dunbari*	A-A'	26	**2.48**	**-3.90**	t	NL	w
TFF-2	*N. dunbari*	A-A'	27	**2.50**	**-3.87**	t	NL	w
TFF-2	*N. dunbari*	A-A'	28	**2.50**	**-3.86**	t	NL	w
TFF-2	*N. dunbari*	A-A'	29	**2.24**	**-3.84**	t	NL	w
TFF-2	*N. dunbari*	A-A'	30	**2.28**	**-3.85**	t	NL	w
TFF-2	*N. dunbari*	A-A'	31	**2.12**	**-3.93**	t	NL	w
TFF-2	*N. dunbari*	A-A'	32	**1.91**	**-3.97**	t	NL	w
TFF-2	*N. dunbari*	A-A'	33	**1.78**	**-4.27**	t	NL	w
TFF-2	*N. dunbari*	A-A'	35	**2.05**	**-4.23**	t	NL	w
TFF-2	*N. dunbari*	A-A'	36	**2.12**	**-4.17**	t	NL	w
TFF-2	*N. dunbari*	A-A'	37	**2.13**	**-4.06**	t	NL	w
TFF-2	*N. dunbari*	A-A'	39	**1.71**	**-4.28**	t	NL	w
TFF-2	*N. dunbari*	A-A'	40	**1.78**	**-4.28**	t	NL	w
TFF-2	*N. dunbari*	A-A'	41	**1.86**	**-4.19**	t	NL	w
TFF-2	*N. dunbari*	A-A'	42	**1.90**	**-4.17**	t	NL	w
TFF-2	*N. dunbari*	B-B'	01	**2.08**	**-4.63**	s	SL/NL	w
TFF-2	*N. dunbari*	B-B'	02	**2.66**	**-4.50**	s	SL/NL	w
TFF-2	*N. dunbari*	B-B'	03	**2.62**	**-4.54**	s	SL/NL	w

Specimen	Species	Transect	Sample #	$\delta^{13}C$	$\delta^{18}O$	Material	L.C.	Fabric
TFF-2	*N. dunbari*	B-B'	04	**2.73**	**-4.39**	s	SL/NL	w
TFF-2	*N. dunbari*	B-B'	05	**2.88**	**-4.22**	s	SL/NL	w
TFF-2	*N. dunbari*	B-B'	06	**2.99**	**-4.22**	s	SL/NL	w
TFF-2	*N. dunbari*	B-B'	07	**2.95**	**-4.13**	s	SL/NL	w
TFF-2	*N. dunbari*	B-B'	08	**2.78**	**-4.37**	s	SL/NL	w
TFF-2	*N. dunbari*	B-B'	09	**2.79**	**-4.32**	s	SL/NL	w
TFF-2	*N. dunbari*	B-B'	10	**2.89**	**-4.31**	t	NL	w
TFF-2	*N. dunbari*	B-B'	11	**2.92**	**-4.28**	t	NL	w
TFF-2	*N. dunbari*	B-B'	12	**2.95**	**-4.24**	t	NL	w
TFF-2	*N. dunbari*	B-B'	13	**2.83**	**-4.15**	t	NL	w
TFF-2	*N. dunbari*	B-B'	14	**2.80**	**-4.17**	t	NL	w
TFF-2	*N. dunbari*	B-B'	15	**2.88**	**-4.00**	t	NL	w
TFF-2	*N. dunbari*	B-B'	16	**2.87**	**-4.07**	t	NL	w
TFF-2	*N. dunbari*	B-B'	17	**2.86**	**-3.93**	t	NL	w
TFF-2	*N. dunbari*	B-B'	19	**2.75**	**-4.02**	t	NL	w
TFF-2	*N. dunbari*	B-B'	20	**2.59**	**-4.04**	t	NL	w
TFF-2	*N. dunbari*	B-B'	21	**2.66**	**-4.01**	t	NL	w
TFF-2	*N. dunbari*	B-B'	22	**2.62**	**-4.09**	t	NL	w
TFF-2	*N. dunbari*	B-B'	23	**2.60**	**-4.11**	t	NL	w
TFF-2	*N. dunbari*	B-B'	24	**2.61**	**-3.99**	t	NL	w
TFF-2	*N. dunbari*	B-B'	25	**2.61**	**-4.05**	t	NL	w
TFF-2	*N. dunbari*	B-B'	26	**2.53**	**-4.07**	t	NL	w
TFF-2	*N. dunbari*	B-B'	27	**2.47**	**-4.03**	t	NL	w
TFF-2	*N. dunbari*	B-B'	28	**2.44**	**-4.03**	t	NL	w
TFF-2	*N. dunbari*	B-B'	29	**2.38**	**-4.20**	t	NL	w
TFF-2	*N. dunbari*	B-B'	30	**2.30**	**-4.16**	t	NL	w
Nn-3	*N. dunbari*	A-A'	1	**2.74**	**-3.74**	s	SL/NL	w
Nn-3	*N. dunbari*	A-A'	2	**2.91**	**-3.67**	s	SL/NL	w
Nn-3	*N. dunbari*	A-A'	3	**3.06**	**-3.79**	s	SL/NL	w
Nn-3	*N. dunbari*	A-A'	4	**3.10**	**-3.86**	s	SL/NL	w
Nn-3	*N. dunbari*	A-A'	5	**3.03**	**-3.98**	t	NL/SL	w
Nn-3	*N. dunbari*	A-A'	6	**2.97**	**-3.96**	t	NL/SL	w
Nn-3	*N. dunbari*	A-A'	7	**2.96**	**-3.87**	t	NL/SL	w
Nn-3	*N. dunbari*	A-A'	8	**2.97**	**-3.85**	t	NL/SL	w
Nn-3	*N. dunbari*	A-A'	9	**3.03**	**-3.88**	t	NL/SL	w
Nn-3	*N. dunbari*	A-A'	10	**3.02**	**-3.86**	t	NL/SL	w
Nn-3	*N. dunbari*	A-A'	11	**3.03**	**-3.93**	t	NL/SL	w
Nn-3	*N. dunbari*	A-A'	12	**3.00**	**-3.89**	t	NL/SL	w
Nn-3	*N. dunbari*	A-A'	13	**2.93**	**-3.91**	t	NL/SL	w

Specimen	Species	Transect	Sample #	$\delta^{13}C$	$\delta^{18}O$	Material	L.C.	Fabric
Nn-3	*N. dunbari*	A-A'	14	**2.76**	**-3.92**	t	NL/SL	w
Nn-3	*N. dunbari*	A-A'	15	**2.49**	**-3.89**	t	NL/SL	w
Nn-3	*N. dunbari*	A-A'	16	**2.19**	**-3.89**	t	NL/SL	w
Nn-3	*N. dunbari*	A-A'	17	**2.08**	**-4.04**	t	NL/SL	w
Nn-3	*N. dunbari*	A-A'	18	**2.38**	**-3.99**	t	NL/SL	w
Nn-3	*N. dunbari*	A-A'	19	**2.55**	**-3.98**	t	NL/SL	w
Nn-3	*N. dunbari*	A-A'	20	**2.61**	**-3.91**	t	NL/SL	w
Nn-3	*N. dunbari*	A-A'	21	**2.44**	**-3.91**	t	NL/SL	w
Nn-3	*N. dunbari*	A-A'	22	**2.40**	**-3.78**	t	NL/SL	w
Nn-3	*N. dunbari*	A-A'	24	**1.72**	**-3.83**	t	NL/SL	w
Nn-3	*N. dunbari*	A-A'	25	**1.55**	**-3.91**	t	NL/SL	w
Nn-3	*N. dunbari*	A-A'	26	**1.59**	**-4.00**	t	NL/SL	w
Nn-3	*N. dunbari*	A-A'	27	**1.68**	**-3.96**	t	NL/SL	w
Nn-3	*N. dunbari*	A-A'	28	**1.64**	**-4.01**	t	NL/SL	w
Nn-3	*N. dunbari*	A-A'	29	**1.46**	**-4.27**	t	NL/SL	w
Nn-3	*N. dunbari*	B-B'	16	**2.93**	**-3.80**	t	NL/SL	w
Nn-3	*N. dunbari*	B-B'	17	**2.77**	**-3.86**	t	NL/SL	w
Nn-3	*N. dunbari*	B-B'	18	**2.91**	**-3.88**	t	NL/SL	w
Nn-3	*N. dunbari*	B-B'	19	**2.68**	**-3.89**	t	NL/SL	w
Nn-3	*N. dunbari*	B-B'	20	**2.67**	**-3.88**	t	NL/SL	w
Nn-3	*N. dunbari*	B-B'	21	**2.54**	**-3.90**	t	NL/SL	w
Nn-3	*N. dunbari*	B-B'	22	**2.43**	**-3.88**	t	NL/SL	w
Nn-3	*N. dunbari*	B-B'	23	**2.36**	**-3.93**	t	NL/SL	w
Nn-3	*N. dunbari*	B-B'	24	**2.38**	**-3.83**	t	NL/SL	w
Nn-3	*N. dunbari*	B-B'	25	**2.34**	**-3.91**	t	NL/SL	w
Nn-3	*N. dunbari*	B-B'	26	**2.53**	**-3.80**	t	NL/SL	w
Nn-3	*N. dunbari*	B-B'	27	**2.45**	**-3.98**	t	NL/SL	w
Nn-3	*N. dunbari*	B-B'	28	**2.42**	**-3.93**	t	NL/SL	w
Nn-3	*N. dunbari*	B-B'	29	**2.38**	**-3.98**	t	NL/SL	w
Nn-3	*N. dunbari*	B-B'	30	**2.32**	**-3.89**	t	NL/SL	w
Nn-3	*N. dunbari*	B-B'	31	**2.12**	**-4.06**	t	NL/SL	w
Nn-3	*N. dunbari*	B-B'	32	**1.93**	**-3.98**	m	L	p
Nn-3	*N. dunbari*	B-B'	33	**1.68**	**-4.00**	m	L	p
CONC	*N. dunbari*	A-A'	1	**2.40**	**-4.07**	t	NL/SL	w
CONC	*N. dunbari*	A-A'	2	**2.37**	**-4.10**	t	NL/SL	w
CONC	*N. dunbari*	A-A'	3	**2.51**	**-4.05**	t	NL/SL	w
CONC	*N. dunbari*	A-A'	4	**2.49**	**-4.05**	t	NL/SL	w
CONC	*N. dunbari*	A-A'	5	**2.64**	**-3.79**	t	NL/SL	w
CONC	*N. dunbari*	A-A'	6	**2.63**	**-3.95**	t	NL/SL	w

Specimen	Species	Transect	Sample #	$\delta^{13}C$	$\delta^{18}O$	Material	L.C.	Fabric
CONC	*N. dunbari*	A-A'	7	**2.67**	**-3.94**	t	NL/SL	w
CONC	*N. dunbari*	A-A'	10	**2.67**	**-3.95**	t	NL/SL	w
CONC	*N. dunbari*	A-A'	11	**2.66**	**-3.86**	t	NL/SL	w
CONC	*N. dunbari*	A-A'	12	**2.69**	**-3.86**	t	NL/SL	w
CONC	*N. dunbari*	A-A'	13	**2.64**	**-3.87**	t	NL/SL	w
CONC	*N. dunbari*	A-A'	14	**2.49**	**-3.96**	t	NL/SL	w
CONC	*N. dunbari*	A-A'	15	**2.68**	**-3.91**	t	NL/SL	w
CONC	*N. dunbari*	A-A'	16	**2.61**	**-4.00**	t	NL/SL	w
CONC	*N. dunbari*	A-A'	17	**2.61**	**-3.97**	t	NL/SL	w
CONC	*N. dunbari*	A-A'	18	**2.58**	**-4.05**	t	NL/SL	w
CONC	*N. dunbari*	A-A'	19	**2.57**	**-4.07**	t	NL/SL	w
CONC	*N. dunbari*	A-A'	20	**2.46**	**-4.17**	t	NL/SL	w
CONC	*N. dunbari*	A-A'	21	**2.34**	**-4.11**	t	NL/SL	w
CONC	*N. dunbari*	A-A'	22	**2.33**	**-4.07**	t	NL/SL	w
CONC	*N. dunbari*	A-A'	23	**2.31**	**-4.07**	t	NL/SL	w
CONC	*N. dunbari*	A-A'	24	**2.26**	**-4.08**	t	NL/SL	w
CONC	*N. dunbari*	A-A'	25	**2.43**	**-4.14**	t	NL/SL	w
CONC	*N. dunbari*	A-A'	26	**2.37**	**-4.31**	t	NL/SL	w
CONC	*N. dunbari*	A-A'	28	**2.45**	**-4.03**	t	NL/SL	w
CONC	*N. dunbari*	A-A'	29	**2.27**	**-4.10**	t	NL/SL	w
CONC	*N. dunbari*	A-A'	30	**2.21**	**-4.05**	t	NL/SL	w
CONC	*N. dunbari*	A-A'	31	**2.25**	**-4.00**	t	NL/SL	w
CONC	*N. dunbari*	A-A'	32	**2.18**	**-4.14**	t	NL/SL	w
CONC	*N. dunbari*	A-A'	33	**2.19**	**-4.03**	t	NL/SL	w
CONC	*N. dunbari*	A-A'	34	**2.21**	**-4.06**	t	NL/SL	w
CONC	*N. dunbari*	A-A'	35	**2.13**	**-4.03**	t	NL/SL	w
CONC	*N. dunbari*	A-A'	36	**1.92**	**-4.10**	t	NL/SL	w
CONC	*N. dunbari*	A-A'	37	**1.57**	**-4.10**	t	NL/SL	w
CONC	*N. dunbari*	A-A'	38	**1.59**	**-4.08**	t	NL/SL	w
CONC	*N. dunbari*	A-A'	39	**1.63**	**-4.20**	t	NL/SL	w
CONC	*N. dunbari*	A-A'	40	**1.86**	**-4.25**	t	NL/SL	w
CONC	*N. dunbari*	A-A'	41	**2.02**	**-4.02**	t	NL/SL	w
CONC	*N. dunbari*	A-A'	42	**2.08**	**-4.28**	t	NL/SL	w
CONC	*N. dunbari*	A-A'	43	**2.16**	**-4.26**	t	NL/SL	w
CONC	*N. dunbari*	A-A'	44	**1.89**	**-4.71**	t	NL/SL	w
CONC	*N. dunbari*	A-A'	45	**2.12**	**-4.14**	t	NL/SL	w
CONC	*N. dunbari*	A-A'	46	**1.93**	**-4.19**	t	SL/NL	W
CONC	*N. dunbari*	B-B'	1	**1.19**	**-3.76**	s	SL/NL	w
CONC	*N. dunbari*	B-B'	2	**2.84**	**-3.73**	t	NL/SL	w

Specimen	Species	Transect	Sample #	$\delta^{13}C$	$\delta^{18}O$	Material	L.C.	Fabric
CONC	*N. dunbari*	B-B'	3	**2.87**	**-3.65**	t	NL/SL	w
CONC	*N. dunbari*	B-B'	4	**2.73**	**-3.91**	t	NL/SL	w
CONC	*N. dunbari*	B-B'	5	**2.79**	**-3.90**	t	NL/SL	w
CONC	*N. dunbari*	B-B'	6	**2.75**	**-3.91**	t	NL/SL	w
CONC	*N. dunbari*	B-B'	7	**2.73**	**-3.91**	t	NL/SL	w
CONC	*N. dunbari*	B-B'	8	**2.63**	**-4.00**	t	NL/SL	w
CONC	*N. dunbari*	B-B'	9	**2.60**	**-3.94**	t	NL/SL	w
CONC	*N. dunbari*	B-B'	10	**2.54**	**-3.91**	t	NL/SL	w
CONC	*N. dunbari*	B-B'	11	**2.54**	**-3.76**	t	NL/SL	w
CONC	*N. dunbari*	B-B'	12	**2.43**	**-4.01**	t	NL/SL	w
CONC	*N. dunbari*	B-B'	13	**2.37**	**-3.77**	t	NL/SL	w
CONC	*N. dunbari*	B-B'	14	**2.22**	**-3.93**	t	NL/SL	w
CONC	*N. dunbari*	B-B'	15	**2.34**	**-3.92**	t	NL/SL	w
CONC	*N. dunbari*	B-B'	16	**2.25**	**-4.06**	t	NL/SL	w
CONC	*N. dunbari*	B-B'	17	**2.22**	**-3.85**	t	NL/SL	w
CONC	*N. dunbari*	B-B'	19	**2.20**	**-4.03**	t	NL/SL	w
CONC	*N. dunbari*	B-B'	20	**2.25**	**-4.01**	t	NL/SL	w
CONC	*N. dunbari*	B-B'	21	**2.26**	**-4.01**	t	NL/SL	w
CONC	*N. dunbari*	B-B'	22	**2.09**	**-4.09**	t	NL/SL	w
CONC	*N. dunbari*	B-B'	23	**2.06**	**-4.09**	t	NL/SL	w
CONC	*N. dunbari*	B-B'	24	**1.78**	**-4.25**	t	SL/NL	w
A01-1	*C. planoconvexa*	n/a	a	**2.75**	**-3.45**	s	NL/SL	W
A01-1	*C. planoconvexa*	n/a	b	**-2.91**	**-4.81**	m	L	n/a
A01-1	*C. planoconvexa*	n/a	c	**2.93**	**-3.51**	s	NL/SL	W
A01-2	*C. planoconvexa*	n/a	a	**2.17**	**-3.75**	s	SL/NL	P
A01-2	*C. planoconvexa*	n/a	b	**-3.50**	**-5.15**	m	L	n/a
A01-6	*C. planoconvexa*	n/a	a	**3.10**	**-3.09**	s	NL/SL	W
A01-6	*C. planoconvexa*	n/a	c	**3.29**	**-2.89**	s	NL/SL	W
A01-6	*C. planoconvexa*	n/a	d	**-3.47**	**-5.65**	m	L	n/a
AMA3-1	*C. planoconvexa*	n/a	a	**1.40**	**-3.59**	s	NL/SL	W
AMA3-1	*C. planoconvexa*	n/a	b	**0.79**	**-3.46**	s	NL/SL	W
AMA3-1	*C. planoconvexa*	n/a	c	**1.69**	**-3.63**	s	NL/SL	W
AMA3-1	*C. planoconvexa*	n/a	d	**-4.87**	**-3.89**	m	L	n/a
AMA3-1	*C. planoconvexa*	n/a	e	**-5.34**	**-4.06**	m	L	n/a
AMA3-2	*C. planoconvexa*	n/a	a	**-3.33**	**-4.03**	s	SL/L	w
AMA3-2	*C. planoconvexa*	n/a	b	**-1.00**	**-3.90**	s	SL/L	w
AMA3-3	*C. planoconvexa*	n/a	a	**-0.02**	**-3.52**	s	SL/L	w
AMA3-3	*C. planoconvexa*	n/a	b	**-0.28**	**-3.58**	s	SL/L	w
AMA5-1	*C. planoconvexa*	n/a	a	**1.09**	**-3.62**	s	SL	w

Specimen	Species	Transect	Sample #	$\delta^{13}C$	$\delta^{18}O$	Material	L.C.	Fabric
AMA5-3	*C. planoconvexa*	n/a	a	**1.67**	**-3.37**	s	SL/L	w
AMA5-3	*C. planoconvexa*	n/a	b	**-1.20**	**-3.91**	s	SL/L	w
AMP1B-1	*C. planoconvexa*	n/a	a	**1.07**	**-4.29**	s	NL/SL	w
AMP1B-1	*C. planoconvexa*	n/a	b	**2.26**	**-3.79**	s	NL/SL	w
AMP1B-2	*C. planoconvexa*	n/a	a	**2.25**	**-3.83**	s	SL/L	w
AMP1B-3	*C. planoconvexa*	n/a	a	**-0.39**	**-5.44**	s	L	w
AMP1B-4	*C. planoconvexa*	n/a	a	**1.93**	**-4.22**	s	NL	w
AMP1B-4	*C. planoconvexa*	n/a	b	**2.35**	**-3.94**	s	NL	w
AMP1B-4	*C. planoconvexa*	n/a	c	**2.15**	**-4.22**	s	NL	w
AMP1B-5	*C. planoconvexa*	n/a	a	**1.41**	**-4.41**	s	NL/SL	w
BELL5-1	*C. planoconvexa*	n/a	a	**1.66**	**-3.67**	s	SL/L	w
BELL5-1	*C. planoconvexa*	n/a	b	**2.27**	**-3.78**	s	SL/L	w
BELL5-4	*C. planoconvexa*	n/a	a	**2.32**	**-3.68**	s	NL/SL	w
BELL5-4	*C. planoconvexa*	n/a	b	**2.40**	**-3.80**	s	NL/SL	w
BELL5-5	*C. planoconvexa*	n/a	a	**2.21**	**-3.65**	s	NL	w
BELL5-5	*C. planoconvexa*	n/a	b	**2.37**	**-3.52**	s	NL	w
BELL5-5	*C. planoconvexa*	n/a	c	**2.20**	**-3.69**	s	NL	w
BELL5-5	*C. planoconvexa*	n/a	d	**-7.84**	**-6.92**	m	L	n/a
BELL5-5	*C. planoconvexa*	n/a	e	**-7.06**	**-6.98**	m	L	n/a
BELL5-6	*C. planoconvexa*	n/a	a	**1.12**	**-4.44**	s	NL/SL	w
BELL5-6	*C. planoconvexa*	n/a	b	**2.59**	**-3.59**	s	NL/SL	w
FAIR4a-1	*C. planoconvexa*	n/a	a	**1.44**	**-3.69**	s	NL/SL	w
FAIR4a-1	*C. planoconvexa*	n/a	b	**2.03**	**-3.68**	s	NL/SL	w
FAIR4a-1	*C. planoconvexa*	n/a	c	**1.42**	**-3.85**	s	NL/SL	w
FAIR4a-2	*C. planoconvexa*	n/a	a	**2.08**	**-3.89**	s	NL/SL	w
FAIR4a-2	*C. planoconvexa*	n/a	b	**1.95**	**-4.09**	s	NL/SL	w
FAIR4a-2	*C. planoconvexa*	n/a	c	**1.98**	**-4.13**	s	NL/SL	w
FAIR4a-3	*C. planoconvexa*	n/a	a	**0.95**	**-4.07**	s	SL/NL	w
FAIR4a-3	*C. planoconvexa*	n/a	b	**1.09**	**-4.06**	s	SL/NL	w
FAIR4a-3	*C. planoconvexa*	n/a	c	**1.22**	**-4.01**	s	SL/NL	w
FAIR4a-4	*C. planoconvexa*	n/a	a	**1.54**	**-3.73**	s	SL/NL	w
FAIR4a-6	*C. planoconvexa*	n/a	a	**1.29**	**-4.42**	s	NL	w
FAIR5-1	*C. planoconvexa*	n/a	a	**1.78**	**-3.77**	s	NL/SL	w
FAIR5-3	*C. planoconvexa*	n/a	a	**1.90**	**-3.74**	s	NL/SL	w
FAIR5-3	*C. planoconvexa*	n/a	b	**2.07**	**-3.82**	s	NL/SL	w
FAIR5-3	*C. planoconvexa*	n/a	c	**2.27**	**-3.65**	s	NL/SL	w
FAIR5-4	*C. planoconvexa*	n/a	a	**1.84**	**-3.94**	s	SL	w
FAIR5-5	*C. planoconvexa*	n/a	a	**1.65**	**-3.93**	s	NL/SL	w
FAIR5-5	*C. planoconvexa*	n/a	b	**1.56**	**-3.86**	s	NL/SL	w

Specimen	Species	Transect	Sample #	$\delta^{13}C$	$\delta^{18}O$	Material	L.C.	Fabric
FAIR5-5	*C. planoconvexa*	n/a	c	**1.99**	**-3.66**	s	NL/SL	w
FAIR5-6	*C. planoconvexa*	n/a	a	**1.62**	**-3.48**	s	SL	w
GRR5a-1	*C. planoconvexa*	n/a	a	**0.44**	**-4.29**	s	NL/SL	w
GRR5a-1	*C. planoconvexa*	n/a	b	**1.27**	**-4.35**	s	NL/SL	w
GRR5a-2	*C. planoconvexa*	n/a	a	**1.50**	**-3.86**	s	SL	w
GRR5a-3	*C. planoconvexa*	n/a	a	**1.32**	**-4.26**	s	SL	w
GRR5a-4	*C. planoconvexa*	n/a	a	**1.59**	**-4.28**	s	NL/SL	w
GRRId-1	*C. planoconvexa*	n/a	a	**1.44**	**-3.75**	s	NL/SL	w
GRRId-1	*C. planoconvexa*	n/a	b	**1.12**	**-3.91**	s	NL/SL	w
GRRId-2	*C. planoconvexa*	n/a	a	**1.73**	**-3.97**	s	NL	w
GRRId-2	*C. planoconvexa*	n/a	b	**1.70**	**-3.89**	s	NL	w
GRRId-2	*C. planoconvexa*	n/a	c	**1.70**	**-3.90**	s	NL	w
GRRId-3	*C. planoconvexa*	n/a	a	**0.35**	**-4.66**	s	SL/NL	w
GRRId-5	*C. planoconvexa*	n/a	a	**0.26**	**-4.46**	s	NL/SL	w
GRRId-5	*C. planoconvexa*	n/a	b	**1.44**	**-3.67**	s	NL/SL	w
GRRId-5	*C. planoconvexa*	n/a	c	**1.28**	**-3.66**	s	NL/SL	w
GRRId-6	*C. planoconvexa*	n/a	a	**1.45**	**-3.92**	s	NL/SL	p
GRRId-7	*C. planoconvexa*	n/a	a	**1.82**	**-4.10**	s	NL/SL	w
GRRId-7	*C. planoconvexa*	n/a	b	**1.72**	**-4.12**	s	NL/SL	w
GRRId-7	*C. planoconvexa*	n/a	c	**1.93**	**-4.10**	s	NL/SL	w
GRRId-8	*C. planoconvexa*	n/a	a	**2.10**	**-4.00**	s	NL/SL	w
GRRId-9	*C. planoconvexa*	n/a	a	**0.74**	**-4.69**	s	NL/SL	p
GRRId-10	*C. planoconvexa*	n/a	a	**1.52**	**-3.82**	s	SL	w
GRRId-M	*C. planoconvexa*	n/a	1	**-6.27**	**-7.95**	m	L	n/a
GRRId-M	*C. planoconvexa*	n/a	2	**-6.97**	**-8.80**	m	L	n/a
GRRIIa-1	*C. planoconvexa*	n/a	a	**1.59**	**-4.11**	s	NL/SL	w
GRRIIa-1	*C. planoconvexa*	n/a	b	**1.66**	**-4.00**	s	NL/SL	w
GRRIIa-4	*C. planoconvexa*	n/a	a	**1.68**	**-4.28**	s	NL/SL	w
GRRIIa-5	*C. planoconvexa*	n/a	a	**1.28**	**-4.11**	s	SL/NL	w
GRRIIa-8	*C. planoconvexa*	n/a	a	**2.09**	**-3.56**	s	NL/SL	w
GRRIIa-8	*C. planoconvexa*	n/a	b	**2.03**	**-3.73**	s	NL/SL	w
GRRIIa-8	*C. planoconvexa*	n/a	c	**-0.33**	**-5.27**	m	NL/SL	w
GRRIIa-12	*C. planoconvexa*	n/a	a	**1.81**	**-3.86**	s	NL/SL	w
GRRVIa-1	*C. planoconvexa*	n/a	a	**-5.23**	**-4.83**	m	L	n/a
GRRVIa-3	*C. planoconvexa*	n/a	a	**-0.42**	**-4.15**	s	L	w
GRRVIa-3	*C. planoconvexa*	n/a	b	**-0.04**	**-4.58**	s	L	w
GRRVIa-3	*C. planoconvexa*	n/a	c	**1.27**	**-4.09**	s	L	w
GRRVIa-3	*C. planoconvexa*	n/a	d	**-7.29**	**-7.46**	m	L	n/a
GRRVIa-3	*C. planoconvexa*	n/a	e	**-6.90**	**-7.67**	m	L	n/a

Specimen	Species	Transect	Sample #	$\delta^{13}C$	$\delta^{18}O$	Material	L.C.	Fabric
GRRVIa-10	*C. planoconvexa*	n/a	a	**1.20**	**-3.41**	s	L	w
GRRVIa-10	*C. planoconvexa*	n/a	b	**1.91**	**-3.35**	s	L	w
GRRVIa-10	*C. planoconvexa*	n/a	c	**-6.15**	**-5.98**	m	L	n/a
GRRVIa-10	*C. planoconvexa*	n/a	d	**-4.59**	**-5.36**	m	L	n/a
A01-3	*C. planoconvexa*	A-A'	1	**2.52**	**-3.55**	s	SL/NL	w
A01-3	*C. planoconvexa*	A-A'	2	**2.92**	**-3.35**	s	SL/NL	w
A01-3	*C. planoconvexa*	A-A'	3	**2.86**	**-3.56**	s	SL/NL	w
A01-3	*C. planoconvexa*	A-A'	4	**3.04**	**-3.43**	s	SL/NL	w
A01-3	*C. planoconvexa*	A-A'	5	**2.63**	**-3.66**	s	SL/NL	w
A01-3	*C. planoconvexa*	A-A'	6	**1.86**	**-1.43**	m	L	n/a
A01-3	*C. planoconvexa*	A-A'	7	**-1.64**	**-4.87**	m	L	n/a
A01-3	*C. planoconvexa*	A-A'	8	**-4.46**	**-6.30**	m	L	n/a
A01-3	*C. planoconvexa*	A-A'	9	**-5.00**	**-6.43**	m	L	n/a
A01-3	*C. planoconvexa*	A-A'	10	**-5.57**	**-6.71**	m	L	n/a
A01-3	*C. planoconvexa*	A-A'	11	**-5.74**	**-6.74**	m	L	n/a
A01-3	*C. planoconvexa*	A-A'	12	**-5.99**	**-7.25**	m	L	n/a
A01-3	*C. planoconvexa*	A-A'	13	**-5.78**	**-7.13**	m	L	n/a
A01-3	*C. planoconvexa*	A-A'	14	**-5.90**	**-6.89**	m	L	n/a
A01-3	*C. planoconvexa*	A-A'	15	**-6.55**	**-7.53**	m	L	n/a
A01-3	*C. planoconvexa*	A-A'	16	**-7.23**	**-8.27**	m	L	n/a
A01-3	*C. planoconvexa*	A-A'	17	**-7.30**	**-8.63**	m	L	n/a
A01-3	*C. planoconvexa*	A-A'	18	**-6.99**	**-8.05**	m	L	n/a
E01-3	*C. planoconvexa*	A-A'	1	**1.08**	**-3.81**	s	SL/NL	w
E01-3	*C. planoconvexa*	A-A'	2	**2.19**	**-3.79**	s	SL/NL	w
E01-3	*C. planoconvexa*	A-A'	3	**2.25**	**-3.77**	s	SL/NL	w
E01-3	*C. planoconvexa*	A-A'	4	**2.08**	**-3.78**	s	SL/NL	w
E01-3	*C. planoconvexa*	A-A'	5	**3.27**	**0.43**	s	SL/NL	w
E01-3	*C. planoconvexa*	A-A'	6	**-1.81**	**-4.48**	s	SL/NL	w
E01-3	*C. planoconvexa*	A-A'	7	**-3.94**	**-4.67**	m	L	n/a
E01-3	*C. planoconvexa*	A-A'	8	**-5.73**	**-4.89**	m	L	n/a
E01-3	*C. planoconvexa*	A-A'	9	**-8.42**	**-6.56**	m	L	n/a
E01-3	*C. planoconvexa*	A-A'	10	**-9.72**	**-7.58**	m	L	n/a
E01-3	*C. planoconvexa*	A-A'	11	**-10.33**	**-7.07**	m	L	n/a
E01-3	*C. planoconvexa*	A-A'	12	**-10.18**	**-8.22**	m	L	n/a
E01-3	*C. planoconvexa*	A-A'	13	**-9.58**	**-11.00**	m	L	n/a
E01-3	*C. planoconvexa*	A-A'	14	**-8.84**	**-10.60**	m	L	n/a
E01-3	*C. planoconvexa*	A-A'	15	**-9.74**	**-9.14**	m	L	n/a
E01-3	*C. planoconvexa*	A-A'	16	**-8.79**	**-10.86**	m	L	n/a

APPENDIX II

TRACE ELEMENT DATA

N. dunbari=Neospirifer dunbari; *C. planoconvexa=Crurithyris planoconvexa*
-=concentration below detection limit

Specimen	Species	Transect	Sample #	x/Ca (mmol/mol)							
				Mg	Fe	Mn	Sr	S	Na	Al	Si
BRK	*N. dunbari*	A-A'	1	10.26	0.21	-	1.03	9.03	4.56	0.02	0.03
BRK	*N. dunbari*	A-A'	2	9.73	-	-	1.02	9.03	4.45	-	-
BRK	*N. dunbari*	A-A'	3	7.15	-	-	0.51	9.35	3.70	0.00	-
BRK	*N. dunbari*	A-A'	4	8.74	-	-	1.03	11.70	5.53	0.04	0.04
BRK	*N. dunbari*	A-A'	5	6.16	-	-	1.03	13.01	5.62	0.03	-
BRK	*N. dunbari*	A-A'	6	8.76	-	-	1.55	14.32	6.13	0.03	-
BRK	*N. dunbari*	A-A'	7	8.77	-	-	1.03	14.95	6.94	-	0.02
BRK	*N. dunbari*	A-A'	8	3.57	-	-	1.02	9.52	5.06	-	-
BRK	*N. dunbari*	A-A'	9	2.54	-	-	1.02	9.01	3.83	-	-
BRK	*N. dunbari*	A-A'	10	2.04	-	-	1.02	9.88	4.47	-	-
BRK	*N. dunbari*	A-A'	11	2.03	-	-	1.02	9.54	4.48	-	0.03
BRK	*N. dunbari*	A-A'	12	2.55	-	-	1.02	10.08	4.37	0.03	-
BRK	*N. dunbari*	A-A'	13	2.04	-	-	1.02	13.76	5.55	0.02	-
BRK	*N. dunbari*	A-A'	14	2.55	-	-	0.51	12.39	4.67	0.03	-
BRK	*N. dunbari*	A-A'	15	3.56	-	-	0.51	9.15	3.43	-	-
BRK	*N. dunbari*	A-A'	16	3.05	-	-	0.51	9.38	3.56	-	-
BRK	*N. dunbari*	A-A'	17	2.54	-	-	1.02	10.00	3.82	-	-
BRK	*N. dunbari*	A-A'	18	2.55	0.23	-	1.02	11.35	4.44	-	-
BRK	*N. dunbari*	A-A'	19	3.05	-	-	1.02	9.87	3.70	-	-
BRK	*N. dunbari*	A-A'	20	3.05	-	-	1.02	9.75	4.92	-	-
BRK	*N. dunbari*	A-A'	21	2.55	-	-	0.51	9.71	4.80	0.04	-
BRK	*N. dunbari*	A-A'	22	3.05	-	-	1.02	9.68	4.61	-	-
BRK	*N. dunbari*	A-A'	23	4.15	-	18.14	0.52	9.16	4.74	0.02	-
BRK	*N. dunbari*	A-A'	24	4.60	-	-	0.51	9.15	7.56	-	-
BRK	*N. dunbari*	A-A'	25	4.09	-	-	0.51	8.97	8.06	0.02	-
BRK	*N. dunbari*	B-B'	1	15.97	1.55	0.52	1.03	5.62	3.27	0.07	0.15
BRK	*N. dunbari*	B-B'	2	2.55	-	-	1.02	11.25	4.59	-	-
BRK	*N. dunbari*	B-B'	3	4.07	-	-	0.51	9.85	3.79	-	-
BRK	*N. dunbari*	B-B'	4	2.54	-	-	0.51	9.86	3.53	-	-
BRK	*N. dunbari*	B-B'	5	3.06	-	-	1.02	10.82	3.74	-	-
BRK	*N. dunbari*	B-B'	6	3.57	-	-	1.02	11.20	3.89	-	-
BRK	*N. dunbari*	B-B'	7	2.04	-	-	1.02	10.80	3.85	-	-
BRK	*N. dunbari*	B-B'	8	2.03	-	-	1.01	8.37	2.57	0.02	-

Specimen	Species	Transect	Sample #	x/Ca (mmol/mol)							
				Mg	Fe	Mn	Sr	S	Na	Al	Si
BRK	*N. dunbari*	B-B'	9	3.56	-	-	1.02	8.60	3.25	0.02	0.03
BRK	*N. dunbari*	B-B'	10	3.05	-	-	0.51	7.48	4.22	0.02	-
BRK	*N. dunbari*	B-B'	11	2.54	-	-	1.02	8.54	3.63	0.03	-
BRK	*N. dunbari*	B-B'	12	2.03	-	-	1.01	6.92	2.57	0.02	-
BRK	*N. dunbari*	B-B'	13	2.53	-	0.51	0.51	6.87	2.64	-	-
BRK	*N. dunbari*	B-B'	14	2.54	-	-	1.02	8.06	3.13	-	-
BRK	*N. dunbari*	B-B'	15	3.04	-	-	0.51	8.21	2.84	-	-
BRK	*N. dunbari*	B-B'	16	2.53	-	-	0.51	7.62	3.36	-	-
BRK	*N. dunbari*	B-B'	17	2.03	-	-	0.51	8.49	4.29	-	-
BRK	*N. dunbari*	B-B'	18	2.03	-	-	0.51	8.86	3.54	-	0.02
BRK	*N. dunbari*	B-B'	19	2.03	0.51	-	0.51	8.66	3.55	0.04	-
BRK	*N. dunbari*	B-B'	20	2.54	-	-	1.02	9.32	3.27	-	-
BRK	*N. dunbari*	B-B'	21	3.05	-	-	1.02	7.92	3.11	-	-
BRK	*N. dunbari*	B-B'	22	7.20	-	-	1.03	12.49	6.94	-	-
BRK	*N. dunbari*	B-B'	23	2.55	-	-	1.02	11.93	4.88	-	-
BRK	*N. dunbari*	B-B'	24	2.55	-	-	1.02	11.42	5.75	-	-
BRK	*N. dunbari*	B-B'	25	6.63	-	-	0.51	7.63	4.83	-	-
GRR-1	*N. dunbari*	A-A'	1	6.11	-	0.51	1.53	7.15	4.54	-	-
GRR-1	*N. dunbari*	A-A'	2	3.04	-	0.68	0.51	7.08	5.99	-	-
GRR-1	*N. dunbari*	A-A'	3	2.54	-	0.29	1.01	8.45	5.03	0.35	0.05
GRR-1	*N. dunbari*	A-A'	4	2.02	-	-	1.01	8.04	4.93	0.27	-
GRR-1	*N. dunbari*	A-A'	5	3.04	-	0.51	1.01	7.31	3.95	0.26	0.02
GRR-1	*N. dunbari*	A-A'	6	2.53	-	0.39	1.01	9.17	6.06	0.30	-
GRR-1	*N. dunbari*	A-A'	7	3.03	-	0.42	0.51	8.49	5.95	-	-
GRR-1	*N. dunbari*	A-A'	8	2.02	-	-	1.01	7.45	5.42	0.04	-
GRR-1	*N. dunbari*	A-A'	9	3.03	-	-	1.01	8.15	5.74	-	0.07
GRR-1	*N. dunbari*	A-A'	10	3.54	-	0.21	1.01	7.82	4.68	-	-
GRR-1	*N. dunbari*	A-A'	11	2.52	-	0.22	1.01	8.30	5.76	0.36	-
GRR-1	*N. dunbari*	A-A'	12	3.03	-	-	1.01	6.79	5.03	-	0.33
GRR-1	*N. dunbari*	A-A'	13	3.54	0.51	-	1.01	6.68	4.84	-	-
GRR-1	*N. dunbari*	A-A'	14	2.53	-	-	1.01	7.95	4.60	0.20	0.22
GRR-1	*N. dunbari*	A-A'	15	3.04	-	-	1.01	6.20	3.39	-	-
GRR-1	*N. dunbari*	A-A'	16	2.53	-	0.51	1.01	6.78	3.56	-	-
GRR-1	*N. dunbari*	A-A'	17	2.53	-	-	1.01	7.19	-	-	-
GRR-1	*N. dunbari*	A-A'	18	3.03	-	0.69	1.01	9.03	6.44	0.15	-
GRR-1	*N. dunbari*	A-A'	19	3.54	-	0.27	1.01	6.43	4.48	-	0.21
GRR-1	*N. dunbari*	A-A'	20	4.05	-	0.51	1.01	5.90	3.84	0.21	-
GRR-1	*N. dunbari*	A-A'	21	2.53	-	0.20	1.01	6.40	3.93	0.17	-

Specimen	Species	Transect	Sample #	x/Ca (mmol/mol)							
				Mg	Fe	Mn	Sr	S	Na	Al	Si
GRR-1	*N. dunbari*	A-A'	22	5.08	-	-	0.51	6.21	4.34	0.25	-
GRR-1	*N. dunbari*	A-A'	23	3.54	-	-	0.51	4.48	3.05	-	-
GRR-1	*N. dunbari*	A-A'	24	3.03	0.19	-	1.01	5.62	3.40	-	-
GRR-1	*N. dunbari*	A-A'	25	4.55	-	-	0.51	6.11	3.35	0.17	-
GRR-1	*N. dunbari*	A-A'	26	3.04	-	-	1.01	7.71	4.33	0.18	-
GRR-1	*N. dunbari*	A-A'	27	3.55	0.21	0.41	1.01	11.65	6.79	-	-
GRR-1	*N. dunbari*	A-A'	28	3.03	-	0.55	1.01	11.92	6.05	-	-
GRR-1	*N. dunbari*	A-A'	29	2.52	-	-	0.50	8.65	4.57	0.34	-
GRR-1	*N. dunbari*	A-A'	30	5.59	-	0.51	0.51	8.82	5.40	0.33	0.09
GRR-9	*N. dunbari*	A-A'	1	3.03	-	-	0.50	3.82	2.02	0.23	-
GRR-9	*N. dunbari*	A-A'	2	3.05	-	-	1.02	8.40	3.28	-	0.25
GRR-9	*N. dunbari*	A-A'	3	2.54	-	-	1.02	9.62	3.86	-	-
GRR-9	*N. dunbari*	A-A'	4	2.52	-	-	0.50	4.61	1.76	0.13	-
GRR-9	*N. dunbari*	A-A'	5	4.05	-	-	0.51	5.72	2.17	-	-
GRR-9	*N. dunbari*	A-A'	6	3.05	-	-	1.02	8.35	2.79	-	-
GRR-9	*N. dunbari*	A-A'	7	3.57	-	-	1.02	11.01	4.58	-	0.28
GRR-9	*N. dunbari*	A-A'	8	3.05	-	-	0.51	10.30	4.13	-	-
GRR-9	*N. dunbari*	A-A'	9	2.54	-	-	1.02	9.04	3.53	-	-
GRR-9	*N. dunbari*	A-A'	10	2.54	-	-	1.02	8.69	3.10	-	-
GRR-9	*N. dunbari*	A-A'	11	2.52	-	-	0.50	2.93	1.38	-	-
GRR-9	*N. dunbari*	A-A'	12	2.02	-	-	0.51	5.78	2.09	-	0.20
GRR-9	*N. dunbari*	A-A'	13	3.03	-	-	1.01	4.93	1.79	-	0.22
GRR-9	*N. dunbari*	A-A'	14	3.02	-	-	1.01	2.84	1.38	-	-
GRR-9	*N. dunbari*	A-A'	15	4.05	-	-	0.51	5.08	2.26	-	-
GRR-9	*N. dunbari*	A-A'	16	3.05	-	0.23	0.51	8.05	4.12	-	-
GRR-9	*N. dunbari*	A-A'	17	2.02	-	-	1.01	4.84	2.10	-	-
GRR-9	*N. dunbari*	A-A'	18	3.56	-	-	1.02	7.11	4.00	0.33	-
GRR-9	*N. dunbari*	A-A'	19	3.04	-	-	1.01	6.67	2.86	-	-
GRR-9	*N. dunbari*	A-A'	20	3.04	0.51	0.51	0.51	6.07	2.57	-	0.29
GRR-9	*N. dunbari*	A-A'	21	3.57	0.51	-	1.02	9.56	4.78	-	-
GRR-9	*N. dunbari*	A-A'	22	3.05	-	-	1.02	8.16	3.95	-	0.22
GRR-9	*N. dunbari*	A-A'	23	3.04	-	-	0.51	6.92	3.43	-	-
GRR-9	*N. dunbari*	A-A'	24	3.56	-	-	0.51	8.21	3.91	-	0.24
GRR-9	*N. dunbari*	A-A'	25	4.08	-	-	1.02	9.32	4.51	0.25	-
GRR-9	*N. dunbari*	A-A'	26	3.05	-	-	1.02	7.93	4.14	0.30	-
GRR-9	*N. dunbari*	A-A'	27	3.05	-	-	1.02	7.99	3.43	0.32	-
GRR-9	*N. dunbari*	A-A'	28	5.58	-	-	0.51	5.46	2.74	-	0.32
GRR-9	*N. dunbari*	A-A'	29	3.56	-	-	1.02	7.86	3.47	-	-

Specimen	Species	Transect	Sample #	x/Ca (mmol/mol)							
				Mg	Fe	Mn	Sr	S	Na	Al	Si
GRR-9	*N. dunbari*	A-A'	30	4.05	-	-	0.51	4.78	2.03	0.41	-
GRR-9	*N. dunbari*	A-A'	31	3.55	-	-	1.01	5.76	2.48	-	0.31
GRR-9	*N. dunbari*	A-A'	32	4.58	-	-	0.51	7.94	3.91	-	0.03
GRR-9	*N. dunbari*	A-A'	33	4.58	0.19	-	1.02	7.52	4.10	-	0.06
GRR-9	*N. dunbari*	A-A'	34	3.04	-	-	0.51	7.16	3.36	-	-
GRR-9	*N. dunbari*	A-A'	35	3.56	-	-	1.02	7.29	3.99	0.30	-
GRR-9	*N. dunbari*	A-A'	36	4.07	-	0.51	1.02	7.32	3.67	-	0.03
GRR-9	*N. dunbari*	A-A'	37	4.07	-	-	1.02	7.59	3.53	-	-
GRR-9	*N. dunbari*	A-A'	38	4.07	-	-	1.02	7.81	4.47	-	-
GRR-9	*N. dunbari*	A-A'	39	4.59	-	-	1.02	9.18	5.30	-	-
GRR-9	*N. dunbari*	A-A'	40	5.09	-	-	1.02	7.12	4.56	0.81	-
MID-2	*N. dunbari*	A-A'	1	2.04	-	-	0.51	8.54	3.28	2.96	-
MID-2	*N. dunbari*	A-A'	2	2.57	-	-	1.03	10.20	3.87	11.35	-
MID-2	*N. dunbari*	A-A'	3	2.56	-	0.51	0.51	9.15	3.54	6.44	-
MID-2	*N. dunbari*	A-A'	4	2.54	-	-	1.02	8.37	3.44	1.63	-
MID-2	*N. dunbari*	A-A'	5	3.08	-	-	1.03	10.83	4.90	6.40	0.43
MID-2	*N. dunbari*	A-A'	6	2.55	0.24	-	1.02	10.25	3.53	4.75	0.20
MID-2	*N. dunbari*	A-A'	7	5.13	-	-	1.03	12.20	4.86	1.59	0.27
MID-2	*N. dunbari*	A-A'	8	2.57	-	-	1.03	9.03	3.24	10.33	0.23
MID-2	*N. dunbari*	A-A'	9	2.55	-	-	0.51	8.26	2.93	4.72	-
MID-2	*N. dunbari*	A-A'	10	4.09	-	0.21	1.02	9.35	3.52	4.21	-
MID-2	*N. dunbari*	A-A'	11	3.56	-	-	0.51	8.88	3.41	1.38	-
MID-2	*N. dunbari*	A-A'	12	5.09	-	-	1.02	6.43	5.59	-	0.27
MID-2	*N. dunbari*	A-A'	13	3.05	-	-	0.51	6.35	3.33	1.93	-
MID-2	*N. dunbari*	A-A'	14	2.54	-	-	1.01	6.75	3.26	0.23	-
MID-2	*N. dunbari*	A-A'	15	2.54	-	-	1.01	6.99	3.55	0.36	-
MID-2	*N. dunbari*	A-A'	16	3.56	-	-	0.51	7.62	4.32	0.25	0.22
MID-2	*N. dunbari*	A-A'	17	2.03	-	-	1.01	6.32	3.07	-	-
MID-2	*N. dunbari*	A-A'	18	2.03	-	-	0.51	6.87	3.08	0.00	0.33
MID-2	*N. dunbari*	A-A'	19	2.54	-	-	1.02	7.20	2.91	1.11	-
MID-2	*N. dunbari*	A-A'	20	3.56	-	-	1.02	7.53	3.75	0.19	-
MID-2	*N. dunbari*	A-A'	21	4.07	-	-	0.51	8.24	4.56	-	-
MID-2	*N. dunbari*	A-A'	22	2.02	0.51	-	0.51	4.59	3.23	0.19	-
MID-2	*N. dunbari*	A-A'	23	2.03	-	-	0.00	7.19	3.53	0.29	0.21
MID-2	*N. dunbari*	A-A'	24	2.53	-	-	0.51	5.80	2.58	0.69	-
MID-2	*N. dunbari*	A-A'	25	3.05	-	-	0.51	7.56	3.57	0.26	-
MID-2	*N. dunbari*	A-A'	26	2.03	-	-	1.01	6.40	3.05	0.37	-
MID-2	*N. dunbari*	A-A'	27	2.53	-	-	0.51	5.36	1.53	0.23	-

Specimen	Species	Transect	Sample #	x/Ca (mmol/mol)							
				Mg	Fe	Mn	Sr	S	Na	Al	Si
MID-2	*N. dunbari*	A-A'	28	5.10	-	-	1.02	10.05	4.15	-	0.52
MID-2	*N. dunbari*	A-A'	29	7.15	-	-	0.51	9.31	3.85	0.33	-
MID-2	*N. dunbari*	A-A'	30	9.78	-	0.51	1.03	11.81	6.09	0.51	0.33
MID-2	*N. dunbari*	B-B'	1	3.05	-	-	0.51	7.79	3.16	0.40	-
MID-2	*N. dunbari*	B-B'	2	4.58	-	-	1.02	7.52	4.31	0.55	-
MID-2	*N. dunbari*	B-B'	3	3.56	-	-	0.51	7.25	4.51	-	0.38
MID-2	*N. dunbari*	B-B'	4	2.53	-	-	0.51	7.26	3.25	-	-
MID-2	*N. dunbari*	B-B'	5	4.07	-	-	1.02	8.27	4.61	0.88	-
MID-2	*N. dunbari*	B-B'	6	2.54	-	-	1.01	6.68	3.63	0.89	-
MID-2	*N. dunbari*	B-B'	7	3.04	0.21	-	1.01	6.48	3.12	-	-
MID-2	*N. dunbari*	B-B'	8	2.54	-	-	1.02	7.80	3.74	0.75	-
MID-2	*N. dunbari*	B-B'	9	2.54	-	-	1.01	7.65	3.01	0.20	-
MID-2	*N. dunbari*	B-B'	10	3.04	-	-	1.01	6.17	3.02	0.32	0.04
MID-2	*N. dunbari*	B-B'	11	3.05	-	-	1.02	7.59	3.83	0.41	0.17
MID-2	*N. dunbari*	B-B'	12	3.05	-	-	1.02	8.69	3.90	1.25	-
MID-2	*N. dunbari*	B-B'	13	3.55	-	-	0.51	6.07	2.09	1.07	0.18
MID-2	*N. dunbari*	B-B'	14	4.58	-	-	0.51	8.55	4.03	1.19	-
MID-2	*N. dunbari*	B-B'	15	2.54	-	-	1.02	9.53	3.41	0.92	0.20
MID-2	*N. dunbari*	B-B'	16	2.54	-	-	0.51	7.95	3.35	0.61	-
MID-2	*N. dunbari*	B-B'	17	2.53	0.21	-	0.51	7.04	2.38	0.33	-
MID-2	*N. dunbari*	B-B'	18	3.56	-	-	0.51	9.25	3.73	-	-
MID-2	*N. dunbari*	B-B'	19	2.53	-	-	0.51	5.66	1.39	0.32	-
MID-2	*N. dunbari*	B-B'	20	5.06	0.23	-	0.00	5.38	1.45	-	-
MID-2	*N. dunbari*	B-B'	21	3.06	-	-	1.02	10.55	4.03	-	0.20
MID-2	*N. dunbari*	B-B'	22	3.05	-	-	1.02	8.69	3.42	0.24	-
MID-2	*N. dunbari*	B-B'	23	5.09	0.23	-	0.51	8.03	2.35	0.39	0.25
MID-2	*N. dunbari*	B-B'	24	2.03	-	-	0.51	7.38	2.18	0.32	-
MID-2	*N. dunbari*	B-B'	25	4.56	-	-	0.51	5.62	1.74	0.67	-
MID-2	*N. dunbari*	B-B'	26	6.65	-	-	1.02	10.37	4.95	0.18	0.22
MID-2	*N. dunbari*	B-B'	27	5.09	-	-	1.02	8.09	4.23	0.45	0.08
MID-2	*N. dunbari*	B-B'	28	2.54	-	-	0.00	6.96	2.89	4.69	-
MID-2	*N. dunbari*	B-B'	29	2.53	-	-	0.51	6.22	2.63	0.20	-
MID-2	*N. dunbari*	B-B'	30	36.71	-	7.34	0.52	1.48	0.02	0.96	1.23
RED	*N. dunbari*	A-A'	1	4.07	-	0.51	0.51	7.58	5.94	-	-
RED	*N. dunbari*	A-A'	2	3.56	0.20	-	0.51	8.86	4.47	-	0.32
RED	*N. dunbari*	A-A'	3	4.09	-	-	0.51	11.31	5.23	0.18	0.18
RED	*N. dunbari*	A-A'	4	4.09	-	0.51	1.02	12.16	5.12	-	-
RED	*N. dunbari*	A-A'	5	4.08	-	0.51	0.51	9.51	4.19	-	-

Specimen	Species	Transect	Sample #	x/Ca (mmol/mol)							
				Mg	Fe	Mn	Sr	S	Na	Al	Si
RED	*N. dunbari*	A-A'	6	4.08	-	0.51	1.02	9.93	4.80	-	-
RED	*N. dunbari*	A-A'	7	5.09	-	0.51	1.02	7.55	3.14	0.25	-
RED	*N. dunbari*	A-A'	8	6.61	-	-	0.51	6.98	3.14	-	-
RED	*N. dunbari*	A-A'	9	3.05	-	0.51	1.02	8.79	4.05	0.37	0.24
RED	*N. dunbari*	A-A'	10	4.61	-	-	1.02	12.61	5.57	-	0.31
RED	*N. dunbari*	A-A'	11	3.06	-	-	1.02	11.95	4.89	-	0.26
RED	*N. dunbari*	A-A'	12	3.08	-	-	1.03	14.88	6.49	0.17	-
RED	*N. dunbari*	A-A'	13	2.55	-	-	0.51	12.81	5.15	-	-
RED	*N. dunbari*	A-A'	14	2.55	-	-	1.02	12.68	5.13	-	0.28
RED	*N. dunbari*	A-A'	15	3.58	0.51	-	1.02	13.77	4.98	-	-
RED	*N. dunbari*	A-A'	16	3.07	-	0.51	1.02	14.46	4.75	0.21	-
RED	*N. dunbari*	A-A'	17	3.59	-	-	1.03	14.39	6.09	-	0.25
RED	*N. dunbari*	A-A'	18	3.06	-	-	0.51	12.42	5.16	0.25	-
RED	*N. dunbari*	A-A'	19	3.06	-	-	0.51	12.71	5.11	-	-
RED	*N. dunbari*	A-A'	20	2.04	-	-	0.51	12.53	5.53	-	-
RED	*N. dunbari*	A-A'	21	3.07	-	-	1.02	12.70	5.12	-	0.43
RED	*N. dunbari*	A-A'	22	3.07	-	-	1.02	13.45	5.35	-	-
RED	*N. dunbari*	A-A'	23	2.55	-	-	1.02	11.86	4.80	-	-
RED	*N. dunbari*	A-A'	24	3.07	-	-	1.02	13.85	5.43	-	0.22
RED	*N. dunbari*	A-A'	25	3.04	-	-	0.51	7.74	2.58	-	0.34
RED	*N. dunbari*	A-A'	26	3.05	-	-	1.02	7.97	2.97	-	-
RED	*N. dunbari*	A-A'	27	3.07	-	-	0.51	12.22	5.73	-	-
RED	*N. dunbari*	A-A'	28	2.54	0.23	-	1.02	8.65	3.10	0.22	-
RED	*N. dunbari*	A-A'	29	2.54	-	-	0.51	7.61	3.12	-	0.19
RED	*N. dunbari*	A-A'	30	6.62	-	-	1.02	7.19	3.10	-	-
RED	*N. dunbari*	B-B'	1	4.60	-	0.22	0.51	10.93	6.92	-	-
RED	*N. dunbari*	B-B'	2	4.08	-	-	0.51	10.80	4.19	-	-
RED	*N. dunbari*	B-B'	3	3.56	-	0.51	1.02	9.00	3.69	-	-
RED	*N. dunbari*	B-B'	4	3.58	-	-	0.51	13.21	5.09	0.38	0.19
RED	*N. dunbari*	B-B'	5	3.14	-	-	0.52	11.33	4.50	26.94	0.25
RED	*N. dunbari*	B-B'	6	3.05	-	-	0.51	9.83	4.79	-	-
RED	*N. dunbari*	B-B'	7	3.58	-	0.51	0.51	12.39	5.94	0.31	-
RED	*N. dunbari*	B-B'	8	4.60	-	-	1.02	10.65	4.75	0.17	0.27
RED	*N. dunbari*	B-B'	9	4.08	-	-	0.51	10.76	5.02	0.21	-
RED	*N. dunbari*	B-B'	10	4.08	-	0.51	1.02	10.15	3.74	0.18	-
RED	*N. dunbari*	B-B'	11	5.11	-	-	1.02	10.84	4.53	-	-
RED	*N. dunbari*	B-B'	12	3.06	-	-	1.02	10.95	3.39	-	0.20
RED	*N. dunbari*	B-B'	13	3.58	-	-	1.02	12.85	5.48	-	-

Specimen	Species	Transect	Sample #	x/Ca (mmol/mol)							
				Mg	Fe	Mn	Sr	S	Na	Al	Si
RED	*N. dunbari*	B-B'	14	3.07	-	-	1.02	12.58	5.63	0.20	-
RED	*N. dunbari*	B-B'	15	3.06	-	0.25	1.02	12.03	5.18	-	-
RED	*N. dunbari*	B-B'	16	2.55	-	-	1.02	10.99	4.58	-	-
RED	*N. dunbari*	B-B'	17	2.55	-	-	1.02	11.91	4.27	0.18	0.38
RED	*N. dunbari*	B-B'	18	2.04	-	0.51	1.02	12.28	4.97	-	0.23
RED	*N. dunbari*	B-B'	19	3.57	-	-	1.02	11.58	4.37	-	-
RED	*N. dunbari*	B-B'	20	2.55	0.23	-	1.02	12.29	4.16	-	0.27
RED	*N. dunbari*	B-B'	21	3.57	-	-	0.51	10.79	3.89	-	0.39
RED	*N. dunbari*	B-B'	22	2.55	-	-	0.51	11.71	4.00	0.23	-
RED	*N. dunbari*	B-B'	23	3.57	-	-	1.53	11.15	4.09	-	-
RED	*N. dunbari*	B-B'	24	3.03	-	-	0.51	5.67	1.85	-	0.39
RED	*N. dunbari*	B-B'	25	4.06	-	-	1.02	8.05	2.67	-	-
RED	*N. dunbari*	B-B'	26	3.60	-	0.24	0.51	15.66	7.93	-	-
RED	*N. dunbari*	B-B'	27	3.58	-	-	0.51	13.45	6.17	-	0.28
RED	*N. dunbari*	B-B'	28	8.79	-	0.52	1.03	16.84	7.11	0.25	-
RED	*N. dunbari*	B-B'	29	9.81	-	-	1.03	14.63	7.33	-	-
RED	*N. dunbari*	B-B'	30	7.70	-	-	1.03	9.55	7.03	-	0.39
TFF-1	*N. dunbari*	A-A'	1	17.71	-	-	1.56	15.12	7.09	0.22	-
TFF-1	*N. dunbari*	A-A'	2	4.58	-	-	0.51	8.97	2.72	-	0.20
TFF-1	*N. dunbari*	A-A'	3	2.54	-	-	1.02	10.39	3.17	-	-
TFF-1	*N. dunbari*	A-A'	4	2.03	-	-	1.02	10.19	2.74	-	-
TFF-1	*N. dunbari*	A-A'	5	3.59	-	-	1.54	15.09	5.58	-	-
TFF-1	*N. dunbari*	A-A'	6	2.54	0.27	-	1.02	10.04	3.13	-	0.24
TFF-1	*N. dunbari*	A-A'	7	2.54	-	-	1.02	9.54	3.27	-	-
TFF-1	*N. dunbari*	A-A'	8	2.04	-	-	1.02	11.72	3.93	-	-
TFF-1	*N. dunbari*	A-A'	9	2.55	-	-	1.02	12.21	5.17	-	-
TFF-1	*N. dunbari*	A-A'	10	2.04	-	-	1.02	12.19	3.90	0.17	-
TFF-1	*N. dunbari*	A-A'	11	1.53	-	-	1.02	12.10	3.65	-	-
TFF-1	*N. dunbari*	A-A'	12	2.04	-	-	1.02	12.78	4.75	-	-
TFF-1	*N. dunbari*	A-A'	13	6.17	-	-	1.03	14.36	6.23	0.02	0.29
TFF-1	*N. dunbari*	A-A'	14	2.04	-	0.20	0.51	10.53	4.01	-	-
TFF-1	*N. dunbari*	A-A'	15	2.04	-	-	1.02	11.33	3.80	-	-
TFF-1	*N. dunbari*	A-A'	16	2.55	-	-	1.02	13.64	3.53	-	0.34
TFF-1	*N. dunbari*	A-A'	17	2.03	-	-	1.01	8.18	2.31	0.18	-
TFF-1	*N. dunbari*	A-A'	18	2.53	-	-	1.01	7.39	2.23	-	0.21
TFF-1	*N. dunbari*	A-A'	19	3.05	-	-	1.02	10.57	2.86	-	-
TFF-1	*N. dunbari*	A-A'	20	2.03	-	-	1.02	10.42	2.43	-	-
TFF-1	*N. dunbari*	A-A'	21	3.05	-	-	0.51	9.16	3.40	-	0.15

Specimen	Species	Transect	Sample #	x/Ca (mmol/mol)							
				Mg	Fe	Mn	Sr	S	Na	Al	Si
TFF-1	*N. dunbari*	A-A'	22	2.04	-	-	0.51	11.31	3.58	-	-
TFF-1	*N. dunbari*	A-A'	23	3.06	-	-	1.02	12.54	3.74	-	0.46
TFF-1	*N. dunbari*	A-A'	24	2.55	-	-	0.51	13.27	4.07	0.23	-
TFF-1	*N. dunbari*	A-A'	25	2.55	-	-	1.02	12.53	3.58	-	-
TFF-1	*N. dunbari*	A-A'	26	2.55	-	-	1.02	12.89	4.41	-	-
TFF-1	*N. dunbari*	A-A'	27	3.07	-	-	1.02	12.83	4.94	-	0.32
TFF-1	*N. dunbari*	A-A'	28	2.54	-	-	1.02	10.27	3.58	-	-
TFF-1	*N. dunbari*	A-A'	29	4.07	-	-	1.02	8.18	4.28	-	-
TFF-1	*N. dunbari*	A-A'	30	4.60	-	-	1.02	10.67	5.88	0.17	-
TFF-1	*N. dunbari*	B-B'	1	15.54	0.37	-	1.04	13.63	5.65	-	-
TFF-1	*N. dunbari*	B-B'	2	6.16	-	-	0.51	13.07	6.57	-	-
TFF-1	*N. dunbari*	B-B'	3	6.11	-	-	0.51	8.18	3.10	0.19	-
TFF-1	*N. dunbari*	B-B'	4	2.54	-	-	0.51	10.28	3.39	-	-
TFF-1	*N. dunbari*	B-B'	5	2.54	-	-	1.02	10.16	3.57	-	-
TFF-1	*N. dunbari*	B-B'	6	2.54	-	-	1.02	10.54	3.61	0.19	-
TFF-1	*N. dunbari*	B-B'	7	2.54	-	-	1.01	8.58	2.67	-	-
TFF-1	*N. dunbari*	B-B'	8	2.04	-	-	1.02	12.72	3.81	-	-
TFF-1	*N. dunbari*	B-B'	9	2.04	-	-	0.51	12.88	4.27	0.38	-
TFF-1	*N. dunbari*	B-B'	10	1.53	-	-	1.02	11.82	4.33	-	0.01
TFF-1	*N. dunbari*	B-B'	11	2.04	-	-	1.02	11.26	4.79	0.39	-
TFF-1	*N. dunbari*	B-B'	12	4.61	-	-	1.02	12.06	5.14	-	0.21
TFF-1	*N. dunbari*	B-B'	13	2.55	-	-	0.51	12.20	5.20	-	-
TFF-1	*N. dunbari*	B-B'	14	2.03	-	-	1.02	10.01	3.66	-	-
TFF-1	*N. dunbari*	B-B'	15	2.54	-	-	1.01	8.33	2.32	0.37	-
TFF-1	*N. dunbari*	B-B'	16	2.54	-	-	0.51	10.09	3.58	-	-
TFF-1	*N. dunbari*	B-B'	17	2.03	-	-	1.02	9.28	2.97	0.16	0.58
TFF-1	*N. dunbari*	B-B'	18	2.54	-	-	1.02	9.71	3.24	-	0.21
TFF-1	*N. dunbari*	B-B'	19	2.03	-	-	0.51	9.31	3.39	-	0.01
TFF-1	*N. dunbari*	B-B'	20	2.55	-	-	0.51	11.88	4.57	0.02	-
TFF-1	*N. dunbari*	B-B'	21	2.04	-	-	1.02	12.14	4.19	-	0.01
TFF-1	*N. dunbari*	B-B'	22	5.14	-	-	1.54	13.98	7.14	-	-
TFF-1	*N. dunbari*	B-B'	23	2.04	-	-	1.02	11.93	3.37	0.21	-
TFF-1	*N. dunbari*	B-B'	24	2.55	-	-	1.02	11.43	4.13	0.19	-
TFF-1	*N. dunbari*	B-B'	25	4.60	-	-	1.02	12.70	4.45	-	-
TFF-1	*N. dunbari*	B-B'	26	3.06	-	-	1.02	11.60	4.48	-	-
TFF-1	*N. dunbari*	B-B'	27	3.05	-	-	1.02	10.96	2.95	-	-
TFF-1	*N. dunbari*	B-B'	28	4.09	-	-	1.02	12.24	4.28	-	0.41
TFF-1	*N. dunbari*	B-B'	29	3.58	-	-	1.02	10.37	5.55	0.18	0.63

Specimen	Species	Transect	Sample #	x/Ca (mmol/mol)							
				Mg	Fe	Mn	Sr	S	Na	Al	Si
TFF-1	*N. dunbari*	B-B'	30	3.57	-	-	0.51	10.51	5.42	0.25	0.31
TFF-2	*N. dunbari*	A-A'	1	2.03	0.00	0.00	0.51	9.47	4.17	0.28	-
TFF-2	*N. dunbari*	A-A'	2	1.52	0.00	0.00	0.51	9.50	4.35	0.17	0.00
TFF-2	*N. dunbari*	A-A'	3	1.52	0.00	0.00	1.02	10.15	3.65	-	-
TFF-2	*N. dunbari*	A-A'	4	1.01	0.00	0.00	1.01	8.87	3.69	0.20	0.15
TFF-2	*N. dunbari*	A-A'	5	1.53	0.00	0.00	1.02	11.07	4.56	0.00	0.16
TFF-2	*N. dunbari*	A-A'	6	2.04	0.00	0.00	1.02	11.28	3.84	0.00	-
TFF-2	*N. dunbari*	A-A'	7	2.04	0.00	0.00	0.51	10.44	3.90	0.17	-
TFF-2	*N. dunbari*	A-A'	8	2.54	0.21	0.00	1.02	8.90	3.05	-	0.31
TFF-2	*N. dunbari*	A-A'	9	2.03	0.00	0.00	0.51	9.71	3.64	-	-
TFF-2	*N. dunbari*	A-A'	10	2.54	0.51	0.00	0.51	9.71	3.43	-	-
TFF-2	*N. dunbari*	A-A'	11	4.55	0.00	0.00	0.51	4.72	1.84	0.00	-
TFF-2	*N. dunbari*	A-A'	12	2.57	0.00	0.00	1.03	15.06	7.77	0.21	-
TFF-2	*N. dunbari*	A-A'	13	2.56	0.00	0.00	1.03	14.09	6.37	1.42	-
TFF-2	*N. dunbari*	A-A'	14	2.55	0.00	0.00	0.51	12.07	4.82	-	-
TFF-2	*N. dunbari*	A-A'	15	2.55	0.00	0.00	1.02	11.49	6.19	-	-
TFF-2	*N. dunbari*	A-A'	16	2.56	0.00	0.00	1.02	12.31	5.65	2.63	-
TFF-2	*N. dunbari*	A-A'	17	3.58	0.00	0.00	1.02	12.38	6.31	0.25	-
TFF-2	*N. dunbari*	A-A'	18	5.67	0.00	0.21	1.03	15.81	6.73	0.36	-
TFF-2	*N. dunbari*	A-A'	19	3.61	0.00	0.00	1.03	16.55	8.44	0.17	-
TFF-2	*N. dunbari*	A-A'	20	9.25	0.51	0.00	1.03	9.83	7.54	-	-
TFF-2	*N. dunbari*	A-A'	21	8.76	0.00	0.52	1.03	14.66	6.01	0.00	-
TFF-2	*N. dunbari*	A-A'	22	4.62	0.00	0.00	1.03	14.96	6.36	-	-
TFF-2	*N. dunbari*	A-A'	23	5.12	0.00	0.00	0.51	12.36	5.94	0.37	-
TFF-2	*N. dunbari*	A-A'	24	3.05	0.00	0.00	0.51	8.82	3.84	-	0.29
TFF-2	*N. dunbari*	A-A'	25	5.62	0.51	0.00	0.51	11.02	4.22	-	-
TFF-2	*N. dunbari*	A-A'	26	5.62	0.00	0.00	0.51	10.33	4.69	0.20	-
TFF-2	*N. dunbari*	A-A'	27	5.11	0.00	0.00	1.02	11.59	4.83	-	-
TFF-2	*N. dunbari*	A-A'	28	8.79	0.00	0.00	0.52	17.07	8.39	0.21	0.03
TFF-2	*N. dunbari*	A-A'	29	5.66	0.00	0.00	1.03	14.69	7.08	0.17	-
TFF-2	*N. dunbari*	A-A'	30	4.09	0.00	0.00	1.02	12.87	5.99	0.00	0.03
TFF-2	*N. dunbari*	A-A'	31	3.07	0.00	0.51	1.02	12.67	5.32	0.33	-
TFF-2	*N. dunbari*	A-A'	32	3.04	0.00	0.00	0.51	7.36	2.54	0.22	-
TFF-2	*N. dunbari*	A-A'	33	16.49	0.00	0.00	0.52	9.53	4.02	-	-
TFF-2	*N. dunbari*	A-A'	34	7.72	0.00	0.00	1.03	13.92	5.73	-	-
TFF-2	*N. dunbari*	A-A'	35	4.58	0.00	0.00	0.51	9.46	3.46	-	-
TFF-2	*N. dunbari*	A-A'	36	7.19	0.00	0.00	0.51	12.90	5.54	0.24	0.21
TFF-2	*N. dunbari*	A-A'	37	3.59	0.00	0.00	1.03	14.12	6.18	-	-

Specimen	Species	Transect	Sample #	x/Ca (mmol/mol)							
				Mg	Fe	Mn	Sr	S	Na	Al	Si
TFF-2	*N. dunbari*	A-A'	38	2.56	0.00	0.00	0.51	14.71	6.05	0.23	-
TFF-2	*N. dunbari*	A-A'	39	4.56	0.00	0.00	0.51	6.35	2.41	0.00	-
TFF-2	*N. dunbari*	A-A'	40	4.09	0.00	0.00	1.02	12.38	5.11	-	-
TFF-2	*N. dunbari*	B-B'	1	2.54	-	-	0.51	7.98	3.57	0.51	0.60
TFF-2	*N. dunbari*	B-B'	2	2.54	-	0.22	0.51	6.72	4.01	-	0.24
TFF-2	*N. dunbari*	B-B'	3	2.03	0.20	-	0.51	7.34	3.60	0.62	-
TFF-2	*N. dunbari*	B-B'	4	2.54	-	-	1.02	9.27	4.30	-	0.18
TFF-2	*N. dunbari*	B-B'	5	2.53	-	-	0.51	7.07	2.80	0.21	-
TFF-2	*N. dunbari*	B-B'	6	2.54	-	-	1.02	7.42	3.78	0.39	-
TFF-2	*N. dunbari*	B-B'	7	2.03	-	-	1.01	7.79	3.19	0.19	-
TFF-2	*N. dunbari*	B-B'	8	2.03	-	-	1.01	7.65	3.51	-	-
TFF-2	*N. dunbari*	B-B'	9	2.03	-	-	0.51	7.90	3.02	0.26	-
TFF-2	*N. dunbari*	B-B'	10	2.04	-	-	3.06	10.94	4.11	0.27	-
TFF-2	*N. dunbari*	B-B'	11	2.03	-	-	1.02	9.34	3.86	-	0.34
TFF-2	*N. dunbari*	B-B'	12	2.04	-	-	0.51	9.35	3.77	2.56	-
TFF-2	*N. dunbari*	B-B'	13	2.54	-	-	1.02	9.43	3.97	0.60	0.30
TFF-2	*N. dunbari*	B-B'	14	1.52	-	-	1.02	8.78	3.19	0.82	-
TFF-2	*N. dunbari*	B-B'	15	1.52	-	-	0.51	9.17	4.30	-	-
TFF-2	*N. dunbari*	B-B'	16	1.53	-	-	0.51	10.29	4.50	0.29	-
TFF-2	*N. dunbari*	B-B'	17	2.03	-	-	1.02	9.04	4.12	0.19	-
TFF-2	*N. dunbari*	B-B'	18	1.52	-	-	1.01	8.43	3.27	-	-
TFF-2	*N. dunbari*	B-B'	19	1.52	-	-	1.02	9.92	3.74	-	0.17
TFF-2	*N. dunbari*	B-B'	20	2.04	-	-	1.02	11.05	4.29	-	-
TFF-2	*N. dunbari*	B-B'	21	3.57	-	0.51	1.02	10.75	4.30	0.29	-
TFF-2	*N. dunbari*	B-B'	22	4.10	-	-	1.03	14.39	5.90	-	-
TFF-2	*N. dunbari*	B-B'	23	11.40	-	0.52	1.04	16.21	7.13	0.45	-
TFF-2	*N. dunbari*	B-B'	24	10.37	0.52	0.52	1.56	15.75	8.38	-	0.29
TFF-2	*N. dunbari*	B-B'	25	9.83	-	-	1.55	15.79	7.17	0.20	0.29
Nn-3	*N. dunbari*	A-A'	1	3.04	-	-	0.51	5.06	4.31	-	-
Nn-3	*N. dunbari*	A-A'	2	3.57	-	-	0.51	10.46	5.21	0.27	0.40
Nn-3	*N. dunbari*	A-A'	3	3.05	-	-	1.02	9.90	3.44	-	0.25
Nn-3	*N. dunbari*	A-A'	4	2.54	-	-	1.02	9.41	3.03	-	-
Nn-3	*N. dunbari*	A-A'	5	3.06	-	-	0.51	10.78	5.21	-	0.33
Nn-3	*N. dunbari*	A-A'	6	3.05	0.51	-	1.02	9.76	4.11	-	-
Nn-3	*N. dunbari*	A-A'	7	3.05	-	-	1.02	9.53	3.87	-	0.37
Nn-3	*N. dunbari*	A-A'	8	5.60	-	-	1.02	8.68	3.35	-	0.32
Nn-3	*N. dunbari*	A-A'	9	3.04	0.20	-	0.51	6.99	3.58	-	-
Nn-3	*N. dunbari*	A-A'	10	7.11	-	-	0.51	5.91	2.10	-	-

Specimen	Species	Transect	Sample #	x/Ca (mmol/mol)							
				Mg	Fe	Mn	Sr	S	Na	Al	Si
Nn-3	*N. dunbari*	A-A'	11	3.07	-	-	1.02	12.11	5.17	-	0.27
Nn-3	*N. dunbari*	A-A'	12	3.05	-	-	1.02	9.66	3.07	-	0.16
Nn-3	*N. dunbari*	A-A'	13	3.57	-	-	1.02	11.18	4.34	-	-
Nn-3	*N. dunbari*	A-A'	14	3.05	0.51	-	0.51	10.04	3.52	0.18	0.21
Nn-3	*N. dunbari*	A-A'	15	3.05	-	-	0.51	9.86	3.41	-	-
Nn-3	*N. dunbari*	A-A'	16	5.58	-	-	0.51	5.82	1.64	-	0.55
Nn-3	*N. dunbari*	A-A'	17	15.94	-	-	0.51	8.18	2.91	-	-
Nn-3	*N. dunbari*	A-A'	18	2.55	-	-	0.51	11.22	4.11	-	-
Nn-3	*N. dunbari*	A-A'	19	8.15	-	-	0.51	6.67	2.42	0.29	0.27
Nn-3	*N. dunbari*	A-A'	20	4.58	-	-	1.02	9.01	3.52	-	-
Nn-3	*N. dunbari*	B-B'	1	2.54	-	-	1.02	7.56	4.13	-	-
Nn-3	*N. dunbari*	B-B'	2	3.06	-	-	0.51	10.01	5.73	-	0.22
Nn-3	*N. dunbari*	B-B'	3	2.54	-	-	0.51	7.55	3.94	-	-
Nn-3	*N. dunbari*	B-B'	4	4.07	-	-	1.02	8.93	3.64	0.33	-
Nn-3	*N. dunbari*	B-B'	5	3.04	-	-	0.51	6.55	3.96	-	-
Nn-3	*N. dunbari*	B-B'	6	2.54	-	-	1.01	7.96	2.12	-	0.23
Nn-3	*N. dunbari*	B-B'	7	4.08	-	-	1.02	9.97	4.21	-	0.27
Nn-3	*N. dunbari*	B-B'	8	3.05	-	-	0.51	7.92	4.10	-	-
Nn-3	*N. dunbari*	B-B'	9	3.05	-	-	1.02	8.05	3.07	-	0.20
Nn-3	*N. dunbari*	B-B'	10	2.54	-	-	0.51	7.54	3.23	-	-
Nn-3	*N. dunbari*	B-B'	11	2.53	-	-	1.01	7.84	2.63	-	-
Nn-3	*N. dunbari*	B-B'	12	3.05	-	-	0.51	7.93	3.46	-	-
Nn-3	*N. dunbari*	B-B'	13	2.54	-	-	1.02	7.70	3.38	0.29	0.19
Nn-3	*N. dunbari*	B-B'	14	2.54	-	-	0.51	9.28	4.08	0.26	-
Nn-3	*N. dunbari*	B-B'	15	3.04	-	-	1.01	6.11	3.94	-	0.21
Nn-3	*N. dunbari*	B-B'	16	3.56	-	-	0.51	8.67	3.87	-	-
Nn-3	*N. dunbari*	B-B'	17	2.03	-	-	1.02	9.16	3.50	0.23	0.51
Nn-3	*N. dunbari*	B-B'	18	2.54	-	-	1.02	8.57	3.52	0.31	0.23
Nn-3	*N. dunbari*	B-B'	19	2.03	-	0.51	0.51	9.13	3.41	0.26	0.19
Nn-3	*N. dunbari*	B-B'	20	2.03	-	-	0.51	9.04	3.83	-	0.26
Nn-3	*N. dunbari*	B-B'	21	2.03	-	-	0.51	8.30	2.76	0.18	-
Nn-3	*N. dunbari*	B-B'	22	2.03	-	-	1.01	7.64	3.30	0.21	-
Nn-3	*N. dunbari*	B-B'	23	2.54	-	-	1.01	7.83	2.92	-	0.32
Nn-3	*N. dunbari*	B-B'	24	2.03	-	-	1.01	7.44	3.00	0.16	0.21
Nn-3	*N. dunbari*	B-B'	25	2.54	-	-	1.01	8.20	3.26	-	-
Nn-3	*N. dunbari*	B-B'	26	2.54	-	-	0.51	9.24	3.73	0.18	-
Nn-3	*N. dunbari*	B-B'	27	2.54	-	-	0.51	9.74	4.20	-	-
Nn-3	*N. dunbari*	B-B'	28	2.03	-	-	1.02	9.42	4.04	0.23	-

Specimen	Species	Transect	Sample #	x/Ca (mmol/mol)							
				Mg	Fe	Mn	Sr	S	Na	Al	Si
Nn-3	*N. dunbari*	B-B'	29	2.54	-	-	1.02	9.96	3.81	0.20	0.28
Nn-3	*N. dunbari*	B-B'	30	2.55	-	-	1.53	10.00	4.15	-	-
Nn-3	*N. dunbari*	B-B'	31	2.54	-	-	0.51	9.70	3.75	-	0.26
Nn-3	*N. dunbari*	B-B'	32	2.55	-	-	0.51	11.47	4.20	0.21	-
Nn-3	*N. dunbari*	B-B'	33	3.05	-	-	1.02	9.45	3.45	-	-
Nn-3	*N. dunbari*	B-B'	34	2.03	0.22	-	1.02	8.90	2.98	-	-
Nn-3	*N. dunbari*	B-B'	35	2.03	-	-	0.51	8.48	3.13	-	-
Nn-3	*N. dunbari*	B-B'	36	2.03	-	-	1.01	6.36	4.14	-	0.22
Nn-3	*N. dunbari*	B-B'	37	2.03	-	-	1.02	8.79	4.00	-	0.32
Nn-3	*N. dunbari*	B-B'	38	2.03	-	-	1.02	10.30	3.26	-	-
Nn-3	*N. dunbari*	B-B'	39	2.03	-	-	1.02	9.41	4.07	0.34	-
Nn-3	*N. dunbari*	B-B'	40	2.55	-	0.24	1.53	8.57	5.52	-	0.68
CONC	*N. dunbari*	A-A'	1	2.02	-	-	1.01	4.53	4.22	-	-
CONC	*N. dunbari*	A-A'	2	2.53	-	-	0.51	4.56	3.90	0.24	0.31
CONC	*N. dunbari*	A-A'	3	2.02	-	-	1.01	4.74	2.97	-	-
CONC	*N. dunbari*	A-A'	4	3.04	-	-	0.51	5.22	4.16	0.56	-
CONC	*N. dunbari*	A-A'	5	2.03	-	-	1.01	5.64	3.17	-	0.40
CONC	*N. dunbari*	A-A'	6	2.53	-	0.20	0.51	4.54	4.34	-	-
CONC	*N. dunbari*	A-A'	7	2.02	-	-	0.50	4.86	2.37	-	-
CONC	*N. dunbari*	A-A'	8	2.02	-	-	0.51	4.34	2.87	0.16	0.17
CONC	*N. dunbari*	A-A'	9	2.02	-	-	1.01	5.03	2.71	-	-
CONC	*N. dunbari*	A-A'	10	2.02	-	-	1.01	4.62	3.45	-	-
CONC	*N. dunbari*	A-A'	11	1.52	-	-	0.51	5.27	2.83	-	-
CONC	*N. dunbari*	A-A'	12	2.03	-	-	0.51	5.05	4.20	0.20	0.17
CONC	*N. dunbari*	A-A'	13	2.53	-	-	1.01	5.81	2.85	-	0.20
CONC	*N. dunbari*	A-A'	14	3.04	-	-	1.01	5.07	3.16	-	-
CONC	*N. dunbari*	A-A'	15	4.06	-	-	0.51	7.16	3.36	-	0.34
CONC	*N. dunbari*	A-A'	16	2.53	-	-	0.51	5.80	2.93	-	-
CONC	*N. dunbari*	A-A'	17	2.57	-	17.50	1.03	4.67	2.86	-	0.36
CONC	*N. dunbari*	A-A'	18	3.04	-	-	0.51	6.90	3.30	-	-
CONC	*N. dunbari*	A-A'	19	2.53	-	-	0.51	6.28	3.48	-	-
CONC	*N. dunbari*	A-A'	20	2.53	-	-	1.01	5.27	3.01	-	-
CONC	*N. dunbari*	A-A'	21	6.11	-	-	0.51	5.84	2.76	2.02	0.34
CONC	*N. dunbari*	A-A'	22	4.57	-	-	0.51	6.70	3.51	-	-
CONC	*N. dunbari*	A-A'	23	3.04	-	-	1.01	5.72	2.83	-	-
CONC	*N. dunbari*	A-A'	24	3.55	-	-	1.01	6.24	2.94	-	-
CONC	*N. dunbari*	A-A'	25	3.04	-	-	0.51	6.12	2.63	0.32	-
CONC	*N. dunbari*	A-A'	26	2.53	-	-	1.01	5.93	2.40	-	0.19

Specimen	Species	Transect	Sample #	x/Ca (mmol/mol)							
				Mg	Fe	Mn	Sr	S	Na	Al	Si
CONC	*N. dunbari*	A-A'	27	3.04	-	-	1.01	6.26	2.93	-	-
CONC	*N. dunbari*	A-A'	28	3.04	-	-	0.51	5.91	2.73	-	-
CONC	*N. dunbari*	A-A'	29	7.61	-	-	0.51	4.94	1.98	-	-
CONC	*N. dunbari*	A-A'	30	2.54	-	-	0.51	9.57	4.25	-	-
CONC	*N. dunbari*	A-A'	31	2.55	-	-	0.51	10.97	4.89	-	-
CONC	*N. dunbari*	A-A'	32	2.55	-	-	1.02	9.94	4.99	-	-
CONC	*N. dunbari*	A-A'	33	2.54	-	0.24	0.51	10.54	4.09	0.21	-
CONC	*N. dunbari*	A-A'	34	3.05	-	-	0.51	8.32	4.54	-	-
CONC	*N. dunbari*	A-A'	35	2.54	-	-	1.02	8.62	3.91	-	-
CONC	*N. dunbari*	B-B'	1	5.60	-	-	0.51	6.68	6.31	-	-
CONC	*N. dunbari*	B-B'	2	4.07	-	0.20	1.02	6.10	4.76	0.37	-
CONC	*N. dunbari*	B-B'	3	3.04	-	-	1.01	6.02	3.69	-	0.24
CONC	*N. dunbari*	B-B'	4	3.04	-	-	0.51	6.45	4.02	-	-
CONC	*N. dunbari*	B-B'	5	2.02	-	-	1.01	5.81	2.18	-	0.19
CONC	*N. dunbari*	B-B'	6	2.53	-	-	0.51	5.46	3.00	0.17	-
CONC	*N. dunbari*	B-B'	7	2.53	-	-	0.51	6.66	0.00	-	-
CONC	*N. dunbari*	B-B'	8	2.02	-	-	1.01	4.93	2.40	-	-
CONC	*N. dunbari*	B-B'	9	2.02	-	-	1.01	5.37	2.66	-	-
CONC	*N. dunbari*	B-B'	10	2.02	-	-	0.51	5.00	2.63	-	-
CONC	*N. dunbari*	B-B'	11	2.02	-	-	1.01	5.10	3.01	-	-
CONC	*N. dunbari*	B-B'	12	2.02	-	-	1.01	4.95	2.59	-	0.23
CONC	*N. dunbari*	B-B'	13	3.04	-	-	0.51	5.00	3.03	-	-
CONC	*N. dunbari*	B-B'	14	3.03	-	-	0.50	2.90	2.73	-	-
CONC	*N. dunbari*	B-B'	15	2.53	-	-	1.52	5.15	3.20	-	-
CONC	*N. dunbari*	B-B'	16	2.53	-	-	0.51	4.82	2.04	-	0.21
CONC	*N. dunbari*	B-B'	17	32.24	1.15	1.15	6.91	75.53	33.23	1.34	-
CONC	*N. dunbari*	B-B'	18	6.67	-	0.51	1.03	12.16	6.54	-	-
CONC	*N. dunbari*	B-B'	19	14.44	-	-	0.52	10.16	6.29	-	-
CONC	*N. dunbari*	B-B'	20	13.45	0.21	-	1.03	12.70	6.67	0.41	-
A01-1	*C. planoconvexa*	n/a	1	6.23	0.52	-	1.56	17.47	12.26	0.19	-
A01-1	*C. planoconvexa*	n/a	2	10.94	0.52	0.52	1.56	16.09	12.84	0.01	0.29
A01-1	*C. planoconvexa*	n/a	3	4.66	-	-	1.55	15.97	12.97	-	-
A01-1	*C. planoconvexa*	n/a	4	6.73	-	-	1.04	15.01	11.29	0.30	0.13
A01-2	*C. planoconvexa*	n/a	1	6.21	-	0.52	1.04	18.81	9.34	-	-
A01-2	*C. planoconvexa*	n/a	2	7.80	-	0.52	1.04	18.53	11.66	-	0.18
A01-2	*C. planoconvexa*	n/a	3	4.66	-	0.52	2.07	17.79	10.75	0.01	-
A01-2	*C. planoconvexa*	n/a	4	4.63	-	-	1.54	14.18	9.19	-	0.05
AMA3-1	*C. planoconvexa*	n/a	1	3.10	-	0.52	1.55	17.14	10.28	0.03	0.08

Specimen	Species	Transect	Sample #	x/Ca (mmol/mol)							
				Mg	Fe	Mn	Sr	S	Na	Al	Si
CONC	*N. dunbari*	A-A'	27	3.04	-	-	1.01	6.26	2.93	-	-
CONC	*N. dunbari*	A-A'	28	3.04	-	-	0.51	5.91	2.73	-	-
CONC	*N. dunbari*	A-A'	29	7.61	-	-	0.51	4.94	1.98	-	-
AMA3-2	*C. planoconvexa*	n/a	1	8.89	-	-	1.05	23.53	11.49	0.38	0.09
AMA3-2	*C. planoconvexa*	n/a	2	6.23	-	0.52	1.56	20.28	10.13	0.12	0.11
AMA3-2	*C. planoconvexa*	n/a	3	5.18	-	-	1.04	19.75	9.29	0.19	-
AMA3-2	*C. planoconvexa*	n/a	4	5.18	0.52	2.07	1.04	18.11	8.95	0.18	0.20
AMA5_1	*C. planoconvexa*	n/a	1	7.81	-	0.52	1.04	19.60	12.23	0.49	0.27
AMA5_2	*C. planoconvexa*	n/a	2	6.78	-	0.52	1.04	20.82	12.68	0.63	0.18
AMA5_3	*C. planoconvexa*	n/a	3	5.73	0.52	0.52	1.56	20.74	11.59	0.97	0.03
AMA5_4	*C. planoconvexa*	n/a	4	7.29	-	-	1.56	19.89	11.70	0.14	0.38
AMP1B-3	*C. planoconvexa*	n/a	1	12.59	-	1.05	1.05	20.56	12.91	0.27	-
AMP1B-3	*C. planoconvexa*	n/a	2	5.21	-	0.52	1.04	21.87	12.07	0.15	0.28
AMP1B-3	*C. planoconvexa*	n/a	3	5.18	-	-	1.55	18.87	9.76	0.06	0.11
AMP1B-4	*C. planoconvexa*	n/a	1	5.16	-	0.52	1.55	15.19	10.29	0.04	0.16
AMP1B-4	*C. planoconvexa*	n/a	2	4.67	-	-	1.56	19.54	11.59	-	0.18
AMP1B-4	*C. planoconvexa*	n/a	3	5.18	-	-	1.55	18.55	9.82	0.13	-
BELL5-5	*C. planoconvexa*	n/a	1	4.15	-	-	1.56	20.67	11.41	0.30	-
BELL5-5	*C. planoconvexa*	n/a	2	3.64	-	0.52	1.56	21.66	13.57	0.28	-
BELL5-5	*C. planoconvexa*	n/a	3	7.85	-	0.52	1.57	22.52	14.21	0.27	0.05
BELL5-5	*C. planoconvexa*	n/a	4	9.95	-	0.52	1.05	22.44	12.38	0.27	0.41
BELL5-6	*C. planoconvexa*	n/a	1	6.20	0.52	0.52	2.07	13.67	10.36	0.06	-
BELL5-6	*C. planoconvexa*	n/a	2	4.15	-	-	1.04	17.97	13.38	0.03	0.12
BELL5-6	*C. planoconvexa*	n/a	3	6.22	-	-	2.07	16.05	12.05	0.78	0.01
BELL5-6	*C. planoconvexa*	n/a	4	10.40	-	-	1.56	16.10	11.62	-	0.10
FAIR4a-1	*C. planoconvexa*	n/a	1	4.13	-	0.52	1.55	15.98	10.69	0.15	0.17
FAIR4a-1	*C. planoconvexa*	n/a	2	3.63	-	-	1.04	18.83	11.29	0.23	-
FAIR4a-1	*C. planoconvexa*	n/a	3	5.21	-	0.52	1.56	21.91	13.14	0.07	0.06
FAIR4a-1	*C. planoconvexa*	n/a	4	6.27	-	-	1.57	23.78	12.19	-	0.26
FAIR4a-2	*C. planoconvexa*	n/a	1	6.71	0.52	-	1.55	13.08	10.82	0.02	0.20
FAIR4a-2	*C. planoconvexa*	n/a	2	7.23	-	-	1.55	12.60	10.40	0.27	0.20
FAIR4a-2	*C. planoconvexa*	n/a	3	7.80	-	-	1.56	19.18	12.08	0.05	-
FAIR4a-2	*C. planoconvexa*	n/a	4	7.80	1.04	0.52	1.56	15.94	11.64	0.66	-
FAIR4a-4	*C. planoconvexa*	n/a	1	7.27	-	-	1.56	18.78	10.71	-	0.20
FAIR4a-4	*C. planoconvexa*	n/a	2	15.18	0.52	-	1.57	16.31	13.32	0.21	0.18
FAIR4a-4	*C. planoconvexa*	n/a	3	9.36	-	0.52	1.56	17.32	11.21	0.00	0.29
FAIR4a-4	*C. planoconvexa*	n/a	4	9.34	-	-	1.04	15.84	10.40	0.11	0.31
FAIR4a-6	*C. planoconvexa*	n/a	1	6.19	-	0.52	1.55	13.37	9.56	0.09	0.11

Specimen	Species	Transect	Sample #	x/Ca (mmol/mol)							
				Mg	Fe	Mn	Sr	S	Na	Al	Si
FAIR4a-6	*C. planoconvexa*	n/a	2	9.33	-	0.52	1.04	16.29	9.53	0.09	0.27
FAIR4a-6	*C. planoconvexa*	n/a	3	9.31	-	-	1.03	13.34	9.81	0.23	0.19
FAIR4a-6	*C. planoconvexa*	n/a	4	16.13	0.52	1.04	1.56	12.13	9.31	0.10	0.01
FAIR5-5	*C. planoconvexa*	n/a	1	3.61	-	-	1.55	14.97	10.06	0.43	0.22
FAIR5-5	*C. planoconvexa*	n/a	2	6.68	-	0.51	1.03	9.59	9.66	-	-
FAIR5-5	*C. planoconvexa*	n/a	3	5.66	0.51	0.51	1.54	10.90	10.40	0.20	0.06
FAIR5-5	*C. planoconvexa*	n/a	4	5.12	-	-	1.02	9.94	8.19	0.21	0.14
FAIR5-6	*C. planoconvexa*	n/a	1	13.56	-	0.52	1.56	14.75	11.88	0.06	0.28
FAIR5-6	*C. planoconvexa*	n/a	2	9.86	-	0.52	1.04	15.21	11.03	0.01	0.06
FAIR5-6	*C. planoconvexa*	n/a	3	7.76	-	0.52	1.03	14.41	11.31	-	-
FAIR5-6	*C. planoconvexa*	n/a	4	10.92	-	0.52	1.56	15.25	11.50	0.09	0.05
GRR5A-1	*C. planoconvexa*	n/a	1	7.30	-	0.52	1.56	20.86	11.42	0.45	0.20
GRR5A-1	*C. planoconvexa*	n/a	2	5.19	-	-	0.52	20.60	11.95	0.01	0.06
GRR5A-1	*C. planoconvexa*	n/a	3	8.88	0.52	0.52	1.57	20.26	13.06	0.24	-
GRR5A-1	*C. planoconvexa*	n/a	4	6.29	-	-	1.05	24.80	14.81	-	-
GRR5A-3	*C. planoconvexa*	n/a	1	5.68	-	-	1.03	13.50	11.73	-	0.40
GRR5A-3	*C. planoconvexa*	n/a	2	8.84	-	0.52	2.08	14.86	9.35	3.38	0.03
GRR5A-3	*C. planoconvexa*	n/a	3	7.79	-	0.52	1.56	16.53	12.21	0.05	0.20
GRR5A-3	*C. planoconvexa*	n/a	4	6.22	-	0.52	1.04	16.50	11.69	0.05	0.42
GRR5A-4	*C. planoconvexa*	n/a	1	4.66	0.52	0.52	1.03	14.64	12.71	0.23	0.26
GRR5A-4	*C. planoconvexa*	n/a	2	6.73	-	0.52	2.07	13.76	13.14	0.09	0.06
GRR5A-4	*C. planoconvexa*	n/a	3	5.18	-	0.00	1.55	15.59	12.86	0.18	0.28
GRR5A-4	*C. planoconvexa*	n/a	4	5.71	-	0.52	1.56	17.73	12.25	0.33	0.43
GRRId-1	*C. planoconvexa*	n/a	1	5.69	-	-	1.04	17.44	10.19	0.11	-
GRRId-1	*C. planoconvexa*	n/a	2	4.65	-	-	1.03	17.19	9.38	-	0.12
GRRId-1	*C. planoconvexa*	n/a	3	8.84	-	-	1.56	19.02	9.94	0.12	0.28
GRRId-2	*C. planoconvexa*	n/a	1	9.32	-	0.52	1.55	14.47	9.02	0.05	0.07
GRRId-2	*C. planoconvexa*	n/a	2	7.78	-	0.52	1.04	17.66	10.05	0.25	-
GRRId-2	*C. planoconvexa*	n/a	3	17.83	-	0.52	1.57	17.51	11.50	-	0.24
GRRId-2	*C. planoconvexa*	n/a	4	6.74	-	-	1.55	18.84	9.57	-	-
GRRId-5	*C. planoconvexa*	n/a	1	11.42	0.52	-	1.56	14.01	10.46	-	0.12
GRRId-5	*C. planoconvexa*	n/a	2	9.33	-	-	1.56	15.64	10.45	0.01	-
GRRId-5	*C. planoconvexa*	n/a	3	6.71	-	-	1.55	13.85	10.07	-	0.10
GRRId-5	*C. planoconvexa*	n/a	4	7.78	-	-	2.08	15.05	12.72	-	0.05
GRRId-7	*C. planoconvexa*	n/a	1	9.28	-	-	1.55	10.36	9.52	-	0.27
GRRId-7	*C. planoconvexa*	n/a	2	7.73	-	-	1.03	12.58	9.31	0.21	0.16
GRRId-7	*C. planoconvexa*	n/a	3	5.19	-	0.52	1.56	15.86	14.18	0.40	0.33
GRRId-7	*C. planoconvexa*	n/a	4	4.14	-	0.52	2.07	16.64	11.09	0.00	0.22

Specimen	Species	Transect	Sample #	x/Ca (mmol/mol)							
				Mg	Fe	Mn	Sr	S	Na	Al	Si
GRRId-8	*C. planoconvexa*	n/a	1	13.51	-	0.52	0.00	13.79	11.14	0.14	0.05
GRRId-8	*C. planoconvexa*	n/a	2	8.88	-	0.52	1.57	19.45	13.77	0.10	0.28
GRRId-8	*C. planoconvexa*	n/a	3	6.23	-	0.52	1.04	17.74	12.74	0.04	0.00
GRRId-8	*C. planoconvexa*	n/a	4	6.75	-	0.52	1.04	18.99	10.48	0.19	0.03
GRRIIa-11	*C. planoconvexa*	n/a	1	16.20	-	0.52	1.57	14.43	11.76	0.20	0.32
GRRIIa-11	*C. planoconvexa*	n/a	2	7.28	-	0.52	1.04	18.77	11.45	0.32	-
GRRIIa-11	*C. planoconvexa*	n/a	3	8.80	0.52	-	1.55	12.82	11.53	0.10	0.07
GRRIIa-11	*C. planoconvexa*	n/a	4	13.06	0.52	0.52	1.04	16.49	12.59	0.11	0.27
GRRIIa-12	*C. planoconvexa*	n/a	1	6.21	-	-	1.55	15.19	11.25	0.40	0.27
GRRIIa-12	*C. planoconvexa*	n/a	2	4.65	-	-	1.55	15.99	11.74	0.16	0.14
GRRIIa-12	*C. planoconvexa*	n/a	3	4.13	-	-	1.55	15.51	11.40	0.10	0.24
GRRIIa-12	*C. planoconvexa*	n/a	4	6.73	-	-	2.07	13.42	12.13	0.15	0.18
GRRIIa-5	*C. planoconvexa*	n/a	1	4.14	0.52	0.52	1.04	17.89	10.87	0.08	-
GRRIIa-5	*C. planoconvexa*	n/a	2	5.69	-	0.52	1.04	17.58	10.34	0.32	-
GRRIIa-5	*C. planoconvexa*	n/a	3	3.60	-	0.51	1.03	14.90	9.31	0.24	0.18
GRRIIa-5	*C. planoconvexa*	n/a	4	6.19	-	-	0.52	14.81	9.07	0.40	0.14
GRRIIa-7	*C. planoconvexa*	n/a	1	7.78	0.52	-	1.04	19.47	9.22	0.12	0.12
GRRIIa-7	*C. planoconvexa*	n/a	2	8.83	-	-	1.04	19.19	8.43	0.18	-
GRRIIa-7	*C. planoconvexa*	n/a	3	23.26	0.53	1.06	1.06	19.62	11.21	0.31	0.04
GRRIIa-8	*C. planoconvexa*	n/a	1	4.13	-	-	1.55	17.71	9.37	0.11	0.14
GRRIIa-8	*C. planoconvexa*	n/a	2	4.65	-	-	1.03	18.16	9.57	0.17	0.15
GRRIIa-8	*C. planoconvexa*	n/a	3	15.06	-	-	1.04	14.48	7.57	0.12	-
GRRIIa-8	*C. planoconvexa*	n/a	4	6.73	-	-	1.04	18.44	9.01	0.47	-
GRRVIa-3	*C. planoconvexa*	n/a	1	13.03	0.52	0.52	1.56	16.46	10.66	0.15	-
GRRVIa-3	*C. planoconvexa*	n/a	2	7.27	-	0.52	1.56	20.06	9.37	0.19	0.03
GRRVIa-3	*C. planoconvexa*	n/a	3	6.20	-	0.52	1.03	16.50	7.99	0.07	0.13
GRRVIa-3	*C. planoconvexa*	n/a	4	9.82	-	-	1.03	15.05	7.82	0.21	0.03